



Universiteit
Leiden
The Netherlands

Another Brick in the Wall: the role of the actinobacterial cell wall in antibiotic resistance, phylogeny and development

Aart, L.T. van der

Citation

Aart, L. T. van der. (2019, March 20). *Another Brick in the Wall: the role of the actinobacterial cell wall in antibiotic resistance, phylogeny and development*. Retrieved from <https://hdl.handle.net/1887/70209>

Version: Not Applicable (or Unknown)

License: [Licence agreement concerning inclusion of doctoral thesis in the Institutional Repository of the University of Leiden](#)

Downloaded from: <https://hdl.handle.net/1887/70209>

Note: To cite this publication please use the final published version (if applicable).

Cover Page



Universiteit Leiden



The handle <http://hdl.handle.net/1887/70209> holds various files of this Leiden University dissertation.

Author: Aart, L.T. van der

Title: Another Brick in the Wall: the role of the actinobacterial cell wall in antibiotic resistance, phylogeny and development

Issue Date: 2019-03-20

Another Brick in the Wall: The role of the actinobacterial cell wall in antibiotic resistance, phylogeny and development

Proefschrift

ter verkrijging van
de graad van Doctor aan de Universiteit Leiden,
op gezag van Rector Magnificus prof. mr. C.J.J.M Stolker,
volgens besluit van het College voor Promoties
te verdedigen op woensdag 20 maart 2019
klokke 10:00 uur

door

Lizah Tanja van der Aart
Geboren te Haarlem, Nederland
7 augustus 1991

Promotiecommissie:

Promotoren: Prof. dr. G.P. van Wezel
Prof. dr. T. Hankemeier

Overige leden: Prof. dr. A.H. Meijer
Prof. dr. P.G.L. Klinkhamer
Prof. dr. M. Bramkamp
Dr. S. Rigali

Contents:

Chapter 1	General Introduction	7
Chapter 2	Polyphasic classification of the gifted natural product producer <i>Streptomyces roseifaciens</i> sp. nov.	23
Chapter 3	High-resolution analysis of the peptidoglycan composition in <i>Streptomyces coelicolor</i>	39
Chapter 4	The peptidoglycan composition of <i>Kitasatospora setae</i> and <i>Kitasatospora viridifaciens</i> is highly modified during sporulation.	57
	Appendix 1	75
Chapter 5	Substrate inhibition of VanA by D-alanine reduces vancomycin resistance in a VanX-dependent manner.	83
Chapter 6	Structural and functional characterization of the alanine racemase from <i>Streptomyces coelicolor</i> A3(2)	105
Chapter 7	General Discussion	117
	Nederlandse Samenvatting	122
	References	128
	Curriculum Vitae	149
	Publications	150

CHAPTER 1

General Introduction

Lizah T. van der Aart & Gilles P. van Wezel

Streptomyces biology

Streptomyces are multicellular, Gram-positive bacteria in the phylum of actinobacteria which produce a high amount of bioactive natural products of which the expression is tightly coordinated with the lifecycle. During growth of *Streptomyces*, cell growth and division are two separate processes. Exponential growth of vegetative hyphae is achieved by apical growth and mycelial branching, driven by DivIVA (Flårdh, 2010). Cell division does not physically separate cells at this stage, instead long hyphae are formed which are separated by occasional cross-walls (Jakimowicz & van Wezel, 2012, Celler *et al.*, 2016). Canonical division occurs during sporulation, which requires all components of the divisome. At this stage, the long aerial hyphae are separated by up to a hundred septa and spores are formed by a highly coordinated process of cell division and DNA segregation (Zhang *et al.*, 2016a). One of the most renowned properties of streptomycetes is that they can grow without cell division, thus uniquely enabling the deletion of the cell division gene *ftsZ* (McCormick *et al.*, 1994). These remarkable properties make streptomycetes a unique model for the study of growth and cell division (McCormick, 2009).

Streptomyces are well-known for the production of a wide range of antibiotics, immune suppressants and anti-cancer compounds (Berdy, 2012, Hopwood, 2007, Barka *et al.*, 2016). The production of this high amount of specialized metabolites is commonly attributed to the lifecycle of these bacteria, consisting of growth of an intricate hyphal network, development of reproductive spores and an event of programmed cell death where old mycelia are broken down and become available in the direct environment (Figure 1). The production of secondary metabolites occurs at the onset of morphological differentiation from vegetative to reproductive growth (van der Heul *et al.*, 2018, van Wezel & McDowall, 2011). The hunt for novel antimicrobial compounds has led to the isolation of huge numbers of actinobacteria from soil and aquatic environments, leading to the discovery of more than 600 type strains of streptomycetes (Labeda *et al.*, 2017, Hopwood, 2007). These were then screened for the production of novel bioactive molecules, resulting in many different medicines from actinobacterial sources. This strategy was very successful and supported the discovery of a large amount of secondary metabolites in the past, but the amount of novel antibiotics found by this same process has decreased to a rate that this is no longer feasible (Kolter & van Wezel, 2016). A breakthrough in the field occurred when the first *Streptomyces* genomes were sequenced: it became clear that *Streptomyces* are capable of producing ten times more secondary metabolites than previously discovered (Ikeda *et al.*, 2003, Bentley *et al.*, 2002). This sparked interest in novel approaches, such as ‘awakening’ silent gene clusters (Rutledge & Challis, 2015, Zhu *et al.*, 2014a, Bentley *et al.*, 2002). Research to find novel antimicrobials is mostly driven with the natural environment and life cycle as a starting point. Scientists do not just ask ‘what’ is being produced, but also ‘why’ and ‘when’. Having the biology in mind, researchers have several different approaches: Firstly, competition between bacteria can be mimicked by co-cultivation. For example, when the filamentous fungus *Aspergillus niger* and the filamentous bacteria *Streptomyces coelicolor* are cultured together, the combination of strains produce metabolites neither organism would produce when grown solitary (Wu *et al.*, 2015). This suggests that secondary metabolites can be produced as a signal to predation or to a social cue (van der Meij *et al.*, 2017). Secondly, when strains are grown on different media they behave in a different manner, which is one of the reasons that growth on 7 different media is an essential part of *Streptomyces* taxonomy (Shirling & Gottlieb, 1966).

Rich or poor growth conditions, or the presence of specific eliciting compounds such *N*-acetyl glucosamine, can make all the difference in terms of antibiotic production (Swiatek *et al.*, 2012, Zhu *et al.*, 2014b, Rigali *et al.*, 2008). Thirdly, novel bacteria are increasingly isolated from underexplored and extreme habitats are used in order to look for more novel species with the potential to produce novel secondary metabolites (Bull *et al.*, 2016). This approach has led to the isolation of the new family of *Salinispora* sp. and a large amount of novel secondary metabolites (Ahmed *et al.*, 2013, Ziemert *et al.*, 2014, Maldonado *et al.*, 2005).

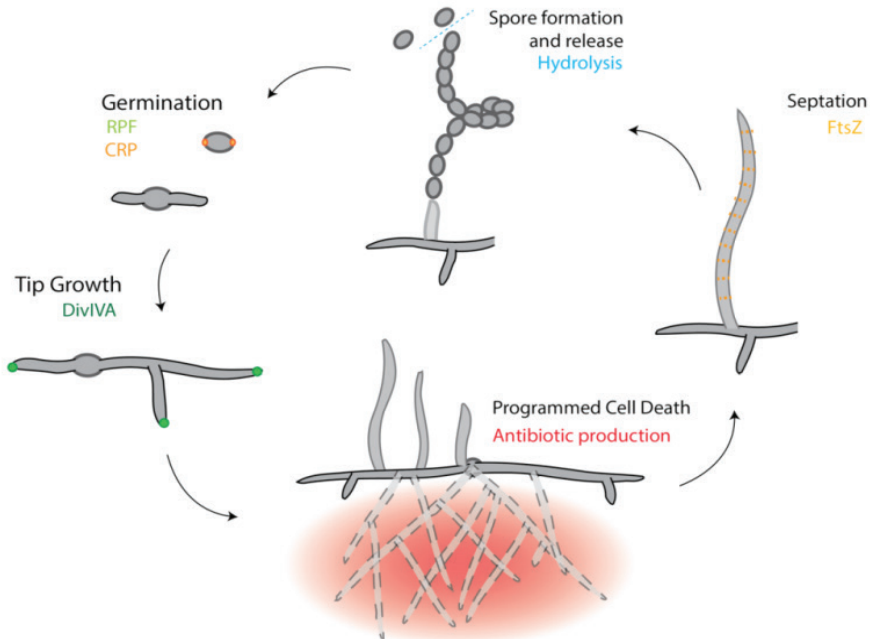


Figure 1. Schematic representation of the *Streptomyces* life cycle. Germination of spores is controlled by the cAMP receptor protein CRP and supported by RPF like proteins and muramidases. Vegetative hyphae then grow by tip growth, driven by DivIVA and eventually form a complex multicellular vegetative mycelium. When nutrients are exhausted, an event of PCD occurs simultaneously with antibiotic production and the growth of aerial hyphae. Spores are formed by simultaneous constriction of hundreds of FtsZ-rings, which are later released in order for life to start anew.

Transcriptional regulation of aerial mycelium formation is due to '*bld*' genes, named after the bald phenotype of a *Streptomyces* without aerial mycelia (Merrick, 1976). The *bld* mutants do not form aerial hypae but are often also disturbed in carbon utilization and antibiotic production, emphasizing the relation between nutrient utilization, antibiotic production and development (Pope *et al.*, 1996). Of the *bld* genes, *bldD* is a global transcription factor that represses most developmental genes during vegetative growth, including *bldN*, *whiG*, *sigH* and *ssgB* (den Hengst *et al.*, 2010, Elliot *et al.*, 2001). Especially interesting is the indirect regulation by *bldA* which specifies a leucyl-tRNA for the translation of UUA codons, which is extremely rare in the GC-rich streptomycetes. The BldA tRNA posttranslationally controls genes involved in development and antibiotic production (Lawlor *et al.*, 1987, Leskiw *et al.*, 1991). The *whi* genes are named after the white phenotype of *Streptomyces*

that fail to produce grey-pigmented spores (Chater *et al.*, 1989), and typically encode transcriptional regulators that regulate processes related to the onset of sporulation. WhiG is a sigma factor that controls the early stage of spore formation, with null mutants forming straight aerial hyphae without septa. WhiB controls the onset of sporulation and is the archetypal member of the Wbl (WhiB-like) proteins (Molle *et al.*, 2000). WhiB and WhiA co-control sporulation, and *whiA* and *whiB* mutants have very similar phenotypes, producing long, curly aerial hyphae without spores (Ainsa *et al.*, 2000, Ainsa *et al.*, 1999). Sporulation is further regulated by the SsgA-like proteins (SALPS), which are small proteins (125-142 aa) with an average amino acid similarity of 30-40% between them (Traag & van Wezel, 2008). All sporulating actinobacteria have at least one SALP and the amount of SALPS increases with the complexity of the organism (Keijser *et al.*, 2003). Deletion mutants lacking *ssgA* have sporulation defects, while overexpression of this gene causes an increase of the amount of germ tubes from a spore and a higher branching frequency (van Wezel *et al.*, 2006, van Wezel *et al.*, 2000a).

When nutrients become scarce, the vegetative mycelium undergoes a large event of Programmed Cell Death (PCD), resulting in breakdown of the vegetative or substrate hyphae for the benefit of the growth of aerial hyphae (Tenconi *et al.*, 2018, Manteca *et al.*, 2006, Miguelez *et al.*, 2000). During PCD, a large part of the vegetative cell wall is hydrolyzed in order to reuse cell-wall derived aminosugars, and in particular *N*-acetyl Glucosamine (GlcNAc), or to recycle for *de novo* cell wall synthesis (Urem *et al.*, 2016, Rigali *et al.*, 2008). At the time of PCD, streptomycetes are in a sensitive position when their own vegetative mycelium is partly hydrolyzed, as nutrients are being released at a time of scarcity. This will attract other bacteria via chemotaxis, and the only way for a slow growing bacterium to defend itself is by producing bioactive compounds, and notably antibiotics. Prodigionines, DNA-damaging agents which serve as anti-cancer compounds, are produced as a molecular trigger to eradicate most of the vegetative mycelium and this way provide nutrients for the surviving, reproductive cells (Tenconi *et al.*, 2018). Understanding cell growth and development, especially that of PCD, will greatly contribute to our understanding of antibiotic production and lead to the discovery of novel antibiotics.

The Bacterial Cell Wall

At first, bacterial shape might seem a trivial feature, at most an easy way to distinguish one species from the other. However, cell shape is subject to heavy environmental pressure and each shape requires a different type of regulation from cell wall biosynthetic machineries (Kysela *et al.*, 2016). In Gram-positive bacteria, cell shape is maintained by the peptidoglycan (PG) layer. PG forms a dynamic macromolecule that is actively remodeled to enable cell growth and differentiation through a tightly regulated interplay of hydrolytic and biosynthetic enzymes (Egan *et al.*, 2017). The chemical structure of PG is extremely well conserved, consisting of a glycan chain backbone of interchanging *N*-acetyl glucosamine (GlcNAc) and *N*-acetyl muramic acid (MurNAc). The glycan chain is cross-linked by peptide chains of non-ribosomally synthesized L- and D- amino acids, which in turn are linked to the lactate group of MurNAc. Although the chemical composition is conserved, the structure (degree of cross-linking/glycan strand length) can vary widely, depending on the species, growth phase and environment (Vollmer *et al.*, 2008a). PG architecture research is an important tool for bacterial biologists in finding mechanisms for cell shape determination. This has shown that the helical shape of *Helicobacter pylori* is maintained

by regulated cross-linking and hydrolysis (Sycuro *et al.*, 2012).

In Gram-positive bacteria, growth can be regulated in two different manners, namely via lateral growth or tip growth, depending on the phylogeny. Well-known representatives are firmicutes (lateral growth) and actinobacteria (tip growth). These bacterial families can be discerned based on features such as G+C content of the DNA, lateral growth vs tip growth and the production of endospores as opposed to external spores. Growth and division in firmicutes and actinobacteria is shown in Figure 2. Firmicutes grow by lateral growth: the cytoskeletal protein MreB forms filaments around the lateral wall of the bacteria and supports PG incorporation and cross-linking, elongating the cell (Hussain *et al.*, 2018). In contrast, actinobacteria grow by tip extension where new PG material is built in solely at the tips of rods or hyphae, a mechanism independent of MreB or FtsZ (Flårdh, 2010, Mazza *et al.*, 2006, Flårdh & Buttner, 2009). Tip growth in actinobacteria is driven by DivIVA (Flårdh *et al.*, 2012). This protein localizes at sites with a negative membrane curvature, and recruits the cell wall construction machinery (Hamoen & Errington, 2003). In *Streptomyces*, DivIVA supports the growth of long hyphae. The signal or mechanism by which branching sites are decided is unknown.

In *Bacillus subtilis*, localization of the septum at midcell is controlled by the Min and Noc systems. The Min complex prevents cell division away from mid-cell, while the nucleoid occlusion system Noc ensures that the chromosomes are well segregated prior to septum synthesis, to avoid DNA damage (Errington *et al.*, 2003, Lutkenhaus, 2007, Margolin, 2005, Wu & Errington, 2011). In most unicellular bacteria, FtsZ is tethered to the membrane by FtsA. The FtsZA complex forms filaments, which encircle the cell at the division site referred to as an FtsZ-ring. The FtsZA complex then recruits PG synthases such as PBPs to build a septum that divides the cell in two (Bisson-Filho *et al.*, 2017). In *Streptomyces*, canonical cell division that requires the divisome proteins exclusively occurs in aerial hyphae. Here, FtsZ is actively recruited to septal sites by SsgB in an SsgA-dependent manner (Willemse *et al.*, 2011). The SsgB-FtsZ complex is tethered to the membrane by SepG (Zhang *et al.*, 2016a). Thus, in streptomycetes, cell division is positively controlled, in contrast to the Min-dependent negative control systems found in many other bacteria.

Regulation of both growth and division is fundamentally different in Actinobacteria and Firmicutes, not a single regulatory protein from Firmicutes has the same function in Actinobacteria. Together, this shows that the Actinobacteria are an especially interesting model organism to investigate cell growth and division.

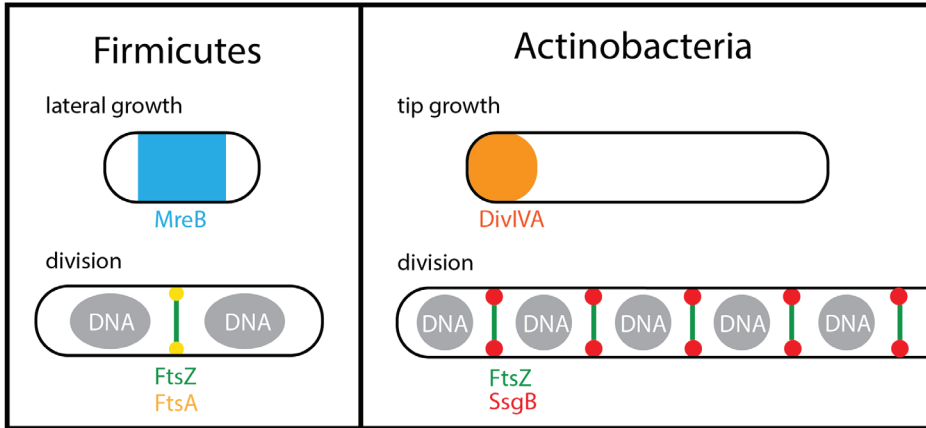


Figure 2. Growth and division in *Firmicutes* and *Actinobacteria* is regulated differently. *Firmicutes* elongate along the lateral wall, driven by MreB. Actinobacteria grow at the tip, driven by DivIVA. *Firmicutes* have a single division site in the center of the cell, where the FtsZ/A complex constricts the cell. Actinobacteria can have several division planes in a single cell during spore formation, regulated by positive control of SsgA and SsgB.

Cell wall construction

Bacterial peptidoglycan construction is a highly conserved and regulated process. The amino acids in the pentapeptide chain consist of interchanging L- and D-amino acids. This structure assists in resistance against non-specific peptidases, who would normally cleave chains of L-amino acids (Cava *et al.*, 2011). The production of D-amino acids is performed by specialized racemases, which convert L-amino acids into D-Amino acids (Radkov & Moe, 2014). The alanine racemase (Alr) converts L-Ala to D-Ala, an essential part of the peptidoglycan. An *alr* knock-out mutant of *S. coelicolor* causes the strain to become dependent on exogenous D-Ala (Tassoni *et al.*, 2017, Walsh, 1989). Lipid II, the building brick of PG, is constructed in the cytoplasm by a set of exceptionally well-conserved Mur-proteins, as shown in Figure 3. Mur-proteins ligate glycans and amino acids in a step-by-step manner, MurA and MurB produce undecaprenol (UDP) MurNAc from UDP-GlcNAc. MurC, MurD and MurE then together ensure the attachment of L-Ala, D-Glu and LL-DAP to the D-lactate group of MurNAc (Smith, 2006). The dipeptide D-Ala-D-Ala is ligated by the D-Ala-D-Ala ligase Ddl, and subsequently attached to the growing peptide chain by MurF. MraY connects the peptidoglycan precursors to the lipid-associated bactoprenyl-phosphate to yield Lipid I. Then MurG attaches GlcNAc and FemX connects Gly to LL-DAP, finishing the Lipid II molecule. The entire structure is then flipped across the lipid membrane by FtsW and/or MurJ. FtsW was shown *in vitro* to have affinity to Lipid II and for flipping activity (Mohammadi *et al.*, 2014, Mohammadi *et al.*, 2011). But this protein appeared to be inactive during *in vivo* studies. MurJ is an essential membrane protein of which a deletion causes accumulation of Lipid II in the cytoplasm and cell lysis. While *in vitro* data supports FtsW as a flippase, *in vivo* data prefers MurJ (Meeske *et al.*, 2015, Sham *et al.*, 2014, Mohammadi *et al.*, 2011). Finally, Lipid II is displayed on the cell surface and can be incorporated into the mature murein by glycosyltransferases and transpeptidases, among which RodA, PBPs and LDT. Figure 3 features cytoplasmic production of Lipid II in *S. coelicolor*.

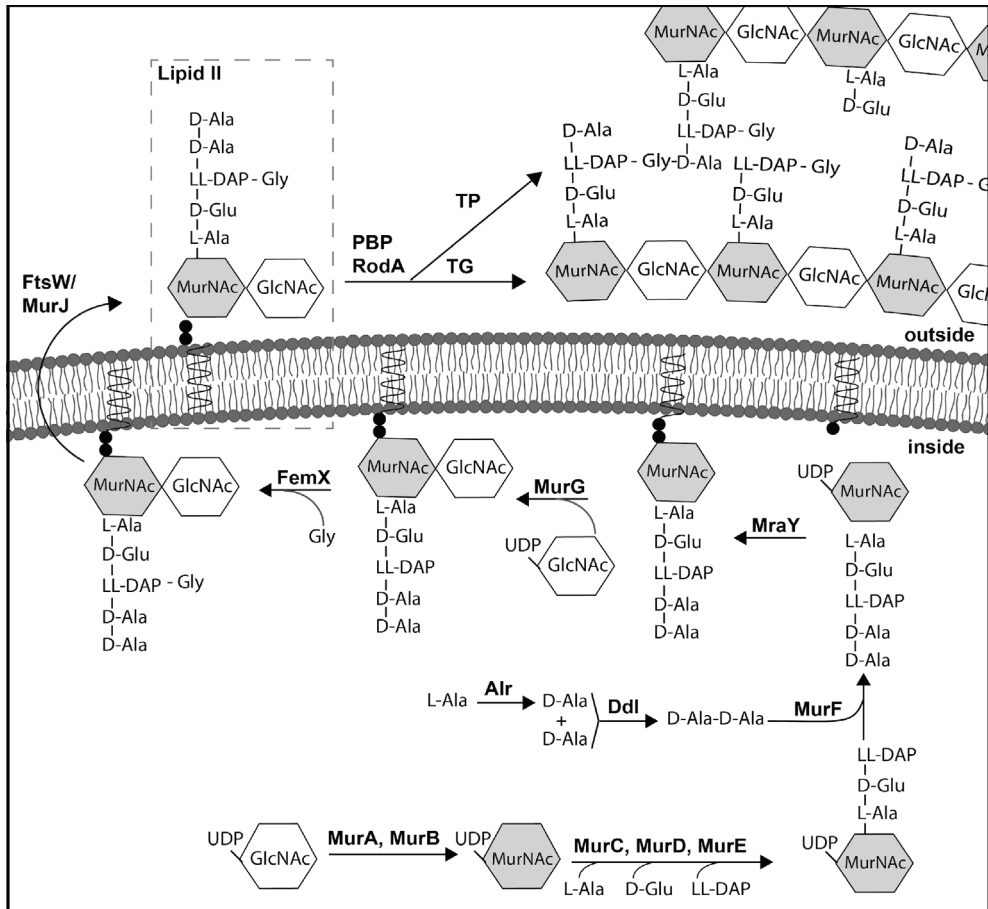


Figure 3. Construction of Lipid II is performed by Mur-genes in the cytoplasm. UDP-GlcNAc is transferred into UDP-MurNAc. To MurNAc, the first three amino acids, L-Ala, D-Glu and LL-DAP are attached by MurC, MurD and MurE, respectively. L-Ala is modified to D-Ala by Alr, after which D-Ala and D-Ala are ligated by Ddl. Then, D-Ala-D-Ala is connected to the growing PG precursor by MurF. Following this, MurY connects the PG precursor to C₅₅-phosphate, and thus connects it to the lipid membrane. MurG ligates UDP-GlcNAc to MurNAc and finally FemX attaches a single Gly to LL-DAP. This structure is flipped over the lipid membrane by either or both FtsW and MurJ. Lipid II is later cross-linked by RodA, LDTs and PBPs.

Peptidoglycan cross-linking

Lipid II construction is highly conserved among bacteria, with minor modifications at the point of the interpeptide bridge (Schleifer & Kandler, 1972). The cross-linking process afterwards is dependent on cell shape and growth mode (Vollmer *et al.*, 2008a). The two major modes of growth, lateral and tip growth, are regulated in a different way and have different mechanistic constraints. During lateral growth, the cell wall expands along the lateral wall of a cell, where new tips are generated only during septation. During tip growth, only the bacterial tip extends. Mechanistically, this means that in laterally growing cells, 'old' cell wall material is located at the tip, whereas in tip growing bacteria the 'old' cell wall material is located along the lateral wall (Kysela *et al.*, 2016). Bacteria that grow at the apex only generate novel peptidoglycan at the spherical tip and require remodeling along the wall of the hyphae to generate a cylindrical cell wall. A lack of remodeling enzymes leads to a bloated, round cells (Baranowski *et al.*, 2018). Here, we discuss PG cross-linking in tip growing bacteria.

After Lipid II translocation over the cell membrane, the new building blocks are incorporated into glycan strands, which are connected to the growing murein by proteins with glycosyltransferase (GT) activity, such as RodA and bifunctional Penicillin Binding Proteins (PBPs) (Emami *et al.*, 2017, Meeske *et al.*, 2016, Leclercq *et al.*, 2017). The peptide chain is cross-linked by transpeptidase (TP) activity by PBPs and L, D-transpeptidases (LDTs). PBPs have been discovered early on due to their ability to bind (and hence sensitivity to) penicillin, and only later it became clear that these proteins are mostly responsible for cell wall construction. Class A PBPs have bifunctional activity as both GT and TP, class B PBPs only have TP activity. PBPs form a 3-4 cross-link, conveniently named for creating a link between the 3rd and 4th amino acid in the pentapeptide chain of mucopeptides (Daniel *et al.*, 2000). PBPs require at least one pentapeptide as a donor strand to form a cross-link, this donor strand loses the terminal D-Ala[5] and PBPs cross-link two mucopeptides via the Gly cross-bridge of the acceptor strand. The requirement for pentapeptides demands that PBPs are present at the site of active peptidoglycan construction (Egan *et al.*, 2015).

PBPs are mostly responsible for PG cross-linking in firmicutes and bacteria with lateral cell wall growth. LDTs are penicillin-insensitive proteins that are able to replace a part of the function of PBP's by cross-linking two peptide chains at LL-DAP[3] and LL-DAP[3], creating a 3-3 cross-link (Mainardi *et al.*, 2005, Mainardi *et al.*, 2002). 3-3 cross-links are especially prevalent in micro-organisms that grow at the apex and have been linked to penicillin-insensitivity. Many actinobacteria contain a high amount of 3-3 cross links, such as *Mycobacterium* (30-80%), *Corynebacterium* (38%) and *Streptomyces* (30-60%) (Lavollay *et al.*, 2011, Hugonnet *et al.*, 2014, Lavollay *et al.*, 2009, van der Aart *et al.*, 2018). In contrast, bacteria with lateral cell wall growth like *E.coli* (>10%) and *E.faecium* (>3%) have a much lower amount of 3-3 cross-links (Pisabarro *et al.*, 1985, Sacco *et al.*, 2010). LDTs attach to tetrapeptides and form a cross-link between glycine and LL-DAP[3]. Here, the D-Ala[4] is considered a donor for the cross-link. The requirement of tetrapeptides in contrast to pentapeptides allow LDTs to remodel the cell wall after in the post-apical area. In mycobacteria, 3-4 cross-linking by PBPs occurs solely at the tips, at the site of peptidoglycan construction. Along the lateral wall, where the peptidoglycan is more highly modified and has a higher amount of tetrapeptides, LDTs produce 3-3 cross-links to remodel the peptidoglycan (Figure 4) (Baranowski *et al.*, 2018).

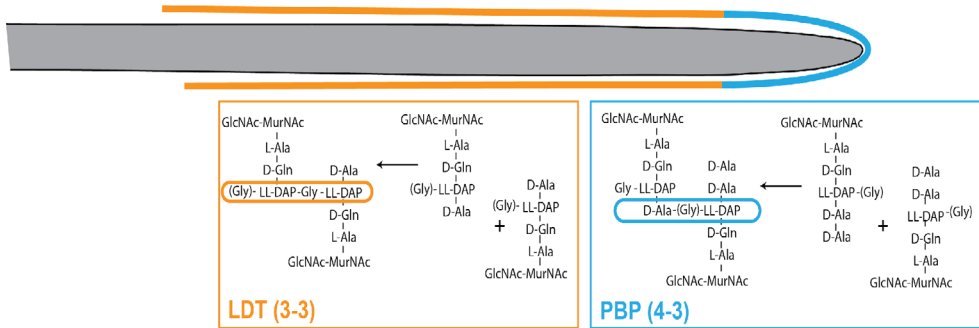


Figure 4. Peptidoglycan cross-linking at the tip and the lateral wall. In *Streptomyces*, cell wall construction takes place at the tips, with cell wall modifications along the lateral wall. At the tip, there is a high abundance of pentapeptides, the necessary donors for PBP's to form a 4-3 cross-link. Further from the tip complex, pentapeptides are modified by D,D-carboxypeptidases and PBP's, presenting a higher amount of tetrapeptides on the cell surface. At this point, LDT's modify the peptidoglycan by forming 3-3 cross-links, using tetrapeptides as a donor muropeptide.

Programmed Cell Death and cell wall hydrolysis

Over the course of growth, new peptidoglycan is continuously generated and broken down. Cell wall hydrolysis has several roles in the life of *Streptomyces*: hydrolyzing PG to allow incorporation of new glycan strands, hydrolyzing the cell wall material between mature spores to allow single spores to disperse, breaking down the thick spore wall during germination and the developmental step of PCD (Haiser *et al.*, 2009). The function of different modifying proteins is summarized in Figure 5. The *Streptomyces coelicolor* genome contains a high amount of hydrolysis-associated genes, consisting of 60 different genes encoding the four functional groups of amidases, carboxypeptidases, endopeptidases and *N*-acetylglucosaminidases (Haiser *et al.*, 2009). The large number of cell-wall modifying enzymes suggests a high degree of redundancy, in line with the multi-stage lifecycle of *Streptomyces*.

Amidases hydrolyze the lactyl bond between MurNAc and L-Ala, these enzymes are found to be essential for cell separation, as a knockdown of amidases or FtsE/FtsX will generate filaments in *E. coli* (Uehara *et al.*, 2010, Heidrich *et al.*, 2001). FtsE and FtsX are suggested to act as ATP-binding cassette transporters (ABC transport proteins), which transport amidases across the membrane (Yang *et al.*, 2011a). In *E. coli*, FtsE and FtsX function in association with FtsZ, in order to separate daughter cells after septum formation. An *ftsX* knockout mutant in *Streptomyces* still showed peptidoglycan linkage between spores, suggesting incomplete hydrolysis of the peptidoglycan (Noens, 2007). The *S. coelicolor* peptidoglycan contains a large amount of dimers which have a cross-linked set of amino acids but has lost one set of glycans, reflecting high activity of PG amidases (van der Aart *et al.*, 2018). This effect was especially pronounced in vegetative cells grown in liquid media. As pellets grow and develop, the shift from exponential to stationary growth occurs with a round of PCD, during which a large part of the cell wall in the centre is hydrolyzed (Manteca *et al.*, 2008).

Carboxypeptidases cleave the terminal amino acid from muropeptides, D,D-carboxypeptidases cleave the 5th D-Ala from a pentapeptide, while L,D-carboxypeptidases cleave the 4th D-Ala from a tetrapeptide. D,D-carboxypeptidases play a key role in spore wall maturation in *S. coelicolor* (Rioseras *et al.*, 2016), while the spore

cell walls mostly consist of tetrapeptides that lack a terminal D-Ala (van der Aart *et al.*, 2018). The product of D,D-carboxypeptidases, namely tetrapeptides, are required as donor strands for 3-3 cross links by L,D-transpeptidases. In *Streptomyces*, the role of D,D-carboxypeptidases is partly associated with 3-3 cross-linking.

Lysozyme-like proteins, muramidases and glucosamidases cleave the glycan strands between GlcNAc and MurNAc. In bacteria, muramidase or glycosamidase activity is especially important during the initiation of spore germination. In actinobacteria, 'resuscitation promoting factors' (RPFs) play a major role in spore germination and resuscitation of dormant cells (Keep *et al.*, 2006). RPFs were first described as a growth factor for non-culturable *Micrococcus luteus*, where minute amounts of protein can resuscitate dormant cells (Mukamolova *et al.*, 2002). Later it was shown that RPFs bind to the peptidoglycan and locally act as muralytic enzymes, similar to lysozyme (Mukamolova *et al.*, 2006). Interestingly, RPFs can also resuscitate dormant cells of mycobacteria (Nikitushkin *et al.*, 2013), which shows their potential as target for drug development, particularly because dormant cells are a major problem in terms of drug treatment. In correspondence with this data, RPFs contribute to germination of *Streptomyces* spores, which can also be considered to be in a state of dormancy (Sexton *et al.*, 2015). RpfA and another muramidase, SCO5466, are controlled by the cAMP-receptor regulon (Piette *et al.*, 2005). In *Streptomyces*, cAMP accumulates during germination and binds to the cAMP-receptor, an important transcriptional regulator (Susstrunk *et al.*, 1998). Mutants lacking the cAMP receptor protein CRP have a much thicker spore wall, suggesting that control mechanisms for spore wall synthesis are impaired (Piette *et al.*, 2005). As a result, it takes much longer for spores to germinate. The germination defect of the *crp* null mutant is explained by the hydrolases encompassed by the *crp*-regulon, among which SCO5466 and RpfA (Piette *et al.*, 2005).

Cell wall biosynthesis and hydrolysis are two inseparable processes, as suggested by the 'make before break' model, first suggested by Koch and Holtje (Höltje, 1993, Koch, 1990). This model, also called the 3-for-1 model, proposes that trimers replace monomers, suggested that after a connection is made, old cell wall material has to be hydrolyzed to allow for expansion of the glycan strand.

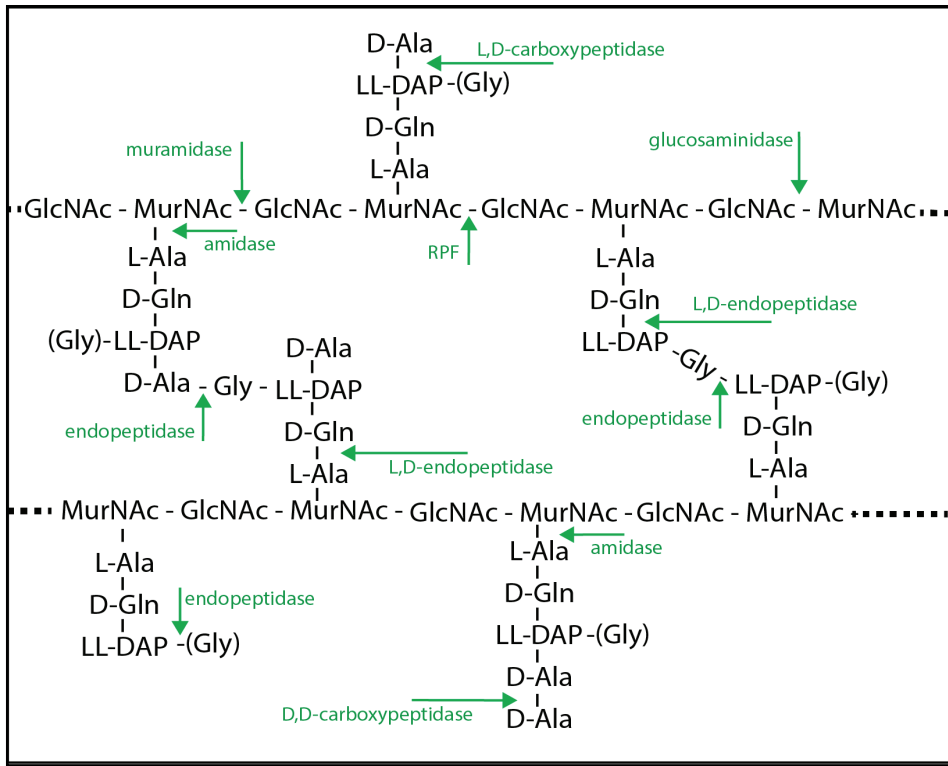


Figure 5. Hydrolysis of the *Streptomyces* peptidoglycan. The peptidoglycan structure of *S. coelicolor* is shown, with LL-DAP at position 3 and Gly which forms the cross-link between two peptide chains. N-acetylglucosaminidases (glucosaminidases) cleave between GlcNAc and MurNAc, N-acetylmuramidases (muramidases) cleave between MurNAc and GlcNAc. RPFs have a muramidase activity. N-acetylmuramyl-L-alanine amidases (amidases) hydrolyze at the site of the lactyl group between MurNAc and L-Ala. L,D-endopeptidases cleave the site between an L-, and D-amino acid in the peptide chain. D,D-, and L,D-carboxypeptidases remove C-terminal D- or L-amino acids. The acetyl group of MurNAc can be removed by a deacetylase, to generate MurN.

The bacterial cell wall and antibiotic resistance

The bacterial cell wall is a favourite target for antibiotics, as it is highly conserved between bacteria, it is conveniently located on the outside of the cell and is essential for growth and the maintenance of turgor pressure. A major advantage for clinical application is that cell wall-targeting antibiotics generally have no cytotoxicity as human cells lack peptidoglycan, and more than 50% of our clinical antibiotics target the bacterial cell wall and cell wall synthesis (Schneider & Sahl, 2010). The PG precursor Lipid II is a highly conserved structure; prior to cross-linking to the mature PG, the lipid tail is lost and can be recycled (Scheffers & Tol, 2015). Due to the essential nature of Lipid II, it is difficult for bacteria to generate resistance against cell wall and Lipid II targeting antibiotics.

In order to prevent antibiotic production from becoming a suicide mission, actinomycetes carry many antibiotic resistance genes, in addition to potential to produce antibiotics (Marshall *et al.*, 1998). Resistance mechanisms found in actinobacteria are also found in clinical isolates, suggesting that genes carrying antibiotic resistance mechanisms readily travel across the bacterial realm, driven by an increase of fitness for the recipient (Perry & Wright, 2013). Here, we focus on (self) resistance against three cell wall antibiotics, vancomycin, D-cycloserine (DCS) and penicillin, and we discuss two new cell wall antibiotics of which resistance mechanisms are still largely unknown, daptomycin and teixobactin.

Vancomycin

The glycopeptide antibiotic vancomycin targets the D-Ala-D-Ala terminus of Lipid II as it is exposed on the cell surface, this way preventing it from being incorporated into the mature peptidoglycan. Notably, vancomycin is incapable of passing the outer membrane of Gram-negative bacteria and only targets Gram-positives. Vancomycin and the related drug Balhimycin, are both produced by *Amycolatopsis orientalis* and *Amycolatopsis balhimicina*, respectively, and both these species are resistant against the glycopeptide antibiotic they produce (Marshall *et al.*, 1998, Schaberle *et al.*, 2011). Vancomycin-resistant bacteria replace the terminal D-Ala-D-Ala by D-Ala-D-Lac in order to decrease vancomycin susceptibility by a thousand-fold. Vancomycin resistance is gained by a conserved set of genes of which the most important ones are: the two-component regulatory system consisting of VanR and VanS; VanH, which converts pyruvate into D-Lac; VanA, a D-Ala-D-Lac ligase; VanX, a dipeptidase which cleaves D-Ala-D-Ala and VanY, a carboxypeptidase which cleaves D-Ala from a pentapeptide precursor (Hong *et al.*, 2004, Arthur *et al.*, 1994). These vancomycin resistance genes occur in the producing bacteria and in clinical isolated of *Enterococcus*, posing a large problem for the medical healthcare (Decousser *et al.*, 2003, Courvalin, 2006).

D-cycloserine

D-cycloserine (DCS) is a cyclic analogue of D-Ala produced by *Streptomyces lavendulae* (Noda *et al.*, 2004a). This antibiotic binds to proteins which would otherwise bind to D-Ala, such as Alr and Ddl, and this way prevents the formation of a functional peptidoglycan layer. In order for the producing bacteria to become resistant against the antibiotic it produces, it has modified both Alr and Ddl to decrease affinity to DCS (Noda *et al.*, 2004b). This modification is different from the resistance mechanism in *Mycobacteria*, which heavily upregulates Alr in order to gain resistance (Caceres *et al.*, 1997).

Penicillin

Penicillin structurally resembles the D-Ala-D-Ala terminus of Lipid II, the recognition site of PBPs, and in this way functions as a suicide substrate for PBP's (Park & Strominger, 1957). As a general rule, penicillin resistance is not gained by changing the function of PBPs, but by producing β -lactamases, which readily break down β -lactam antibiotics like penicillins and cephalosporins (Ogawara *et al.*, 1999). The life of β -lactam antibiotics in the clinic has been extended by the discovery of clavulanic acid, produced by *Streptomyces clavuligerus* (Reading & Cole, 1977). However, PBPs are not the only proteins with GT and TP activity. It has recently been demonstrated that RodA is a penicillin-insensitive glycosyltransferase, of which the overexpression can relieve the absence of Class A PBPs (Emami *et al.*, 2017, Meeske *et al.*, 2016). While PBPs are the major TPs for laterally expanding bacteria, polar growing bacteria rely on LDTs for 30-70% of the cross-links (Lavollay *et al.*, 2008). LDTs in *Streptomyces* recognize the terminus of a tetrapeptide, consisting of LL-DAP and D-Ala, and are insensitive to Penicillin. Structural studies of LDTs have shown that carbapenem antibiotics, originally developed for Gram-negative infections, readily targets LDTs and stay functional in combination with β -lactamase activity (Iannazzo *et al.*, 2016). Potentially, carbapenems could be optimized to target only LDTs, this way producing an antibiotic which specifically targets mycobacteria. It remains open for discussion whether LDTs are developed to support tip growth, or to support antibiotic resistance (Mainardi *et al.*, 2008).

Teixobactin

Recently, the novel cell wall antibiotic Teixobactin has been discovered that uniquely binds to two different targets in the cell wall, which strongly reduces the chance of resistance development (Ling *et al.*, 2015). Teixobactin is a Lipid II targeting antibiotic isolated from a Gram-negative soil bacterium *Efleveria terrae*, which binds to the pyrophosphate-sugar moiety of undecaprenyl-bound cell wall precursors Lipid II and Lipid III. Lipid III is a precursor for teichoic acids, and this dual activity against PG and teichoic acid synthesis, combined with the fact that it does not bind to mature murein, makes this an especially interesting antibiotic (Homma *et al.*, 2016). Teixobactin is active against several Gram-positive bacteria including mycobacteria and staphylococci. Initial studies by the author showed no sign of development of resistance mechanisms by serial passaging of *S. aureus* with the compound, and the mechanism of self-resistance mechanism in the producing strain is also unknown. It is worth noting that vancomycin resistance in *Staphylococci* was also considered negligible during initial studies on vancomycin resistance in 1981 (Griffith, 1981). Vancomycin resistant enterococci were isolated from clinical infections in 1988 (Leclercq *et al.*, 1988).

Daptomycin

Daptomycin is a membrane-targeting lipopeptide antibiotic with activity against Gram-positive bacteria and is clinically important to ward multidrug resistant infections, especially methicillin resistant *Staphylococcus aureus* (MRSA) and vancomycin resistant enterococci (VRE). Daptomycin is produced by *Streptomyces roseosporus*, and like for teixobactin, the self-resistance mechanism is yet unknown (McHenney *et al.*, 1998). Daptomycin functions by depolarizing the lipid membrane (Taylor & Palmer, 2016). Resistance against daptomycin is unusual in clinical settings, but is thought to relate to the charge or fluidity of the lipid membrane, or an

increase in the amount of teichoic acids, which prevent daptomycin from accessing the cell membrane (Gomez Casanova *et al.*, 2017).

Bacteria have been producing antibiotics for half a billion years, and resistance mechanisms co-evolved. This is emphasized by a recent expedition to a cave in Mexico, which had been sealed for 4 million years. Researchers had sampled the microbial community in this cave and encountered bacteria which showed resistance against many different clinical antibiotics, of which some species showed resistance against 14 antibiotics in total (Bhullar *et al.*, 2012). As we isolate many more different species of bacteria and collect more full genome sequences every day, we expect to find novel antibiotics and also resistance mechanisms in for example rare actinobacteria. Antibiotic resistance research will continue to show us amazing features of bacterial versatility.

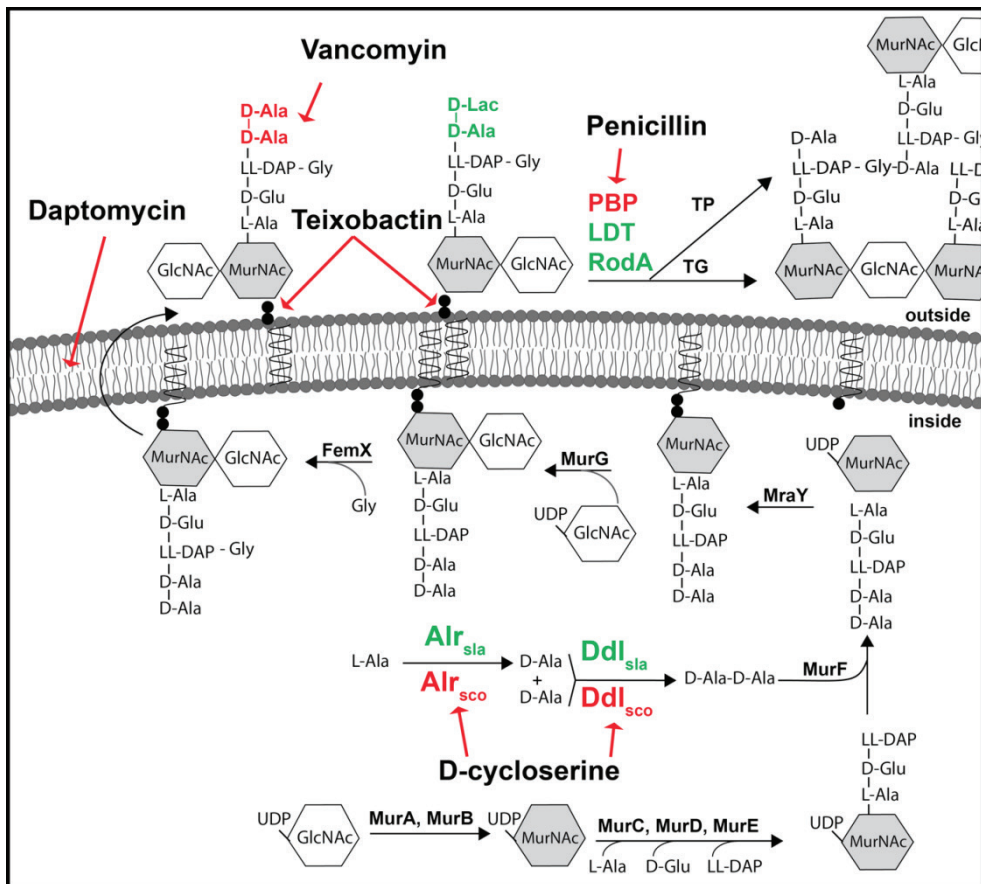


Figure 6. Summary of cell wall antibiotics and their targets. Vancomycin targets the D-Ala-D-Ala terminus of Lipid II. Vancomycin resistant strains mostly replace the terminal D-Ala by D-Lac to relieve vancomycin sensitivity. Penicillin targets PBPs, sensitivity can partially be decreased by upregulation of LDTs and RodA. D-cycloserine targets proteins with a D-Ala binding site, Alr and Ddl. Daptomycin functions by destabilizing the plasma membrane. Teixobactin targets the pyrophosphate-sugar moiety of Lipid II, both vancomycin resistant and vancomycin sensitive.

Outline of the thesis

Streptomycetes are especially interesting bacteria due to their complex morphology and production of secondary metabolites, which has led to the isolation and characterization of more than 600 type strains. Chapter 2 discusses the characterization and taxonomic classification of the novel species *Streptomyces roseofaciens*. This species of *Streptomyces* has an unusual mode of growth, producing spores perpendicular to the aerial mycelia instead of septating the aerial hyphae into long spore chains. The phenotype could be correlated to a different household of SsgA-like proteins, a set of actinobacteria-specific proteins which regulate growth and sporulation.

The complexity of the *Streptomyces* life cycle is astonishing and the consequences for cell wall synthesis are yet unclear. In Chapter 3, the peptidoglycan layer of *S. coelicolor* is analyzed over the course of growth and development. Spores were isolated separately from vegetative mycelium, so as to look for specific changes which could hint towards a germination mechanism. A high-resolution peptidoglycan analysis of *Streptomyces coelicolor* was performed by LC-MS, allowing for easy identification of all muropeptides despite potentially overlapping retention times. The analysis shows that the peptidoglycan is continuously modified and heavily broken down during PCD. An analysis of developmental mutants, $\Delta bldD$ which only produces vegetative mycelium and $\Delta whiG$ which only produces aerial hyphae, emphasizes the function of a muropeptide which was specifically abundant in spores.

Streptomyces and *Kitasatospora* are sister genera within the *Streptomycetaceae*. The genera are morphologically very similar, but can be readily distinguished based on their peptidoglycan composition. The stereoisomers of DAP, LL-DAP and MESO-DAP are a key diagnostic feature in the phylogeny of Actinobacteria, and while members of the genus *Streptomyces* carry LL-DAP, *Kitasatosporae* carry MESO-DAP in vegetative mycelia and LL-DAP in their spore walls. Chapter 4 shows an in-depth peptidoglycan analysis of two species of *Kitasatospora*, *K. setae* and *K. viridifaciens*, to lay a connection between taxonomy and cell wall homeostasis.

Antibiotic resistance is part and parcel of the ability of bacteria to produce antibacterial compounds. *S. coelicolor* carries inducible resistance genes that mediate target resistance against vancomycin, an antibiotic produced by another species of actinomycetes. When vancomycin production is initiated, the molecule is sensed by the producer strain, and resistance is switched on. That results in the production of an altered version of Lipid II with D-Ala-D-Lac as a terminus, resulting in a resistant cell wall, contrary to when the wild-type molecule with a D-Ala-D-Ala terminus is built in. In Chapter 5, we investigated whether vancomycin resistance can be counteracted via metabolic interference with exogenous D-Ala. The experiments revealed a possible novel approach by sensitizing cells with D-Ala in the presence of a VanX inhibitor. Indeed, *vanX* null mutants had a thousand-fold lower MIC against vancomycin in the presence of D-Ala than with L-Ala.

D-amino acids are an essential part of the peptidoglycan, and the D-Ala-D-Ala terminus is a universal part of bacterial peptidoglycan, with the exception being vancomycin resistant bacteria. In Chapter 6 we biochemically and structurally characterized the alanine racemase of *S. coelicolor*. The data in this chapter show that the lack of Alr makes a strain dependent on D-Ala for growth. The crystal structure of the enzyme was resolved at a 2.8 Å resolution, and compared to other Alr enzymes, including that of a strain that is resistant to the Alr-targeting antibiotic D-cycloserine.

The implications of the work for *Streptomyces* biology are discussed in Chapter 7.

CHAPTER 2

Polyphasic classification of the gifted natural product producer *Streptomyces roseifaciens* sp. nov.

Lizah T. van der Aart, Imen Nouioui, Alexander Kloosterman, José Mariano Ingal, Joost Willemse, Michael Goodfellow, Gilles P. van Wezel.

Chapter published as:

International Journal of Systematic and Evolutionary Microbiology (2019)
doi: 10.1099/ijsem.0.003215.

ABSTRACT

A polyphasic study was designed to establish the taxonomic status of a *Streptomyces* strain isolated from soil from the QinLing Mountains, Shaanxi Province, China, and found to be the source of known and new specialized metabolites. Strain MBT76^T was found to have chemotaxonomic, cultural and morphological properties consistent with its classification in the genus *Streptomyces*. The strain formed a distinct branch in the *Streptomyces* 16S rRNA gene tree and was closely related to the type strains of *Streptomyces hiroshimensis* and *Streptomyces mobaraerensis*. Multi-locus sequence analyses based on five conserved house-keeping gene alleles showed that strain MBT76^T is closely related to the type strain of *S. hiroshimensis*, as was the case in analysis of a family of conserved proteins. The organism was also distinguished from *S. hiroshimensis* using cultural and phenotypic features. Average Nucleotide Identity and digital DNA-DNA hybridization values between the genomes of strain MBT76^T and *S. hiroshimensis* DSM 40037^T were 88.96 and 28.4±2.3%, respectively, which is in line with their assignment to different species. On the basis of this wealth of data it is proposed that strain MBT76^T (=DSM 106196^T = NCCB 100637^T), be classified as a new species, *Streptomyces roseifaciens* sp.nov.

Strain MBT76^T is an actinomycete isolated from a soil sample taken from the QinLing mountains in China. Many actinobacteria isolated from this niche turned out to be rich sources of bioactive compounds effective against multi-drug resistant bacterial pathogens (Zhu *et al.*, 2014b). Based on its genome sequence, MBT76 was positioned within the genus *Streptomyces* (Wu *et al.*, 2016). *Streptomyces* sp. MBT76^T is a gifted strain that produces various novel antibiotics and siderophores (Gubbens *et al.*, 2017, Wu *et al.*, 2017a, Wu *et al.*, 2017b, Wu *et al.*, 2016), its genome contains at least 44 biosynthetic gene clusters (BGCs) for specialized metabolites as identified by antiSMASH (Blin *et al.*, 2017). The importance of validly naming novel industrially important streptomycetes is often overlooked despite improvements in the classification of the genus *Streptomyces* (Kämpfer, 2012, Labeda *et al.*, 2017, Labeda *et al.*, 2012) and adherence to the rules embodied in the International Code of Nomenclature of Prokaryotes (Parker *et al.*, 2015).

Actinobacteria are Gram-positive often filamentous bacteria that are a major source of bioactive natural products (Hopwood, 2007, Barka *et al.*, 2016). The genus *Streptomyces*, the type genus of the family *Streptomycetaceae* within the actinobacteria (Waksman & Henrici, 1943), encompasses over 700 species with valid names (<http://www.bacterio.net/streptomyces.html>), many of which have been assigned to multi- and single-membered clades in *Streptomyces* 16S rRNA gene trees (Labeda *et al.*, 2012, Kämpfer, 2012). Despite being the largest genus in the domain *Bacteria*, a steady stream of new *Streptomyces* species are being proposed based on combinations of genotypic and phenotypic features (Kumar & Goodfellow, 2010, Goodfellow *et al.*, 2017). It is particularly interesting that multi-locus sequence analyses (MLSA) of conserved house-keeping genes are providing much sharper resolution of relationships between closely related *Streptomyces* species than corresponding 16S rRNA gene sequence studies (Labeda *et al.*, 2017, Rong & Huang, 2014). Labeda and his colleagues observed correlations between certain morphological traits of streptomycetes and phylogenetic relationships based on MLSA data, as exemplified by the clustering of whorl-forming (verticillate) species (formerly *Streptoverticillium*) into a single well supported clade. Similarly, the sequences of highly conserved proteins (SALPS) have been used to resolve relationships between morphologically complex actinobacteria, including streptomycetes and closely related taxa classified in the family *Streptomycetaceae* (Girard *et al.*, 2013, Traag & van Wezel, 2008).

The aim of the present study was to establish the taxonomic status of *Streptomyces* sp. MBT76^T using a polyphasic approach. The resultant data show that the strain forms the nucleus of a novel verticillate *Streptomyces* species for which we propose the name *Streptomyces roseifaciens* sp.nov.

Streptomyces sp. MBT76^T was isolated from a soil sample (depth 10-20 cm), collected from Shandi Village in the QinLing mountains, Shaanxi Province, China (34°03'28.1"N, 109°22'39.0"E) at an altitude of 660 m (Zhu *et al.*, 2014b). The soil sample (1 g) was enriched with 6% yeast extract broth (Hayakawa & Nomomura, 1989) and incubated at 37°C for 2 h in a shaking incubator. 0.1 mL aliquots of 10⁻² to 10⁻⁴ dilutions of the resultant preparations were spread over selective agar plates (Zhu *et al.*, 2014b) supplemented with nystatin (50 µg/ml) and nalidixic acid (10 mg/ml), that were incubated at 30°C for 4 days. The colony of the test strain was subcultured onto Soy Flour Mannitol agar (SFM) (Kieser *et al.*, 2000). The isolate and *Streptomyces hiroshimensis* DSM 40037^T were maintained on yeast extract-malt extract agar slopes (International *Streptomyces* Project medium [ISP 2]

(Shirling & Gottlieb, 1966)) at room temperature and as suspensions of spores and hyphae in 20%, v/v glycerol at -20°C and -80°C. Biomass for the chemotaxonomic and molecular systematic studies was cultured in shake flasks (180 rpm) of ISP 2 broth after incubation at 30°C for 2 days and washed with distilled water, cells for the detection of the chemical markers were freeze-dried and then stored at room temperature.

The test strain was examined for chemotaxonomic and morphological properties known to be of value in *Streptomyces* systematics (Kämpfer, 2012, Goodfellow *et al.*, 2017). Spore chain arrangement and spore surface ornamentation were determined following growth on oatmeal agar (ISP 3 (Shirling & Gottlieb, 1966)) for 14 days at 28°C, by scanning electron microscopy on a JEOL JSM-7600F instrument (Piette *et al.*, 2005). Key chemotaxonomic markers were sought using standard chromatographic procedures; the strain was examined for isomers of diaminopimelic acid (A₂pm) (Hasegawa *et al.*, 1983), menaquinones and polar lipids (Collins *et al.*, 1985) and whole-organism sugars (Hasegawa *et al.*, 1983). In turn, cellular fatty acids were extracted, methylated and analysed by gas-chromatography (Hewlett Packard, model 6890) using the Sherlock Microbial Identification System (Sasser, 1990) and the ACTINO version 6 database.

Strain MBT76^T was found to have chemotaxonomical and morphological properties consistent with its classification in the genus *Streptomyces* (Kämpfer, 2012). The organism formed branched substrate hyphae that carried filaments bearing short chains of oval to cylindrical, smooth-surfaced spores arranged in verticils (Fig. 1).

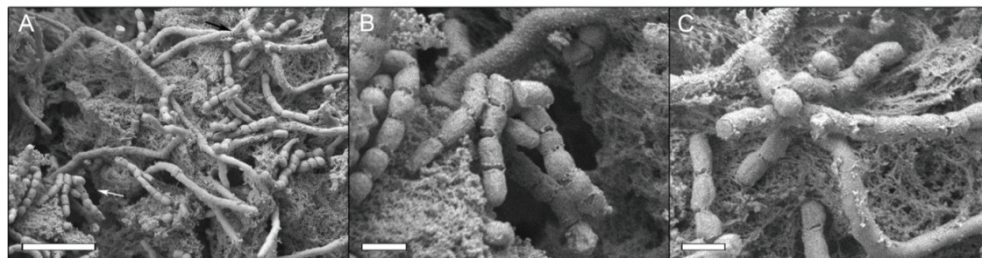


Figure 1. Scanning electron micrograph from a 14-day old culture of *Streptomyces* MBT76^T grown on an ISP-3 agar plate showing the presence of smooth, round to cylindrical verticillate spores. A shows a full overview, the white and black arrows refer to the respective magnifications B and C. Scale bars 1 μM.

Whole-organism hydrolysate of the strain was rich in *LL*-diaminopimelic acid, glucose, mannose and ribose, the isoprenologues were composed of octahydrogenated menaquinone with nine isoprene units (MK-9[H8]) (47%) and lesser amounts of MK-9[H6] (8%) and MK-9[H4] (3%). The polar lipid pattern consisted of diphosphatidylglycerol, glycerophospholipid, phosphatidylethanolamine, phosphatidylinositol, and an unknown compound, as shown in Fig. S1. The cellular fatty acids of the organism contained major proportions (>10%) of *anteiso*-C_{15:0} (34.40%), and *anteiso*-C_{17:0} (10.92%), lower proportions (i.e. <10%) of *iso*-C_{14:0} (8.28%), *iso*-C_{15:0} (5.11%), *iso*-C_{16:0} (7.99%), *anteiso*-C_{16:0} (2.54%), C_{16:1} ω9 (2.84%), C_{16:0} (5.64%), C_{18:1} ω9 (8.93%), C_{20:11} ω11 (4.53%) and summed features C_{18:2} ω9,12/C_{18:0} (8.81%).

A 16S rRNA gene sequence (1,416 nucleotides [nt]) taken from the genome

sequence of *Streptomyces* sp. MBT76^T (Genbank accession number: LNBE00000000.1) was compared with corresponding sequences of the type strains of closely related *Streptomyces* species using the Eztaxon server (Yoon *et al.*, 2017a). The resultant sequences were aligned using CLUSTALW version 1.8 (Thompson *et al.*, 1994) and phylogenetic trees generated using the maximum-likelihood (Felsenstein, 1981), maximum-parsimony (Fitch, 1971) and neighbour-joining (Saitou & Nei, 1987) algorithms taken from MEGA 7 software package (Tamura *et al.*, 2011, Guindon & Gascuel, 2003, Kumar *et al.*, 2016); an evolutionary distance matrix for the neighbour-joining analysis was prepared using the model of Jukes and Cantor (1969) (Jukes & Cantor, 1969). The topologies of the inferred evolutionary trees were evaluated by bootstrap analyses (Felsenstein, 1985) based on 1,000 repeats. The root positions of unrooted trees were estimated using the sequence of *Kitasatospora setae* KM 6054^T (Genbank accession number: AP010968) .

Streptomyces sp. MBT76^T formed a distinct phyletic line in the *Streptomyces* 16S rRNA gene tree (Fig. 2; see also Fig. S2-S3). It was found to be most closely related to the type strains of *Streptomyces hirosimensis* (Witt & Stackebrandt, 1990, Shinobu, 1955), *Streptomyces mobaraensis* (Witt & Stackebrandt, 1990, Nagatsu & Suzuki, 1963) and *Streptomyces cinnamoneus* (Witt & Stackebrandt, 1990, Benedict *et al.*, 1952) sharing 16S rRNA gene sequence similarities with them of 99.37% (9 nt differences), (99.24%) (= 11 nt differences) and 99.17% (=12 nt differences), respectively. The corresponding 16S rRNA gene sequence similarities with the remaining strains fell within the range 98.13 to 99.10%. The test strain was also found to form a distinct phyletic line in the analysis based on the maximum-parsimony and neighbour-joining algorithms.

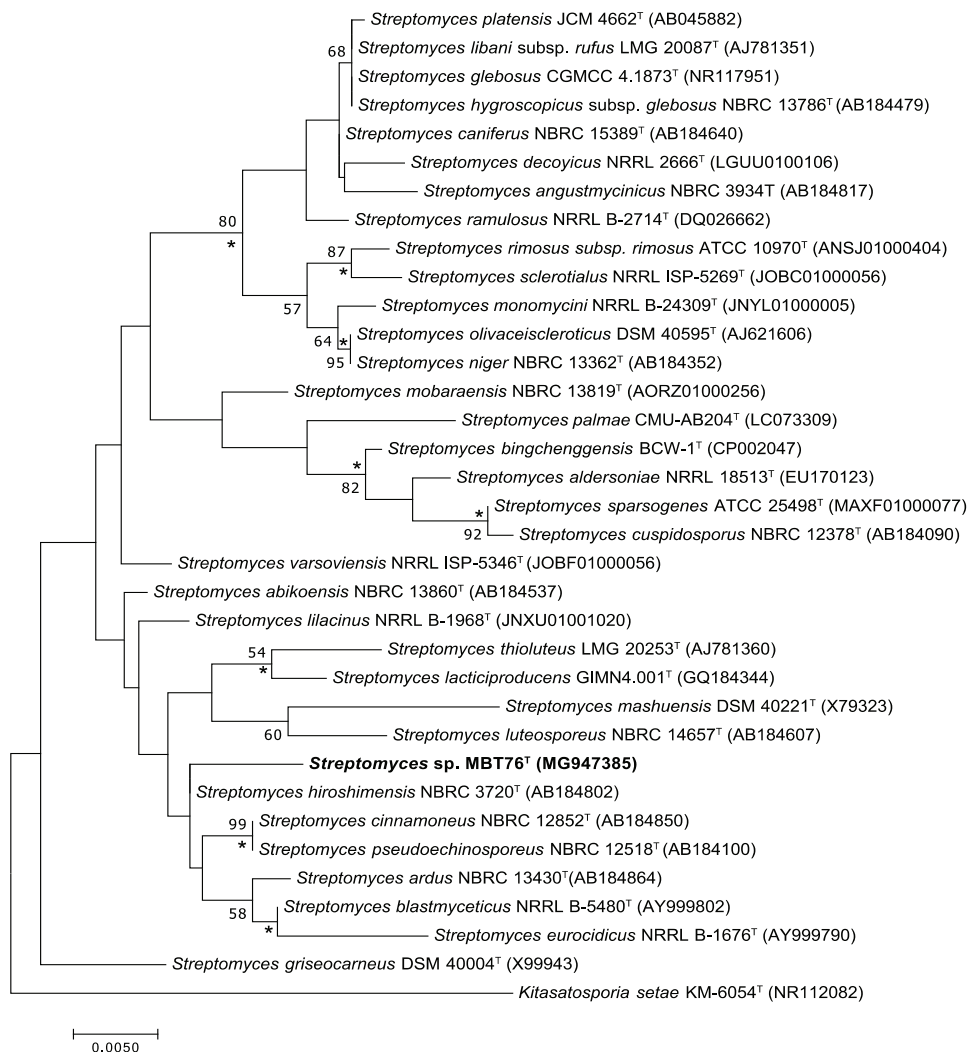


Figure 2. Maximum-likelihood phylogenetic tree based on 16S rRNA gene sequences, showing relationships between isolate MBT76^T and the type strains of closely related *Streptomyces* species. Asterisks indicate branches of the tree that were also recovered using the neighbour-joining and maximum-parsimony tree-making algorithms. Numbers at the nodes indicate levels of bootstrap based on an analysis of 1,000 sampled datasets, only values above 50% are given. The root position of the tree was determined using *Kitasatospora setae* KM-6054^T. GenBank accession numbers are given in parentheses. Scale bar, 0.005 substitutions per nucleotide position.

The partial sequences of five house-keeping genes: *atpD* (encoding ATP synthase F1, β -subunit), *gyrB* (for DNA gyrase B subunit), *recA* (for recombinase A), *rpoB* (for RNA polymerase β -subunit) and *trpB* (for tryptophan synthase, β -subunit) were drawn from the full genome sequence of strain MBT76^T and from corresponding sequences on the *Streptomyces* type strains used to generate the 16S rRNA gene tree (Fig. 3; sequences presented in Table S1). The multilocus sequence analysis was based on the procedure described by Labeda (Labeda, 2011), the sequences of the protein loci of the strains were concatenated head-to-tail and exported in FASTA format, yielding a dataset of 33 strains and 2351 positions. The sequences were inferred using MUSCLE (Edgar, 2004) and phylogenetic relationships defined using the maximum-likelihood algorithm from MEGA 7 software (Tamura *et al.*, 2011, Kumar *et al.*, 2016) based on the General Time Reversible model (Nei & Kumar, 2000). The topology of the inferred tree was evaluated in a bootstrap analysis as described above. Phylogenetic trees were also generated using the maximum-parsimony (Fitch, 1971) and neighbour-joining (Saitou & Nei, 1987) algorithms. Pairwise distances between the sequences of each locus were established using the two parameter model (Kimura, 1980). Strain pairs showing MLSA evolutionary distances <0.007 were taken to be conspecific as determined by Rong and Huang (Rong & Huang, 2012) validating the MLSA scheme for systematics of the whole genus, a value that corresponds to the 70% DNA-DNA threshold recommended for the discrimination of prokaryotic species (Wayne *et al.*, 1987).

MLSA have clarified relationships between closely related streptomycetes, thereby reflecting the strong phylogenetic signal provided by partial sequences of single copy house-keeping genes (Labeda, 2011, Labeda *et al.*, 2017, Labeda *et al.*, 2012, Rong & Huang, 2012). In the present study all of the verticillate-forming streptomycetes fell into a single clade that is sharply separated from associated clades composed of strains that form spores in straight, looped or spiral chains (Fig. 3). Strain MBT76^T and the type strain of *S. hiroshimensis* were found to form a distinct phyletic line supported by all of the tree-making algorithms and a 100% bootstrap value. It can also be seen from Figure 3 that these strains are at the periphery of a well-supported branch composed of an additional eight *Streptomyces* type strains that produce verticillate spore chains. The discovery that the strain can be separated from its closest phylogenetic neighbours by MLSA distances well above 0.007 threshold (Table 1) indicates that it forms a distinct phyletic line within the evolutionary radiation of the genus *Streptomyces* (Rong & Huang, 2014). The results of this study underpin those presented by Labeda *et al.* (Labeda *et al.*, 2017) by showing that streptomycetes which produce verticillate spore chains form a recognizable group in the *Streptomyces* gene tree that can be equated with the genus "*Streptoverticillium*" (Baldacci & Locci, 1974, Baldacci *et al.*, 1966).

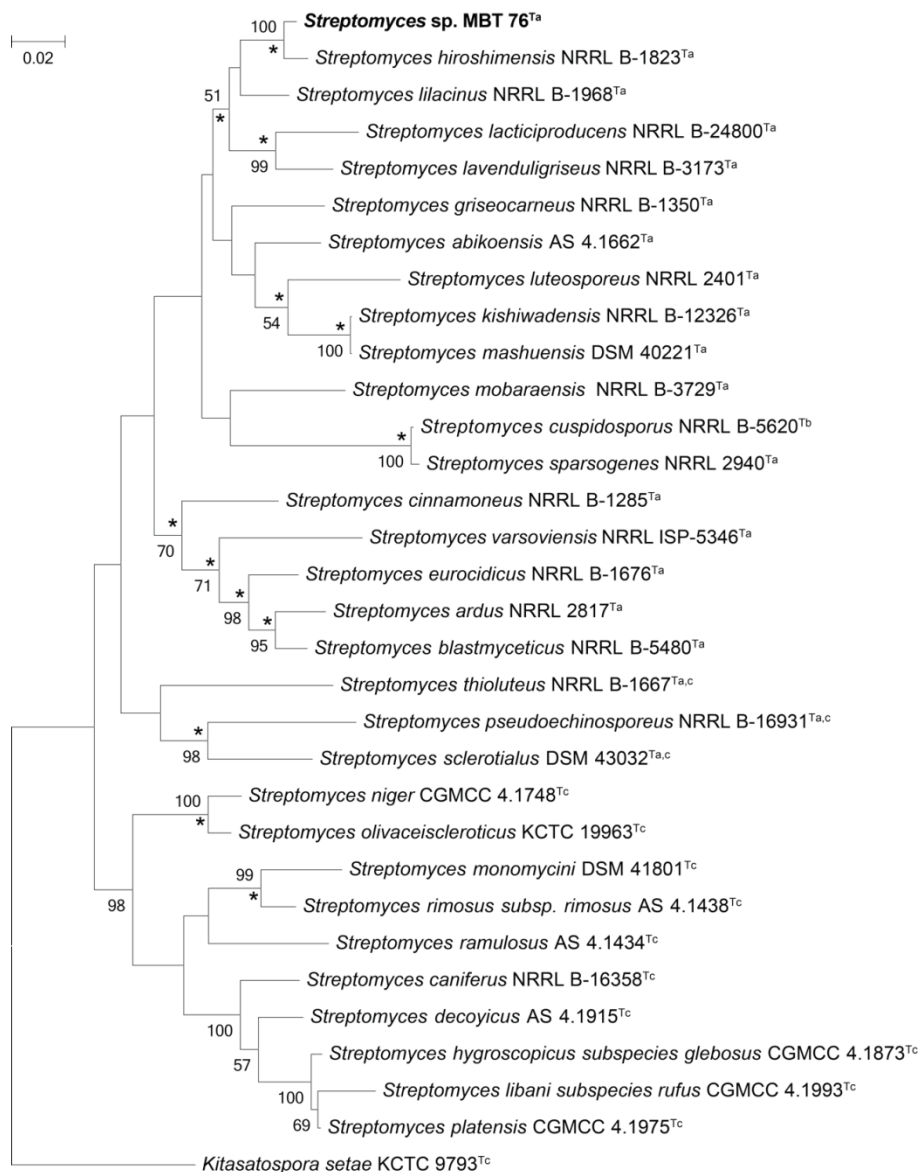


Figure 3. Phylogenetic tree inferred from concatenated partial sequences of house-keeping genes *atpD*, *gyrB*, *recA*, *rpoB* and *trpB* using the maximum-likelihood algorithm, based on the general time reversible model. The final dataset consisted of 2351 positions and 33 strains. Asterisks indicate branches of the tree that were recovered using the maximum-parsimony and neighbor-joining algorithms. Percentages at the nodes represent levels of bootstrap support from 1,000 resampled datasets with values with less than 60% not shown. *Streptomyces* morphology: ^a: verticillate spore chains. ^b: not determined ^c: *Streptomyces* with canonical (apical) spore chains.

Table 1. MLSA distances between strain MBT76^T and the type strains of closely related *Streptomyces* species.

	Strain	MLSA (Kimura 2-parameter) distance											
		1	2	3	4	5	6	7	8	9	10	11	12
1	Strain MBT76 ^T	-											
2	<i>S. abikoensis</i> AS 4.1662 ^T	0.056											
3	<i>S. cuspidosporus</i> NRRL B-5620 ^T	0.097	0.128	0.117									
4	<i>S. griseocarneus</i> NRRL B-1350 ^T	0.059	0.121	0.067	0.075								
5	<i>S. hiroshimensis</i> NRRL B-1823 ^T	0.014	0.114	0.084	0.070	0.063							
6	<i>S. kishiwadensis</i> NRRL B-12326 ^T	0.062	0.106	0.093	0.080	0.068	0.107						
7	<i>S. lacticiproducens</i> NRRL B-24800 ^T	0.065	0.106	0.089	0.090	0.083	0.112	0.078					
8	<i>S. lavenduligriseus</i> NRRL B-3173 ^T	0.055	0.115	0.090	0.086	0.079	0.117	0.077	0.052				
9	<i>S. lilacinus</i> NRRL B-1968 ^T	0.038	0.109	0.075	0.081	0.054	0.115	0.060	0.066	0.109			
10	<i>S. luteosporus</i> NRRL 2401 ^T	0.079	0.106	0.080	0.084	0.092	0.104	0.066	0.088	0.117	0.074		
11	<i>S. mashuensis</i> DSM 40221 ^T	0.062	0.106	0.093	0.081	0.069	0.107	0.001	0.078	0.104	0.060		
12	<i>S. sparsogenes</i> NRRL 2940 ^T	0.100	0.130	0.119	0.123	0.112	0.133	0.102	0.108	0.122	0.097	0.102	

The SsgA-like proteins (SALPs) have recently been proposed as phylogenetic markers for the accurate classification of Actinobacteria (Girard *et al.*, 2013). Members of the SALP protein family are typically between 130 and 145 amino acids (aa) long, and are unique to morphologically complex actinobacteria (Traag & van Wezel, 2008); they coordinate cell division and spore maturation (Noens *et al.*, 2005, Willemse *et al.*, 2011). SsgB shows extremely high conservation within a genus, while there is high diversity even between closely related genera (Girard *et al.*, 2013). Genes encoding SALPs were drawn from the genomes of strains MBT76^T, *S. cinnamoneus* (NZ_MOEP01000440.1), *S. mobaraensis* (NZ_AORZ01000001.1) and *S. hiroshimensis* (NZ_JOFL01000001.1) and from those of non-verticillate reference organisms, namely “*Streptomyces coelicolor*” A3(2) (NC_003888.3), *S. griseus* subspecies *griseus* NBBC 13350^T (NC_010572.1) and “*Streptomyces lividans*” TK24 (NZ_GG657756.1). A second BLAST search was undertaken based on a low cut-off value (e-value 10⁻⁵) to interrogate the genome sequence of “*S. coelicolor*” M145 (NC_003888.3) to verify that the initial hits were *bona fide* SALPs. Sequences showing their best reciprocal hits against SALPs were aligned using MUSCLE (Edgar, 2004) and trees generated using the maximum-likelihood algorithm with default parameters as implemented in MEGA 7 software (Tamura *et al.*, 2011), the robustness of the resultant trees was checked in bootstrap analyses (Felsenstein, 1985) based on 1000 replicates.

The maximum-likelihood tree (Fig. 4) shows that all of the strains have genes that encode for the cell division proteins SsgA, SsgB, SsgD and SsgG (Noens *et al.*, 2005, Traag & van Wezel, 2008). It is also evident that the SsgB-protein, which mediates sporulation-specific division in *Streptomyces* strains (Willemse *et al.*, 2011) encodes for identical proteins in both the verticillate and reference strains. The sequences of the SALP proteins, SsgA and SsgG, underpin the close relationship between the test strain and *S. hirosheimensis* and separate them from the type strains of *S. cinnamomeus* and *S. mobaerensis*. It is particularly interesting that the verticillate strains lack an orthologue of SsgE, which is fully conserved in non-verticillate streptomycetes. SsgE proteins are considered to have a role in morphogenesis and the length of spore chains in "*S. coelicolor*" (Noens *et al.*, 2005). Further comparative studies are needed to determine whether the absence of SsgE in the genomes of verticillate streptomycetes is correlated to their different mode of sporulation.

Strain MBT76^T and *S. hirosheimensis* DSM 40037^T were examined for cultural and phenotypic properties known to be of value in the systematics of the genus *Streptomyces* (Williams *et al.*, 1983, Goodfellow *et al.*, 2017). The cultural properties were recorded from tryptone-yeast extract, yeast extract-malt extract, oatmeal, inorganic-salt starch, glycerol-asparagine, peptone- yeast extract-iron and tyrosine agar (ISP media 1-7, (Shirling & Gottlieb, 1966)) plates following incubation as 28°C for 14 days. Aerial and substrate mycelium colours and those of diffusible pigments were determined by comparison against colour charts (Kelly, 1964). The strains grew well on all of the media forming a range of pigments (Table 2). In general, strain MBT76^T produced a pink aerial spore mass, dark red substrate mycelia and pale brown diffusible pigments, black melanin pigments were formed on ISP 6 agar. In contrast, *S. hirosheimensis* formed a white aerial spore mass, cream, pink or white substrate mycelia and, when produced, a brown diffusible pigment, it also formed melanin pigments on ISP 6 agar.

The enzyme profiles for the test strain and *S. hirosheimensis* were determined using API-ZYM kits (BioMerieux) and a standard inoculum corresponding to 5 on the Mc Farland scale (Murray *et al.*, 1999) and by following the protocol provided by the manufacturer. Similarly, a range of biochemical, degradative and physiological properties were acquired using media and methods described previously (Williams *et al.*, 1983). Identical results were obtained for all of the duplicate cultures.

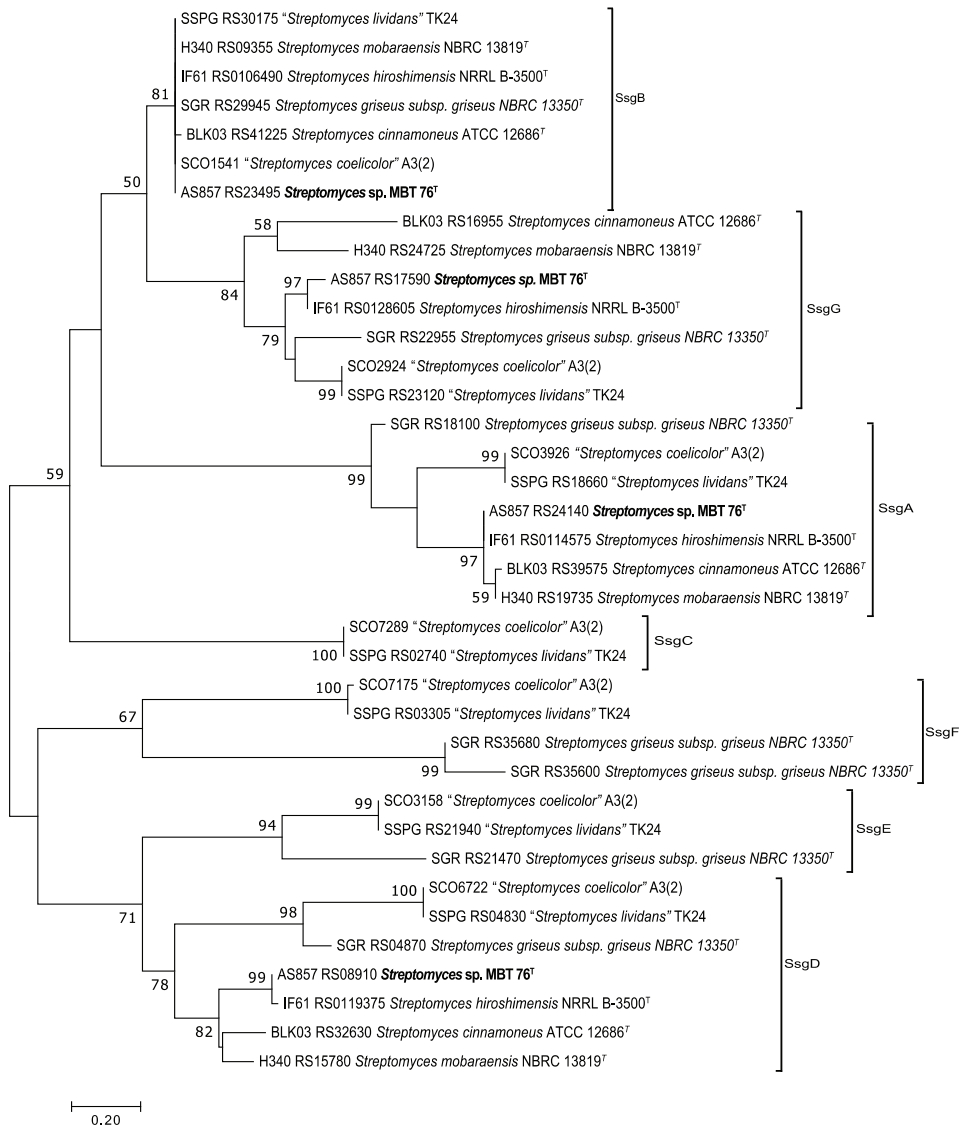


Figure 4. A composite maximum-likelihood tree showing the relationships between strain MBT76^T, the type strains of *S. cinnamoneus*, *S. hiroshimensis*, *S. mobaraensis* and reference strains "*S. coelicolor*", "*S. lividans*" and *S. griseus*, based on the sequences of SALP proteins.

The full genome sequence of strain MBT76^T (GenBank accession number GCF_001445655) was elucidated using Illumina sequencing. The sequences assembled into 18 contigs, giving a total genome size of 8.64 Mb with a G+C content of 72.1%, with an N50 of 2,514,044 and a 200x genome coverage. The genome is predicted to encode 73 RNAs and 7,598 proteins. Gene functions were distributed among different classes using the RAST annotation tool (Fig. S4) (Aziz *et al.*, 2008). A total number of 44 secondary metabolites are predicted by antiSMASH 4.2.0 (Blin *et al.*, 2017), as shown in Table S2. Several genomic metrics are now available to distinguish between orthologous genes of closely related prokaryotes, including the calculation of average nucleotide identity (ANI) and digital DNA-DNA hybridization values (Yoon *et al.*, 2017b, Meier-Kolthoff *et al.*, 2013). In the present study, ANI and dDDH values were determined from the genomes of strain MBT76^T and *S. hiroshimensis* DSM 40037^T using the ortho-ANlu algorithm from Ezbiotaxon (Yoon *et al.*, 2017b) and the genome-to-genome distance calculator (GGDC 2.0) at <http://ggdc.dsmz.de>. The dDDH value between the genomes of the two strains was 28.4% ± 2.3 %, a result well below the 70% threshold for assigning strains to the same species (Wayne *et al.*, 1987), the digital DNA G+C value recorded for strain MBT76^T was 71.9 mol%. Similarly, a low ANI value of 88.96 was found between the two organisms, a result well below the threshold used to delineate prokaryote species (Richter & Rossello-Mora, 2009, Chun & Rainey, 2014).

It can be concluded from the chemotaxonomic, cultural, morphological and phylogenetic data that strain MBT76^T belongs to the genus *Streptomyces*. It can be distinguished from the type strain, *S. hiroshimensis*, its closest phylogenetic neighbour using genotypic and phenotypic procedures, notably by low ANI and dDDH values. Consequentially, strain MBT76^T should be recognised as a new *Streptomyces* species for this we propose the name *Streptomyces roseifaciens* sp.nov.

Table 2. Growth and cultural characteristics of strain MBT76^T and *Streptomyces hiroshimensis* DSM 40037^T after incubation at 30°C for 14 days.

Strain MBT76 ^T	Growth	Aerial spore mass colour	Substrate mycelium colour	Diffusible pigment
Glycerol- asparagine agar (ISP 5)	+++	Pink	Dark red	None
Inorganic salts-starch agar (ISP 4)	+++	Pink	Pink	None
Oatmeal agar (ISP 3)	+++	Pink	Red	Pale brown
Peptone-yeast extract- iron agar (ISP-6)	++	Pink	Grey	Black
Tryptone-yeast extract agar (ISP 1)	+++	Pink	Dark red	Pale brown
Tyrosine agar (ISP 7)	+++	Grey	Dark red	Pale brown
Yeast extract-malt extract agar (ISP 2)	+++	Pink	Dark red	Pale brown
<i>S. hiroshimensis</i> DSM 40037 ^T				
Glycerol- asparagine agar (ISP 5)	+++	White	Pink	None
Inorganic salts-starch agar (ISP 4)	+++	White	White	None
Oatmeal agar (ISP 3)	+++	Pink	Pink	Brown
Peptone-yeast extract- iron agar (ISP 6)	++	None	Grey	Black
Tryptone-yeast extract agar (ISP 1)	+++	White	Cream	Brown
Tyrosine agar (ISP 7)	+++	White	Pink	None
Yeast extract-malt extract agar (ISP 2)	+++	White	Cream	Brown
+++abundant growth. ++, very good growth				

Table 3. Phenotypic properties that distinguish strain MBT76^T from *S.hiroshimensis* DSM 40037^T

Characteristics	Strain MBT76 ^T	<i>S. hiroshimensis</i> DSM 40037 ^T
Cultural characteristics on yeast extract-malt extract agar		
Aerial spore mass	Pink	White
Substrate mycelium	Dark red	Cream
Diffusible pigment	Pale brown	Brown
API ZYM tests:		
α-Chymotrypsin	+	-
β- Glucosidase	+	-
Lipase (C14)	+	-
α -Mannosidase	+	-
Trypsin	+	-
Degradation of:		
Xanthine	-	+
Growth on sole carbon source		
Sucrose	+	-
Fructose	-	+
Growth in presence of:		
3% w/v sodium chloride	-	+

Description of *Streptomyces roseifaciens* sp. nov.

Streptomyces roseifaciens (*ro.se.i.fa'ci.ens* L. *masc. adj. roseus* [*italic type*] *rosy*; L. *pres. part. faciens* [*italic type*] *producing*; N.L. *part. adj. roseifaciens* [*italc type*] *producing rosy colour*). Aerobic, Gram-stain positive actinobacterium which forms an extensively branched substrate mycelium that carries long straight filaments bearing at more or less regular intervals branches arranged in verticils. Each branch of the verticils produces at its apex short chains of 3-5 spores with smooth surfaces. Grows well on all ISP media. A red substrate mycelium, a pink aerial spore mass and a pale brown diffusible pigment are produced on oatmeal agar. Grows from 20-50°C, optimally at ~30°C, from pH 5.0 to pH 11, optimally at pH ~7, and in the presence of 2% NaCl. Produces acid and alkaline phosphatase, α -chymotrypsin, α -cysteine arylamidase, esterase (C4), esterase lipase (C8), *N*-acetyl- β -glucosaminidase, α - and β -glucosidase, α -mannosidase, naphthol-AS-B1-phosphatase, trypsin and valine arylamidase, but not α -fucosidase, α - or β -galactosidase or β -glucuronidase (API-ZYM tests). Degrades casein, gelatin, hypoxanthine, starch and L-tyrosine. Glucose, inositol and sucrose are used as sole carbon sources. Additional phenotype properties are given in Tables 1 and 2. Major fatty acids are anteiso-C_{15:0}' and anteiso-C_{17:0}', the predominant menaquinone is MK-9 (H8), the polar lipid profile contains diphosphatidylglycerol, phosphatidylethanolamine, phosphatidylinositol, glycopospholipid, and an unidentified lipid, the DNA G+C composition is 71.9 mol% and the genome size 8.64 Mbp. The genome contains 44 biosynthetic gene clusters many of which encode for unknown specialized metabolites.

The type strain MBT76^T (=NCCB 100637^T=DSM 106196^T) was isolated from a soil sample from the QinLing mountains, Shaanxi Province, China. The species description is based on a single strain and hence serves as a description of the type strain. The GenBank accession number for the assembled genome of *Streptomyces roseifaciens* is GCA_001445655.1.

Funding statement

This project was supported by an EMBO Short-Term Fellowship (6746) awarded to LvdA, and by the School of Natural and Environmental Sciences (Newcastle University). LN is grateful to Newcastle University for a postdoctoral fellowship.

Conflicts of interest

The authors declare that they have no conflict of interest.

CHAPTER 3

High-resolution analysis of the peptidoglycan composition in *Streptomyces coelicolor*

Lizah T. van der Aart, Gerwin K. Spijksma, Amy Harms, Waldemar Vollmer, Thomas Hankemeier and Gilles P. van Wezel

Chapter published as:
Journal of Bacteriology (2018) 200:e00290-18. (with Cover image)

Supplemental information available at:
<https://jb.asm.org/content/jb/suppl/2018/09/11/JB.00290-18.DCSupplemental/zjb999094886s1.pdf>

ABSTRACT

The bacterial cell wall maintains cell shape and protects against bursting by the turgor. A major constituent of the cell wall is peptidoglycan (PG), which is continuously modified to allow cell growth and differentiation through the concerted activity of biosynthetic and hydrolytic enzymes. Streptomycetes are Gram-positive bacteria with a complex multicellular life style alternating between mycelial growth and the formation of reproductive spores. This involves cell-wall remodeling at apical sites of the hyphae during cell elongation and autolytic degradation of the vegetative mycelium during the onset of development and antibiotic production. Here, we show that there are distinct differences in the cross-linking and maturation of the PG between exponentially growing vegetative hyphae and the aerial hyphae that undergo sporulation. Liquid chromatography-tandem mass spectrometry (LC-MS/MS) analysis identified over 80 different muropeptides, revealing that major PG hydrolysis takes place over the course of mycelial growth. Half of the dimers lacked one of the disaccharide units in transition-phase cells, most likely due to autolytic activity. De-acetylation of MurNAc to MurN was particularly pronounced in spores, and strongly reduced in sporulation mutants with a deletion of *blbD* or *whiG*, suggesting that MurN is developmentally regulated. Taken together, our work highlights dynamic and growth phase-dependent construction and remodeling of PG in *Streptomyces*.

IMPORTANCE

Streptomycetes are bacteria with a complex lifestyle, which are model organisms for bacterial multicellularity. From a single spore, a large multigenomic multicellular mycelium is formed, which differentiates to form spores. Programmed cell death is an important event during the onset of morphological differentiation. In this work, we provide new insights into the changes in the peptidoglycan composition and over time, highlighting changes over the course of development and between growing mycelia and spores. This revealed dynamic changes in the peptidoglycan when the mycelia aged, with extensive PG hydrolysis and, in particular, an increase in the proportion of 3-3-cross-links. Additionally, we identified a muropeptide that is highly abundant specifically in spores, which may relate to dormancy and germination.

INTRODUCTION

Peptidoglycan (PG) is a major component of the bacterial cell wall. It forms a physical boundary that maintains cell shape, protects cellular integrity against the osmotic pressure and acts as a scaffold for large protein assemblies and exopolymers (Vollmer *et al.*, 2008a). The cell wall is a highly dynamic macromolecule that is continuously constructed and deconstructed to allow for cell growth and to meet environmental demands (Kysela *et al.*, 2016). PG is built up of glycan strands of alternating *N*-acetylglucosamine (GlcNAc) and *N*-acetylmuramic acid (MurNAc) residues that are connected by short peptides to form a mesh-like polymer. PG biosynthesis starts with the synthesis of PG precursors by the Mur enzymes in the cytoplasm and cell membrane, resulting in Lipid II precursor, undecaprenylpyrophosphoryl-MurNAc(GlcNAc)-pentapeptide. Lipid II is transported across the cell membrane by MurJ and/or FtsW/SEDS proteins and the PG is polymerized and incorporated into the existing cell wall by the activities of glycosyltransferases and transpeptidases (Egan *et al.*, 2017, Leclercq *et al.*, 2017, Sham *et al.*, 2014).

The Gram-positive model bacterium *Bacillus subtilis* grows via lateral cell-wall synthesis followed by binary fission; in addition, *B. subtilis* forms heat- and desiccation-resistant spores (Popham, 2002, Keep *et al.*, 2006). In contrast, the vegetative hyphae of the mycelial *Streptomyces* grow by extension of the hyphal apex and cell division results in connected compartments separated by cross-walls (Flårdh & Buttner, 2009, Barka *et al.*, 2016, Celler *et al.*, 2016). This makes *Streptomyces* a model taxon for bacterial multicellularity (Claessen *et al.*, 2014). Multicellular vegetative growth poses different challenges to *Streptomyces*, including the synthesis of many chromosomes during vegetative growth and separation of the nucleoids in the large multi-genomic compartments during cross-wall formation (Jakimowicz & van Wezel, 2012, Wolanski *et al.*, 2011). In submerged cultures, streptomycetes typically form complex mycelial networks or pellets (van Dissel *et al.*, 2014). On surface-grown cultures, such as agar plates, these bacteria develop a so-called aerial mycelium, whereby the vegetative or substrate mycelium is used as a substrate. The aerial hyphae eventually differentiate into chains of spores, a process whereby many spores are formed almost simultaneously, requiring highly complex coordination of nucleoid segregation and condensation and multiple cell division (Jakimowicz & van Wezel, 2012, McCormick, 2009, Noens *et al.*, 2005). Streptomycetes have an unusually complex cytoskeleton, which plays a role in polar growth and cell-wall stability (Celler *et al.*, 2013, Holmes *et al.*, 2013). Mutants that are blocked in the vegetative growth phase are referred to as bald or *bld*, for lack of the fluffy aerial hyphae (Merrick, 1976), while those producing aerial hyphae but no spores are referred to as white (*whi*), as they fail to produce grey-pigmented spores (Chater, 1972)

The *Streptomyces* genome encodes a large number of cell wall-modifying enzymes, such as cell wall hydrolases (autolysins), carboxypeptidases and penicillin-binding proteins (PBPs), a complexity that suggests strong heterogeneity of the PG of these organisms (Haiser *et al.*, 2009, Peters *et al.*, 2016). Several concepts that were originally regarded as specific to eukaryotes also occur in bacteria, such as multicellularity (Lyons & Kolter, 2015, Claessen *et al.*, 2014, Shapiro, 1988), and programmed cell death (Hochman, 1997, Rice & Bayles, 2003). Programmed cell death (PCD) likely plays a major role in the onset of morphological development, required to lyse part of the vegetative mycelium to provide the nutrients for the aerial hyphae (Manteca *et al.*, 2005, Miguelez *et al.*, 1999). PCD and cell-wall recycling are

linked to antibiotic production in *Streptomyces* (Urem *et al.*, 2016).

All disaccharide peptide subunits (muropeptides) in the PG are variations on the basic building block present in Lipid II, which in *Streptomyces* typically consists of GlcNAc-MurNAc-L-Ala-D-Glu-LL-diaminopimelate(Gly)-D-Ala-D-Ala (Hugonnet *et al.*, 2014, Schleifer & Kandler, 1972). Here, we have analyzed the cell wall composition of vegetative mycelium and mature spores of *Streptomyces coelicolor* by liquid chromatography-mass spectrometry (LC-MS), to obtain a detailed inventory of the monomers and dimers in the cell wall. This revealed extensive cell wall hydrolysis and remodeling during vegetative growth and highlights the difference in cell wall composition between vegetative hyphae and spores.

MATERIAL AND METHODS

Bacterial strain and culturing conditions

Streptomyces coelicolor A3(2) M145 (Kieser et al., 2000), and its *bldD*, J774 (*cysA15 pheA1 mthB2 bldD53 NF SCP2** (Merrick, 1976) and *whiG*, J2400 (M145 *whiG::hyg* (Flårdh et al., 1999)) mutants, were obtained from the John Innes Centre strain collection. All media and methods for handling *Streptomyces* are described in the *Streptomyces* laboratory manual (Kieser et al., 2000). Spores were collected from Soy Flour Mannitol (SFM) agar plates. Liquid cultures were grown shaking at 30°C in a flask with a spring, using normal minimal medium with phosphate (NMM+) supplemented with 1% (w/v) mannitol as the sole carbon source; polyethylene glycol (PEG) was omitted to avoid interference with the MS identification. Cultures were inoculated with spores at a density of 10⁶ CFU/ML. A growth curve was constructed from dry-weight measurements by freeze-drying washed biomass obtained from 10 mL of culture broth (three biological replicates). To facilitate the harvest of mycelium from agar plates, they were grown on cellophane slips, after which the biomass was scraped of the cellophane. Spores were collected from SFM agar plates by adding 0.01% (w/v) SDS to facilitate spore release from the aerial mycelium, scraping them off with a cotton ball and drawing the solution with a syringe. Spores were filtered with a cotton filter to separate spores from residual mycelium.

PG extraction

Cells were lyophilized for a biomass measurement, 10 mg biomass was directly used for PG isolation. PG was isolated according to (Kühner *et al.*, 2014), using 2 mL screw-cap tubes for the entire isolation. Biomass was first boiled in 0.25% SDS in 0.1 M Tris/HCl pH 6.8, thoroughly washed, sonicated, treated with DNase, RNase and trypsin, inactivation of proteins by boiling and washing with water. Wall teichoic acids were removed with 1 M HCl. PG was digested with mutanolysin and lysozyme (Arbeloa *et al.*, 2004). Muropeptides were reduced with sodium borohydride and the pH was adjusted to 3.5-4.5 with phosphoric acid.

To validate the method, we compared it to the method described previously (Bui *et al.*, 2012). For this, *S. coelicolor* mycelia were grown in 1 L NMM+ media for 24 h. After washing of the mycelia, pellets were resuspended in boiling 5% (w/v) SDS and stirred vigorously for 20 min. Instead of sonicating the cells, they were disrupted using glass beads, followed by removal of the teichoic acids with an HF treatment at 4°C as described.

LC-MS analysis of monomers

The LC-MS setup consisted of a Waters Acquity UPLC system (Waters, Milford, MA, USA) and a LTQ Orbitrap XL Hybrid Ion Trap-Orbitrap Mass Spectrometer (Thermo Fisher Scientific, Waltham, MA, USA) equipped with an Ion Max electrospray source.

Chromatographic separation was performed on an Acquity UPLC HSS T3 C₁₈ column (1.8 μm, 100 Å, 2.1 × 100 mm). Mobile phase A consist of 99.9% H₂O and 0,1% Formic Acid and mobile phase B consists of 95% Acetonitrile, 4.9% H₂O and 0,1% Formic Acid. All solvents used were of LC-MS grade or better. The flow rate was set to 0.5 ml/min. The binary gradient program consisted of 1 min 98% A, 12 min from 98% A to 85% A, and 2 min from 85% A to 0% A. The column was then flushed for 3 min with 100% B, the gradient was then set to 98% A and the column was equili-

brated for 8 min. The column temperature was set to 30°C and the injection volume used was 5 μ L. The temperature of the autosampler tray was set to 8°C. Samples were run in triplicates.

MS/MS was done both on the full chromatogram by data dependent MS/MS and on specific peaks by selecting the mass of interest. Data dependent acquisition was performed on the most intense detected peaks, the activation type was Collision Induced Dissociation (CID). Selected MS/MS was performed when the resolution of a data dependent acquisition lacked decisive information. MS/MS experiments in the ion trap were carried out with relative collision energy of 35% and the trapping of product ions were carried out with a q-value of 0.25, and the product ions were analyzed in the ion trap., data was collected in the positive ESI mode with a scan range of m/z 500–3000 in high range mode. The resolution was set to 15.000 (at m/z 400).

Data analysis

Chromatograms were evaluated using the free software package MZmine (<http://mzmine.sourceforge.net/>) (Pluskal *et al.*, 2010) to detect peaks, deconvolute the data and align the peaks. Only peaks corresponding with a mass corresponding to a muropeptide were saved, other data was discarded. The online tool MetaboAnalyst (Xia *et al.*, 2015) was used to normalize the data by the sum of the total peak areas, then normalize the data by log transformation. The normalized peak areas were exported and a final table which shows peak areas as percentage of the whole was produced in Microsoft Excel.

Muropeptide identification

The basic structure of the peptidoglycan of *S. coelicolor* has been published previously (Hugonnet *et al.*, 2014). Combinations of modifications were predicted and the masses were calculated using ChemDraw Professional (PerkinElmer). When a major peak had an unexpected mass, MS/MS helped resolve the structure. MS/MS was used to identify differences in cross-linking and to confirm predicted structures.

RESULTS

To assess how growth and development translate to variations in the PG composition, we isolated the PG and analyzed the muropeptide profile of spores and of vegetative hyphae during different phases of growth in liquid-grown cultures. In submerged cultures, *S. coelicolor* does not sporulate, while it forms aerial hyphae and spores on solid media. Vegetative mycelia of *S. coelicolor* M145 were harvested from cultures grown in liquid minimal media (NMM+). Samples taken after 18 h and 24 h represented exponential growth, while samples taken after 36 h and 48 h represented mycelia in transition phase (Figure 1A,B). Samples from solid-grown cultures were taken at 24 h to represent vegetative growth, 48 h, representing growth of aerial hyphae and 72 h, when the strain has formed spores (Figure 1C). Spores were harvested from SFM agar plates and filtered to exclude mycelia fragments.

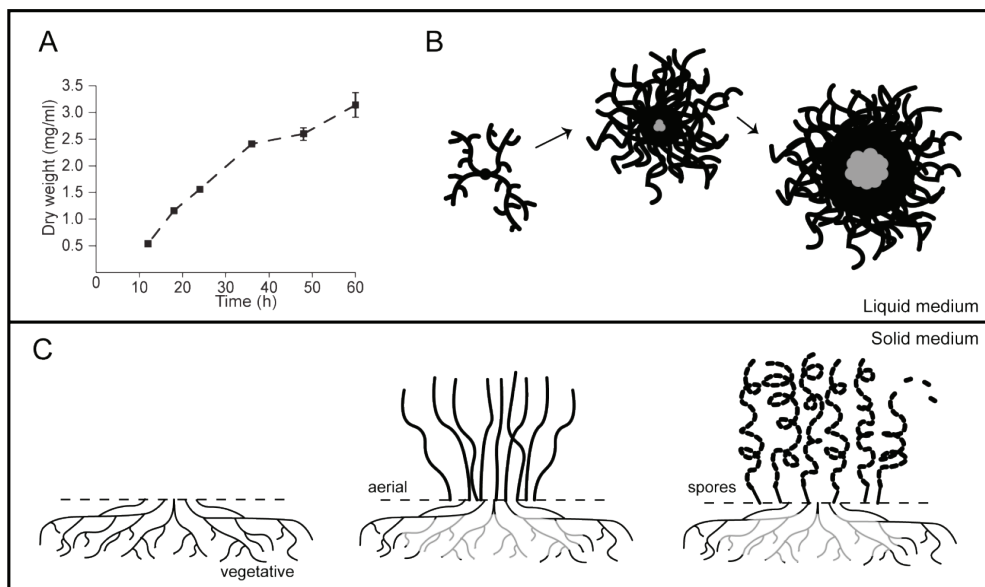


Figure 1. Growth of *S. coelicolor* in liquid and solid medium. (A) Growth curve on NMM+ medium based on triplicate dry weight measurements. (B) Pellet morphology in liquid medium. After spore germination, hyphae emerge through top growth and branching that form an intricate network or pellet. The center of the pellets eventually lyses due to PCD (gray). (C) Growth on solid medium, starting with development of vegetative mycelium, after which aerial hyphae grows into the air, coinciding with an event of PCD at the vegetative mycelium, indicated by grey hyphae. Spores are generated by septation of the aerial hyphae.

To allow analyzing a large number of samples simultaneously and in a reasonable time frame, we adapted a method for rapid PG purification (Kühner *et al.*, 2014) for *S. coelicolor*. The advantage of this method is that it requires only a small amount of input biomass and much faster sample handling. For this, 10 mg of lyophilized cell wall material was isolated by boiling cells in 0.25% SDS in 2-ml microcentrifuge tubes, and secondary cell-wall polymers such as teichoic acids were removed by treatment for 4 h with hydrochloric acid (HCl) (see Materials and Methods section for details). As a control for the validity of the method, it was compared to a more elab-

orate method that is used routinely (Bui *et al.*, 2012). In the latter method, biomass from a 1-liter culture of *S. coelicolor* was boiled in 5% SDS and subsequently treated for 48 hours with hydrofluoric acid (HF) to remove teichoic acids. Comparison of the two methods revealed comparable outcomes between the two methods in peak detection (Table S5). This validated the more rapid method using 0.25% SDS and HCl, which was therefore used in this study.

The isolated PG was digested with mutanolysin (Kühner *et al.*, 2014, Glauner, 1988) and the muropeptide composition was analyzed by LC-MS. Peaks were identified in the m/z range from 500-3000 Da, whereby different m/z 's in co-eluting peaks were further characterized by MS/MS. The eluted m/z values were compared to a dataset of theoretical masses of predicted muropeptides. Table 1 shows a summary of the monomers and dimers that were detected during growth in liquid medium, and Table 2 shows a summary of muropeptides on solid medium. The full datasets are given in Tables S1, S2, S3 and S4. We identified several modifications, including the amidation of D-iGlu to D-iGln at position 2 of the stem peptide, deacytlation of MurNAc to MurN, removal of amino acids to generate mono-, di-, tri- and tetrapeptides, loss of LL-DAP-bound glycine, and the presence of Gly (instead of Ala) at position 1, 4 or 5. The loss of GlcNAc or GlcNAc-MurNAc indicates hydrolysis (Figure 2). For all amino acids in the pentapeptide chain, the position is indicated as [n], whereby n is the number in the chain (with [1] the position closest to the PG backbone, i.e., the MurNAc residue, and [5] being the last amino acid residue).

Growth phase dependent changes in the PG composition

The muropeptide that is incorporated from Lipid II by glycosyltransferases contains a pentapeptide with a Gly residue linked to LL-DAP [3]. In many bacteria pentapeptides are short-lived muropeptides that occur mostly at sites where *de novo* cell-wall synthesis takes place, i.e. during growth and division (Kuru *et al.*, 2015, Morales Angeles *et al.*, 2017). This is reflected by the high abundance of pentapeptides in the samples obtained from exponentially growing cells, with a pentapeptide content of 21% during early exponential growth (18 h), as compared to 14% and 11% during late exponential growth (24 h), transition phase (36 h) and stationary phase (48 h), respectively. Conversely, tripeptides increased over time, from 24% during early exponential phase to 32% in transition-phase cultures. Addition of Gly to the medium and, in consequence, incorporation of Gly in the peptidoglycan can cause changes in morphology (Hammes *et al.*, 1973, Takacs *et al.*, 2013). This property was applied to facilitate lysozyme-mediated formation of protoplasts in *Streptomyces*, used for protoplast transformation methods (Okanishi *et al.*, 1974, Hopwood *et al.*, 1977, Kieser *et al.*, 2000). In *S.coelicolor*, Gly can be found instead of Ala at position 1, 4 or 5 in the pentapeptide chain. During liquid growth, tetrapeptides carrying Gly at position 4 increased from 3% during early growth to 8% during the latest time points. The relative abundance of pentapeptides carrying Gly at position 5 (4-5%) did not vary over time. On solid-grown cultures, the Gly content of the peptidoglycan was around 1%, which is significantly lower than in liquid-grown cultures.

Table 1. Relative abundance(%)^a of muropeptides in vegetative cells from liquid NMM+.

Muropeptide ^a	Abundance (%) ^b in <i>S. coelicolor</i> M145			
	18h	24h	36h	48h
Monomers				
Mono	1.6	2.1	3.3	3.3
Di	14.2	15.5	14.5	13.2
Tri	27.4	32.2	35.1	35.8
Tetra	26.7	24.4	23.9	23.9
Tetra[Gly4] ^c	3.5	5.3	6.9	8.2
Penta	22.7	16.9	13.1	12.9
Penta[Gly5] ^c	4.7	4.8	4.7	4.4
D-Glutamine	67	62	61.1	63.7
Deacetylated	3.9	6.0	7.9	8.0
MurN-Tri	0.1	0.7	1.2	2.3
GlcNAc-MurN-Tri	1.8	2.2	2.6	2.1
Dimers	18h	24h	36h	48h
TriTri (3-3)	4.1	4.8	6.5	7.0
TriTri - MurNAcGlcNAc	8.7	14.8	23.7	34.3
TriTetra(3-3)	23.9	24.2	22.3	16.9
TriTetra(3-4)	1.0	8.7	8.2	6.1
TriTetra - MurNAcGlcNAc	9.6	15.1	16.1	16.2
TetraTetra(3-4)	23.3	13.5	10.1	8.6
TetraTetra - MurNAcGlcNAc	6.0	7.3	4.8	5.6
TetraPenta (3-4)	24.6	9.1	5.6	3.0
MurN	1.8	1.2	1.5	1.2
-GlcNac	0.3	0.6	1.1	1.2
missing MurNAcGlcNAc	24.3	37.2	44.6	56.1
Proportion(%) of 3-3 cross-links	36.5	48.0	54.5	57.3

^aMonomers and dimers are treated as separate datasets.

^bRelative abundance is calculated as the ratio of the peak area over the sum of all peak areas recognized in the chromatogram.

^cGly detected instead of Ala

Table 2. Relative abundance(%)^a of muuropeptides over growth on solid SFM-medium and spores.

Muuropeptide ^a	Abundance (%) ^b in <i>S. coelicolor</i> M145			
	24h	48h	72h	spores
Monomers				
Mono	3.6	4.3	4.1	4.5
Di	21.6	17.6	17.9	13.1
Tri	29.6	34.3	34.2	28.1
Tetra	25.4	29.5	32.0	48.3
Tetra[Gly4] ^c	0.9	1.1	1.0	2.3
Penta	16.8	9.9	7.2	5.3
Penta[Gly5] ^c	1.2	1.4	1.3	4.0
Deacetylated	3.7	4.4	6.1	4.5
D-Glutamine	76.2	80.3	82.9	74.0
Missing GlcNAc	1.5	3.4	5.0	4.8
MurN-Tri	0.6	1.7	3.1	3.5
GlcNAc-MurN-Tri	1.9	1.4	1.6	0.1
Dimers	24h	48h	72h	spores
Tri-Tri (3-3)	7.4	10.5	12.6	4.9
Tri-Tri - MurNacGlcNac	0.6	0.6	0.3	7.1
Tri-Tetra(3-3)	20.4	22.2	21.8	19.1
Tri-Tetra(3-4)	9.7	12.7	11.8	4.7
Tri-Tetra - MurNacGlcNac	13.3	14.5	13.0	6.3
Tetra-Tetra(3-4)	13.3	15.8	15.7	38.9
Tetra-Tetra - MurNacGlcNac	17.3	13.7	13.2	17.1
Tetra-Penta (3-4)	12.7	7.3	5.4	0.7
MurN	1.0	0.3	1.2	0.4
-GlcNAc	0.4	0.2	0.4	0.1
missing MurNacGlcNac	31.1	28.7	26.5	30.4
Proportion(%) of 3-3 cross-links	43.8	47.8	51.1	35.1

^aMonomers and dimers are treated as separate datasets.

^bRelative abundance is calculated as the ratio of the peak area over the sum of all peak areas recognized in the chromatogram.

^cGly detected instead of Ala

The abundance of 3-3 cross-links increases over time

Two types of cross-links are formed via separate mechanisms, namely the canonical D,D-transpeptidases (PBPs) producing 3-4 (D,D) cross-links between LL-DAP[3] and D-Ala[4] and L,D-transpeptidases that form 3-3 (L,D) cross-links between two LL-DAP[3] residues (Figure 2). These types of peptidoglycan cross-linking can be distinguished based on differences in retention time and their MS/MS fragmentation patterns. Dimers containing a tripeptide and a tetrapeptide (TetraTri) may have either cross-link, giving rise to isomeric forms that elute at different retention times, allowing for assessment by MS/MS (Figures 3A and 3B). In *S. coelicolor*, the ratio of 3-3 cross-linking increased over time towards transition phase; the relative abundance increased from 37% of the total amount of dimers at 18 h (exponential phase) to 57% of all dimers at 48 h (Figures 3A and 3B).

PG hydrolysis increases as the culture ages

PG hydrolysis is associated with processes such as separation of daughter cells after cell division and autolysis, and in *E. coli* and other species deletion mutants lacking PG amidases grow in chains of unseparated cells (Heidrich *et al.*, 2002, Vollmer *et al.*, 2008b). On solid media, vegetative hyphae of *Streptomyces* undergo programmed cell death (PCD) and hydrolysis. During spore maturation, spores are separated hydrolytically from one another. Some streptomycetes sporulate in submerged culture, but this is not the case for *S. coelicolor* (Girard *et al.*, 2013). Our data show that as growth proceeds in submerged cultures, the *S. coelicolor* peptidoglycan progressively loses GlcNAc and GlcNAc-MurNAc moieties (Table 1), as a result of N-acetylglucosamidase activity. The proportion of dimers lacking GlcNAc-MurNAc thereby increases in time from 24% at 18 h to 56% at 48 h. Figure 3C shows MS/MS profiles of a TriTri-dimer with a single set of glycans. During growth on solid media the trend was inverted. This may be due to the different developmental stages, whereby 24 h corresponds to early developmental events and PCD, 48 h to aerial growth and sporulation at 72 h. This analysis shows the relative abundance of muropeptides of the total amount of biomass, when hydrolysis has occurred at the vegetative mycelium, while the strain has simultaneously produces a large amount of aerial hyphae, the relative abundance of muropeptides of the entire culture could be misleading (Table 2).

Deacetylation of MurNAc is associated with mycelial aging and sporulation

Modifications to the glycan strand are commonly linked to lysozyme resistance (Meyrand *et al.*, 2007). In particular, N-deacetylation of PG strands is widespread among bacteria, which can occur both at GlcNAc and at MurNAc (Vollmer, 2008). In the case of *S. coelicolor*, the only glycan modification is the deacetylation of MurNAc to MurN. Our data show that this modification becomes more prominent as the vegetative mycelium ages, from 5% during early growth to 8% during later growth stages. On agar plates, 3.7% of the monomers was deacetylated at 24 h, 4.4% at 48 h and 6.1% at 72h. The PG composition of spores and vegetative mycelia was compared to get more insights into the possible correlations between PG composition and important processes such as dormancy and germination. Muropeptides in spores were strongly biased for tetrapeptides, making up 44% of the monomers, as compared to 23-25% of the vegetative PG. Conversely, pentapeptides were found in much lower

High-resolution analysis of the peptidoglycan composition in *Streptomyces coelicolor*

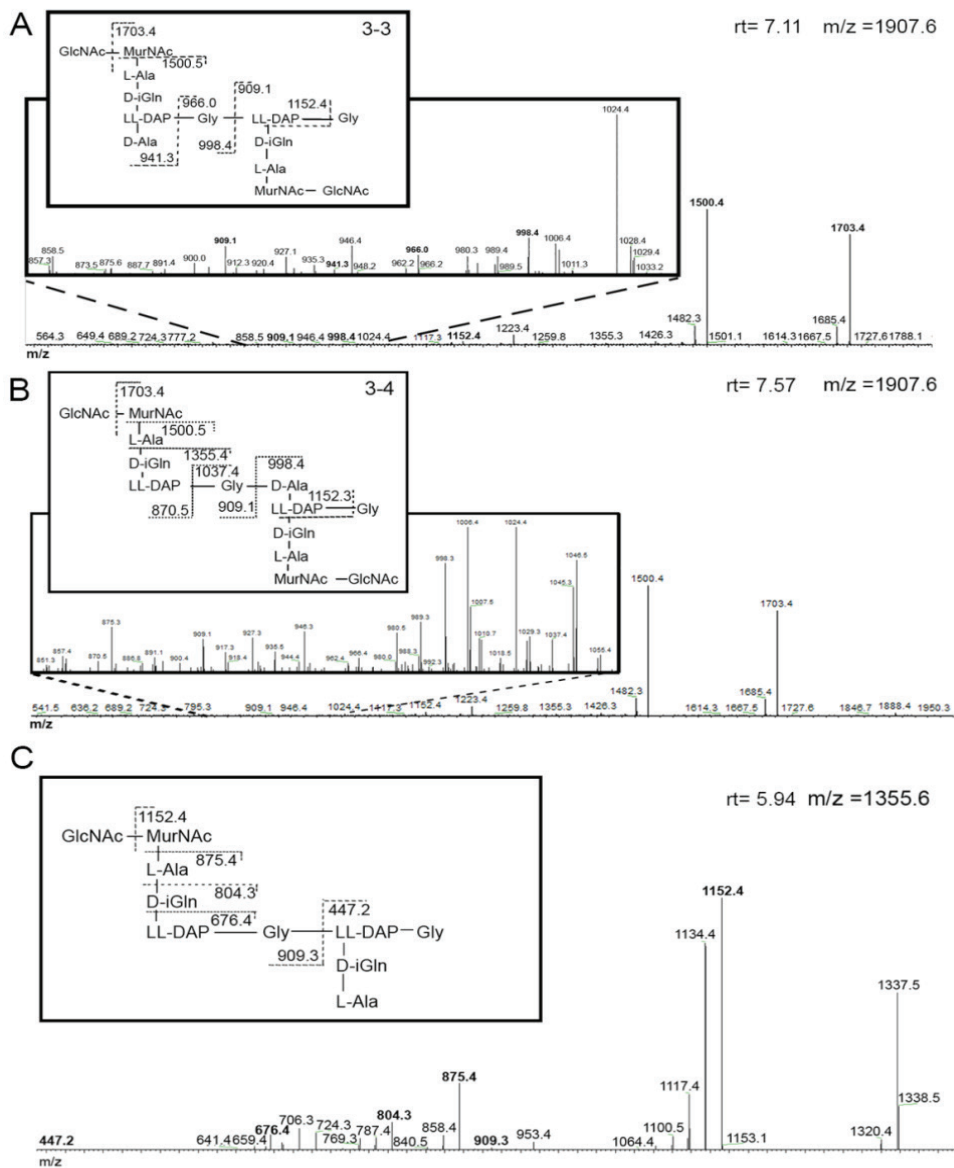


Figure 2. MS/MS fragmentations of TetraTri dimers with either 3-3 cross-link (A) or 3-4 cross-link (B). Differentiation between these two types of cross-links is possible at the point of asymmetry, at Gly attached to LL-DAP. The 3-3 cross-linked dimer (A) fragments into masses of 966.0 m/z and 941.3 m/z, which can be found in the respective MS/MS spectrum. The 3-4 cross-linked dimer (B) fragments into masses of 1037.4 m/z and 870.5 m/z. These masses are found in the MS/MS spectrum. Boxed MS/MS spectra show a magnification of masses between m/z 850 and 1050 to show masses present in lower abundance. (C) a TriTri dimer lacking GlcNAcMurNAc with an M+H of 1355.6, diagnostic fragments are given in the proposed structures.

amounts in spores (5% of the monomers), as compared to 10-22% in vegetative hyphae. A previous study showed that mutation of the gene *dacA* that encodes D-alanyl-D-alanine carboxypeptidase disrupts spore maturation and germination, where one could influence the other. This indicates that either pentapeptides inhibit spore maturation, or that a high amount of tetrapeptides is important (Rioseras *et al.*, 2016). The mucopeptide that stood out in the analysis of the spore PG was a tripeptide which lacks GlcNAc and contains a deacetylated MurNAc, called MurN-Tri (Figure 2). In spores, MurN-Tri made up 3.5% of the monomers, whereas the less modified mucopeptide, GlcNAcMurN-Tri only made up 0.2% of the monomers.

To further investigate this interesting phenomenon, we analyzed two developmental mutants, namely the *bldD* and *whiG* mutants. The *bldD* gene product is a global transcription factor that controls the transcription of many developmental genes and is therefore blocked in an early stage of morphogenesis (den Hengst *et al.*, 2010), while the *whiG* gene product is a σ factor that controls early events of aerial growth. The monomer profile of *S. coelicolor* M145 and its *bldD* and *whiG* mutants are summarized in Table 3. For the wild-type strain M145, 24 h represents vegetative growth, 48 h aerial growth and 72 h spore formation. In line with the notion that MurN-Tri accumulates particularly in spores, the *bldD* mutant accumulated hardly any MurN-Tri (0-0.2%) over the course of time and the *whiG* mutant 0.4%, 0.6% and 1.3% after 24 h, 48 h, and 72 h. respectively. In contrast, M145 had 0.6%, 1.7% and 3.1% MurN-Tri at these time points, strongly suggesting that MurN-Tri accumulates in a sporulation-specific manner.

Table 3. Summary of relative abundance (%)^a of monomers from developmental *bldD*- and *whiG*-mutants and the parent strain, M145.

		Mono	Di	Tri	Tetra	Penta	De-acetylated	MurN-Tri	GlcNAc-MurN-Tri
<i>ΔbldD</i>	24h	4.5	25.7	28.0	23.0	10.8	6.5	0.0	5.3
	48h	4.3	26.3	38.3	23.4	11.1	8.5	0.2	6.6
	72h	4.3	27.2	40.9	19.9	9.5	7.6	0.2	5.8
<i>ΔwhiG</i>	24h	3.5	23.2	27.0	32.5	15.2	3.0	0.4	1.3
	48h	3.6	17.5	44.3	25.5	7.9	5.0	0.6	3.2
	72h	4.1	18.5	48.8	20.9	6.9	6.2	1.3	3.8
M145	24h	3.6	21.6	29.6	25.4	16.8	3.7	0.6	1.9
	48h	4.3	17.6	34.3	29.5	9.9	4.4	1.7	1.4
	72h	4.1	17.9	34.2	32.0	7.2	6.1	3.1	1.6
spores		4.5%	13.1	28.1	48.3	5.3	4.5	3.5	0.1

^aRelative abundance is calculated as the ratio of the peak area over the sum of all peak areas recognized in the chromatogram.

DISCUSSION

The *Streptomyces* cell wall is essential for structural rigidity and, in a pinch, a source of nutrients (Rigali *et al.*, 2008). Here, we analyzed the peptidoglycan composition over the course of growth and development. All masses are identified by MS and MS/MS, by which we were able to identify between dimers which were cross-linked by either 3-3- or 3-4 cross-links. A large event of peptidoglycan recycling was recognized in the hydrolysis of GlcNAc-MurNAc from up to 56% of the dimers in late-exponential cultures. One muropeptide is linked to development, which was confirmed in developmental mutants. In conclusion, *Streptomyces* peptidoglycan is dynamic, being constantly constructed and deconstructed while maintaining cell shape and solidity.

Implications for the biology of actinobacteria

Sporulation is a key feature of *Streptomyces* biology and the spore wall is a major line of defense against environmental stresses, allowing the bacteria to survive under adverse conditions such as heat and cold stress, osmotic pressure, starvation or drought (van der Meij *et al.*, 2017, Okoro *et al.*, 2009). The spores are spread to a new environment, where they germinate as soon as the right conditions are met and start a new mycelium. Not much is known about the environmental and genetic factors that control the onset of germination. In terms of the genetics, we have previously shown that mutants deficient for the cAMP-receptor protein Crp have a much thicker spore wall, presumably due to reduced expression of cell-wall hydrolases and consequently germinate slowly (Piette *et al.*, 2005). Additionally, Crp is a positive regulator of secondary metabolite production where the expression of Crp increases undecylprodigiosin production (Gao *et al.*, 2012). Conversely, strains over-expressing the cell-division activator protein SsgA show an increase in the number of germ tubes per spore (Noens *et al.*, 2007), with on average three germ tubes emerging from a single spore (instead of the two in wild-type spores and significantly less than that in *ssgA* mutants). It is yet unclear how future sites of branching in the hyphae or germination in the spores are marked. However, even after very long storage of spores, germination still occurs at the spore 'poles', suggesting physical marks to the PG, such as rare modifications. Yet, in our analysis, we did not find muropeptide moieties such as muramic d-lactam, which is uniquely found in the spore-cortex of *B. subtilis*, but which is absent in vegetatively growing cells (Popham *et al.*, 1996). The only major difference was the relatively high amount of MurN-Tri in the spore PG, which was hardly seen in *bldD* mutants, and also much less prominent in the *whiG* mutant. This strongly suggests that incorporation of MurN-Tri directly relates to sporulation. It will be interesting to see why this moiety is overrepresented in the spore PG. At the same time, this also shows the importance of analyzing the cell wall of different culture types as it reveals novel features that may play a key role in development. L,D-transpeptidases (LDTs) are especially prevalent in the actinobacterial genera *Mycobacterium*, *Corynebacterium* and *Streptomyces*, and, suggestively, these bacteria have a much higher percentage of 3-3 cross-links, with an abundance of at least 30% 3-3-cross links in investigated actinobacterial peptidoglycan as compared to bacteria with lateral cell-wall growth such as *E. coli* (<10%) and *E. faecium* (3%) (Cameron *et al.*, 2014, Hugonnet *et al.*, 2014, Lavollay *et al.*, 2009). LDTs attach to D-Ala[4] and form a cross-link between glycine and LL-DAP[3]. D-Ala[4] is considered a donor for this type of cross-link (Mainardi *et al.*, 2005). An interesting

feature of these two mechanisms is that 3-4 cross-links can only be formed when a pentapeptide is present to display the D-Ala[5] donor, whereas 3-3 cross-links can be formed with a tetrapeptide as a donor strand. The data agrees with the idea that 3-3 cross-links could be required for remodeling of the cell wall beyond the tip-complex, using available tetrapeptides contrary to newly constructed pentapeptides (Lavollay *et al.*, 2008, Sanders *et al.*, 2014, Sacco *et al.*, 2010, Baranowski *et al.*, 2018).

The cell wall and programmed cell death

Evidence is accumulating that, like eukaryotes, bacteria undergo a process of programmed cell death (PCD). Bacterial multicellularity implies a lifestyle involving cellular heterogeneity and the occasional sacrifice of selected cells for the benefit of survival of the colony (Zhang *et al.*, 2016b, Yague *et al.*, 2010, Yague *et al.*, 2013). PCD is likely a major hallmark of multicellularity (Claessen *et al.*, 2014), and has been described in the biofilm-forming *Streptococcus* (Giral *et al.*, 2005) and *Bacillus* (Engelberg-Kulka *et al.*, 2006), in Myxobacteria that form fruiting bodies (Sogaard-Andersen & Yang, 2008), in the filamentous cyanobacteria (Bornikoel *et al.*, 2017, Ning *et al.*, 2002), and in the branching *Streptomyces* (Manteca *et al.*, 2006, Miguez *et al.*, 1999, Tenconi *et al.*, 2018). In streptomycetes, cell-wall hydrolases support developmental processes like branching and germination (Haiser *et al.*, 2009). Additionally, PCD is likely an important event during the onset of development from a vegetative lifestyle to a reproductive lifestyle, as autolytic degradation of the cell wall is intrinsically linked with the onset of antibiotic production and spore formation (Tenconi *et al.*, 2018). Conceptually, GlcNAc accumulates at high concentrations around colonies during PCD, and GlcNAc is an important signaling molecule for the onset of morphological differentiation and antibiotic production in streptomycetes (Rigali *et al.*, 2008, Urem *et al.*, 2016). The linkage of PCD and antibiotic production is logical from a biological perspective; autolytic dismantling of the vegetative (substrate) mycelium generates building blocks in a nutrient-depleted soil, which will inevitably attract motile competitors. Antibiotics likely serve to fend off these competitors and protect the food source. Thus, cell-wall hydrolysis may facilitate the correct timing of development.

CONCLUSIONS

We have provided a detailed analysis of the peptidoglycan of *Streptomyces* mycelia and spores, and developed a reliable and fast method to compare larger numbers of samples. Our data show significant changes over time, among which changes in the amino acid chain, hydrolysis of dimers, and the accumulation of the rare MurN-Tri specifically in the spores. The cell wall likely plays a major role in the development of streptomycetes, with implications for germination and the switch to development and antibiotic production (via PCD-released cell wall components). The dynamic process that controls the remodeling of the cell wall during tip growth is poorly understood, but we anticipate that the local cell-wall structure at sites of growth and branching may well be different from that in older (non-growing) hyphae. This is consistent with the changes we observed over time, between the younger and older mycelia. Detailed localization of cell-wall modifying enzymes and of specific cell-wall modifications, in both time and space, is required to further reveal the role of the cell wall in the control of growth and development of streptomycetes.

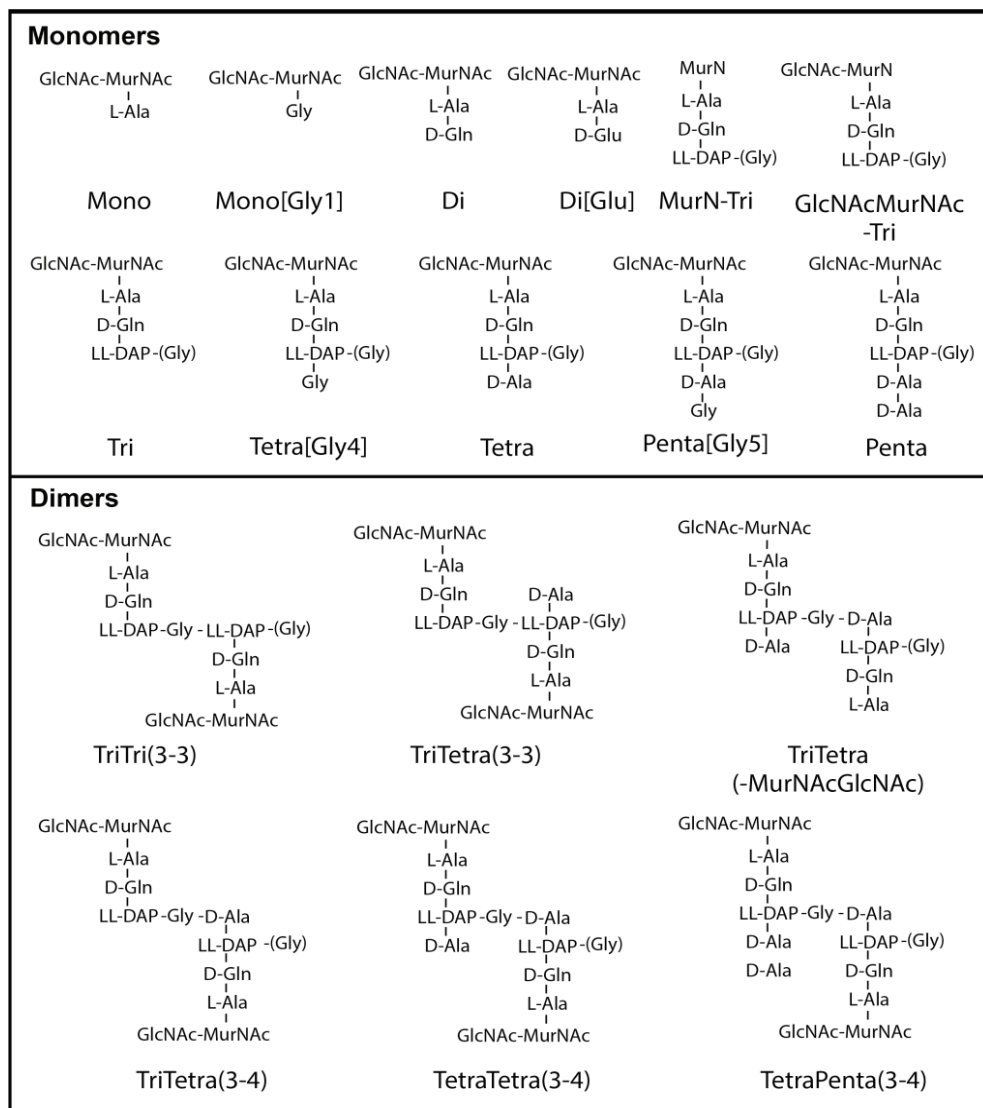


Figure 3. Summary of structures of main monomers and dimers observed in PG from *S. coelicolor*. Modification to the PG include: alteration of the length of the amino acid chain; [Gly1], L-Ala is replaced by Gly; [Glu], where Glutamic acid (Glu) is present instead of D-Glutamine (Gln); [Gly4], where D-Ala(4) is replaced by Gly; [Gly5], where D-Ala(5) is replaced by Gly. Specific for dimers: (3-3) shows a cross-link between LL-DAP(3) to LL-DAP(3) with a Gly-bridge; (3-4) shows a cross-link between LL-DAP(3) and D-Ala(4) with a Gly-bridge; (-MurNacGlcNac) shows hydrolysis of a set of sugars.

Acknowledgments

This work is part of the profile area Antibiotics of the Faculty of Sciences of Leiden University.

Conflict of interest statement

The authors declare that they have no conflicts of interest with the contents of this article.

Author contributions

LvdA performed the experiments with the help of GS. LvdA and GvW conceived the study. LvdA, AH, TH and GvW wrote the article with the help of WV. All authors approved the final manuscript.

CHAPTER 4

The peptidoglycan composition of *Kitasatospora setae* and *Kitasatospora viridifaciens* is highly modified during sporulation

Lizah T. van der Aart, Thomas Hankemeier and Gilles P. van Wezel

Supplementary material available at Appendix 1

ABSTRACT:

Members of the genus *Kitasatospora* are Gram-positive actinomycetes that belong to the family of *Streptomycetaceae*, and strongly resemble *Streptomyces* in terms of their genetics and morphology. However, there are also differences, such as that key developmental genes are missing and their cell wall composition differs significantly. *Kitasatosporae* have a unique switch in peptidoglycan composition during their life cycle, producing a vegetative mycelium with *meso*-DAP in the peptidoglycan, while the spore peptidoglycan contains LL-DAP. Here, we investigate the biological implications of the growth phase-dependent changes in the PG composition. Our work shows that the peptidoglycan of *Kitasatospora setae* and *Kitasatospora viridifaciens* changes composition between the point of vegetative growth and sporulation. An *ssgB* null mutant of *K. viridifaciens*, which fails to sporulate (Ramijan *et al.*, 2018), accumulated muropeptides with a modification at the site of MurNAc, a higher amount of hydrolyzed dimers as compared to the parent strain and has minimal amounts of peptidoglycan with LL-DAP. The data suggests that at the switch from vegetative growth to reproductive growth, *Kitasatospora* species actively hydrolyze most of the vegetative mycelium, potentially in a *meso*-DAP directed manner in order to produce reproductive spores.

INTRODUCTION:

Actinomycetes are Gram-positive bacteria well known for their capability to produce a wide array of secondary metabolites, among which most of our clinical antibiotics (Barka *et al.*, 2016; Hopwood, 2007). The search for novel antibiotic-producing actinobacteria has resulted in the isolation of an huge diversity of taxonomically described actinomycetes. Many of these belong to the genus *Streptomyces*, of which no fewer than 550 type species have been described (Kämpfer, 2012). Besides *Streptomyces*, the family of *Streptomycetaceae* includes *Kitasatospora* and *Streptacidiphilus* (Goodfellow, 2012; Labeda *et al.*, 2012; Labeda *et al.*, 2017). *Kitasatospora* are a sister genus to *Streptomyces* with an indistinguishable morphology, which has caused many *Kitasatospora* species to be mis-assigned to the genus *Streptomyces* (Girard *et al.*, 2014; Ramijan *et al.*, 2017).

During growth of *Kitasatospora*, a single spore germinates and develops vegetative hyphae, which extend by tip growth and branching, thereby developing an intricate vegetative mycelium. Reproductive growth starts with the development of aerial hyphae, which grow into the air and eventually differentiate into long spore chains (Barka *et al.*, 2016). Development from vegetative to aerial mycelium is regulated by the *bld* genes, named after the nonsporulating phenotype of mutants, whereby colonies have a ‘bald’ appearance; spore formation is regulated by the *whi* genes, so-called because *whi* mutants are white, due to their failure to produce the grey-pigmented spores (Chater, 1972; Merrick, 1976). *Kitasatosporae* lack the regulatory genes *bldB* and *whiJ* that are important for development in *Streptomyces*, and the cytoskeletal gene *mbl*, for an MreB-like protein (Celler *et al.*, 2013). BldB is a small protein involved in the regulation of development and antibiotic production, WhiJ mediates repression of *Streptomyces* development (Ainsa *et al.*, 2010; Pope *et al.*, 1998).

These data suggest that at least some aspects of *Kitasatospora* development is regulated different from *Streptomyces* (Girard *et al.*, 2014). Another major difference lies in the so-called SsgA-like proteins. Sporulation of actinobacteria requires one or more proteins that belong to the SsgA-like proteins (SALPS) (Traag, 2008; van Dissel, 2014). All actinobacteria that sporulate contain an orthologue of *ssgB*, while more complex actinomycetes like streptomycetes encode several SALPS (Noens *et al.*, 2005). Of these, *ssgA* and *ssgB* are required for sporulation in streptomycetes; mutants deleted for *ssgA* only form spores on minimal media (van Wezel *et al.*, 2000), while *ssgB* mutants fail to sporulate under any growth condition (Keijser *et al.*, 2003). SsgB recruits FtsZ to septum sites so as to initiate sporulation-specific cell division (Willemse *et al.*, 2011). Several *Kitasatosporae* lack *ssgA* and/or its regulatory gene *ssgR*, again suggesting that the control of development is different in *Kitasatospora* and *Streptomyces*.

One determining feature that sets *Kitasatospora* apart from *Streptomyces* is found in the cell wall composition: diaminopimelic acid (DAP) is a diagnostic features in actinomycetales, and this modified amino acid contains two stereocenters of which two stereoisomers are found in bacteria, LL-DAP and L,D(*meso*)-DAP (Lechevalier and Lechevalier, 1965). *Streptomyces* PG exclusively contains LL-DAP, but *Kitasatospora* species carry *meso*-DAP in PG of the vegetative mycelium and LL-DAP in spore PG, as shown in Figure 1 (Takahashi, 2017; Zhang *et al.*, 1997). Analysis of the cell wall composition of *Streptomyces* failed to identify muropeptides that were unique for either vegetative mycelia or spores; instead, the major differences were seen in

the abundance of muropeptides (van der Aart *et al.*, 2018).

The switch from *meso*- to LL-DAP in the PG between vegetative mycelium and spores of *Kitasatospora* species suggests a form of regulation at the point of the cell wall construction (Takahashi, 2017). In this study, we analyzed the peptidoglycan composition of mycelia and spores of *Kitasatospora setae* KM 6054^T and *Kitasatospora viridifaciens* DSM40239. Analysis of the muropeptides by MS/MS revealed major changes in cell wall composition between vegetative mycelium and spores of both strains. An *ssgB* deletion mutant of *K. viridifaciens* showed a higher degree of cell wall hydrolysis and an unidentified modification at the site of MurNAc.

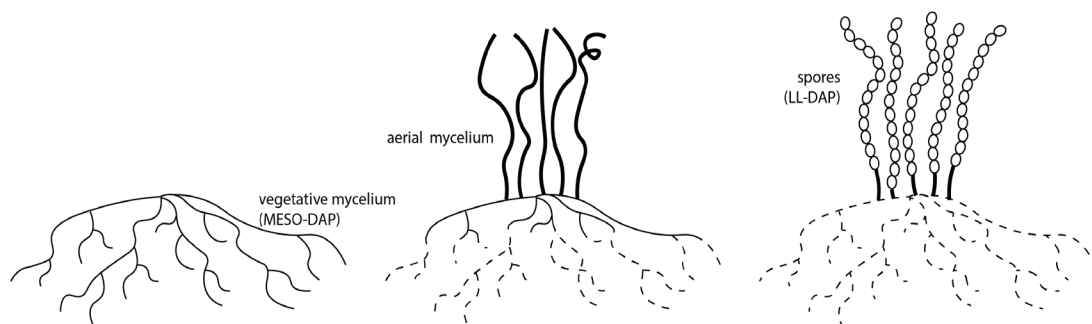


Figure 1. *Kitasatospora* produces a vegetative mycelium with LL-DAP, followed by an aerial mycelium that develops into spores with LL-DAP. Over the course of development, the vegetative mycelium is broken down during a process of programmed cell death, indicated by dashed lines.

MATERIAL AND METHODS

Bacterial strain and culturing conditions:

Kitasatospora setae KM 6054^T and *Kitasatospora viridifaciens* DSM40239 are both obtained from the DSMZ. *K. viridifaciens* was grown on MYM-medium, *K. setae* was grown on ISP-2. Spores are isolated by scraping them off with a cotton ball and drawing the solution with a syringe. The *ssgB*-mutant of *K. viridifaciens* was generated by Karina Ramijan (Ramijan *et al.*, 2018).

PG extraction

Cells were lyophilized for a biomass measurement, 10 mg biomass was directly used for PG isolation. PG was isolated according to Kühner *et al.* (Kühner *et al.*, 2014), using 2 mL screw-cap tubes for the entire isolation. Biomass was first boiled in 0.25% SDS in 0.1 M Tris/HCl pH 6.8, thoroughly washed, sonicated, treated with DNase, RNase and trypsin, inactivation of proteins by boiling and washing with water. Wall teichoic acids were removed with 1 M HCl (van der Aart *et al.*, 2018). PG was digested with mutanolysin and lysozyme (Arbeloa *et al.*, 2004). Muropeptides were reduced with sodium borohydride and the pH was adjusted to 3.5-4.5 with phosphoric acid.

LC-MS analysis of monomers

The LC-MS setup consisted of a Waters Acquity UPLC system (Waters, Milford, MA, USA) and a LTQ Orbitrap XL Hybrid Ion Trap-Orbitrap Mass Spectrometer (Thermo Fisher Scientific, Waltham, MA, USA) equipped with an Ion Max electrospray source.

Chromatographic separation was performed on an Acquity UPLC HSS T3 C₁₈ column (1.8 μ m, 100 Å, 2.1 \times 100 mm). Mobile phase A consist of 99.9% H₂O and 0,1% Formic Acid and mobile phase B consists of 95% Acetonitrile, 4.9% H₂O and 0,1% Formic Acid. All solvents used were of LC-MS grade or better. The flow rate was set to 0.5 ml/min. The binary gradient program consisted of 1 min 98% A, 12 min from 98% A to 85% A, and 2 min from 85% A to 0% A. The column was then flushed for 3 min with 100% B, the gradient was then set to 98% A and the column was equilibrated for 8 min. The column temperature was set to 30°C and the injection volume used was 5 μ L. The temperature of the autosampler tray was set to 8°C. Samples were run in triplicates.

MS/MS was done both on the full chromatogram by data dependent MS/MS and on specific peaks by selecting the mass of interest. Data dependent acquisition was performed on the most intense detected peaks, the activation type was Collision Induced Dissociation (CID). Selected MS/MS was performed when the resolution of a data dependent acquisition lacked decisive information. MS/MS experiments in the ion trap were carried out with relative collision energy of 35% and the trapping of product ions were carried out with a q-value of 0.25, and the product ions were analyzed in the ion trap., data was collected in the positive ESI mode with a scan range of *m/z* 500–2500 in high range mode. The resolution was set to 15.000 (at *m/z* 400).

Data analysis

Chromatograms were evaluated using the free software package MZmine (<http://mzmine.sourceforge.net/>) (Pluskal *et al.*, 2010) to detect peaks, deconvolute the data and align the peaks. Only peaks corresponding with a mass corresponding

to a mucopeptide were saved, other data was discarded. The peak areas were exported and a final table which shows peak areas as percentage of the whole was produced in Microsoft Excel.

Muropeptide identification

The base structure and modifications of *S.coelicolor* PG has been resolved (Hugonnet *et al.*, 2014). Different combinations of modifications were predicted and the masses were calculated using ChemDraw Professional (PerkinElmer). When a major peak had an unexpected mass, MS/MS helped resolve the structure. MS/MS was used to identify differences in cross-linking and to confirm predicted structures.

DAP characterization

2-3 mg of freeze-dried material was dissolved in 200 μ L 6M HCl and boiled for 16 hours. After cooling, the tubes were transferred to the rotary evaporator and dried. The remaining material was dissolved in 100 μ L H₂O. 2 μ L of each sample was applied to the baseline of a cellulose TLC-plate. The tank was filled with Methanol:H₂O:Pyridine:12M HCl (32:7:4:1) (Lechevalier *et al.*, 1971).

RESULTS

Diaminopimelic acid composition in vegetative mycelium and spores.

Mycelia from *K. setae* and *K. viridifaciens* were harvested from solid ISP-2 or MYM agar plates at 16 h (vegetative growth), 30 h (aerial growth), 42 h (onset of sporulation) and 64 h (mature spores) and spores separated from the mycelia by filtering through cotton wool. Mycelium of the non-sporulating *ssgB* null mutant of *K. viridifaciens* was harvested after 64 h, when abundant aerial hyphae were formed, as shown in figure S1. This mutant was used to analyse aerial mycelium after prolonged incubation, in the absence of spores. Then, cell wall material was isolated from all the mycelia and spores as described (Lechevalier *et al.*, 1971). The diaminopimelic acid (DAP) stereochemistry of the samples was assessed by TLC. In agreement with the literature, during vegetative growth (16 h) only *meso*-DAP was identified, while spore samples exclusively contained LL-DAP. Interestingly, *K. setae* cell walls contained a major amount of LL-DAP in 42 h samples and apparently exclusively LL-DAP was found in 64 h samples. For *K. viridifaciens*, this effect was less pronounced, but mycelia that had grown for 64 h had a DAP profile that is highly similar to that of spores. This suggests that after 64h, a large part of the vegetative mycelium has been used as a substrate for the aerial mycelium. The *ssgB* deletion mutant of *K. viridifaciens* carried mostly *meso*-DAP after 64 h of growth, with trace amounts of LL-DAP, suggesting that aerial hyphae are modified before the point of sporulation (Figure S2).

Peptidoglycan analysis

Cell wall material of *K. setae* and *K. viridifaciens* was isolated from the same samples as the DAP isolation, from both *K. setae* and *K. viridifaciens* after 16 h, 30 h, 42 h, and 64 h of growth. Spores were filtered through cotton wool, mycelium from the *ssgB*-mutant of *K. viridifaciens* was harvested at 64 h. PG was isolated as described previously (van der Aart *et al.*, 2018). Most muropeptides found in the profiles of *K. setae* and *K. viridifaciens* have previously been described for *S. coelicolor*. The basal structure of the muropeptides is a glycan backbone consisting of GlcNAc and MurNAc, where a pentapeptide chain is attached to MurNAc consisting of L-Ala-D-Glu-*meso*/LL-DAP-D-Ala-D-Ala with Gly attached to the DAP residue. Cross-links can be formed via the DAP-linked Gly, which then connects to the opposite D-Ala in the case of a 3-4 cross-link or DAP in the case of a 3-3 cross-link.

Modifications to monomers

After 16 h of growth, the PG from both *Kitasatospora* species contained only *meso*-DAP. From 30 h onwards, their PG contained minor amounts of LL-DAP, which is seen in the muropeptide profile where double peaks started to appear. The major switch from *meso*-DAP to LL-DAP occurred with a switch in PG modification, whereby both species of *Kitasatospora* showed major changes in cell wall composition at the time of sporulation. Modification to the PG structure involve: peptidolytic cleavage of amino acids to generate tetra-, tri-, di- or mono-peptides, loss of Gly, amidation of Glu to glutamine (Gln) (Figueiredo *et al.*, 2012), and amidation of DAP (Levefaudes *et al.*, 2015). Modifications to the glycan strand include de-acetylation of MurNAc to MurN, as often seen in older mycelia and spores of *Streptomyces* and amidation of the glycan strands whereby MurNAc-GlcNAc is cleaved off, to give a dimer with a single set of glycans (van der Aart *et al.*, 2018) (Vollmer, 2008).

Table 1. Relative abundance(%)^b of muropeptides from *K. setae*.

Muropeptide ^a	<i>K. setae</i>				
	16h	30h	42h	64h	spores
Monomers	16h	30h	42h	64h	spores
Mono	2.1	2.3	2.4	0.2	0.0
Di	24.5	27.7	27.4	28.8	22.6
Tri	6.0	9.1	6.8	6.2	8.2
Tri (-Gly)	9.8	10.9	13.0	10.4	5.3
Tetra	5.7	7.4	12.8	27.5	51.2
Tetra (-Gly)	37.2	34.3	30.9	21.3	7.3
Penta	0.4	0.2	0.4	1.2	2.5
Penta (-Gly)	13.9	7.9	6.1	3.5	0.5
Penta [Gly5]	0.4	0.2	0.2	0.9	2.3
Deacetylation	0.3	0.8	1.2	1.0	0.9
	<i>K. setae</i>				
Dimers	16h	30h	42h	64h	spores
TriTri [deAc/deAc]	13.7	11.9	15.5	5.3	1.3
TriTri (-GM/ -Gly)	4.0	6.0	3.9	1.6	2.1
TriTri (-GM) [deAc]	12.1	22.6	21.2	10.0	1.8
TriTetra	0.0	0.0	0.0	3.6	6.5
TriTetra [deAc]	23.0	11.3	11.6	4.6	0.3
TriTetra (-GM)	1.8	0.1	1.3	6.6	16.5
TriTetra (-GM) [deAc]	34.1	32.2	25.6	12.4	0.4
TriTetra (-GM) (-Gly)	3.7	6.5	4.7	2.8	1.8
TetraTetra	0.5	0.5	2.7	17.8	25.5
TetraTetra [deAc] [Gly4]	3.9	1.3	0.6	0.1	0.0
TetraTetra [Gly4]	2.6	6.8	7.1	18.1	7.7
TetraTetra (-GM)	0.5	0.8	5.8	17.0	38.1
Deacetylation	86.8	79.3	74.6	32.5	3.8
missing MurNAcGlcNAc	56.2	68.2	62.5	50.5	60.7
3-3 cross-links	92.4	90.7	83.8	47.1	28.8

^a The labels correspond to the labels in Figure 2. (-Gly) misses the DAP-linked Gly, [Gly4] or [Gly5] has Gly instead of the 4th or 5th D-Ala, [deAc] carries MurN instead of MurNAc, (-G) lacks GlcNAc, (-GM) lacks GlcNAcMurNAc. Monomers and dimers are treated as separate datasets.

^bRelative abundance is calculated as the ratio of the peak area over the sum of all peak areas recognized in the chromatogram.

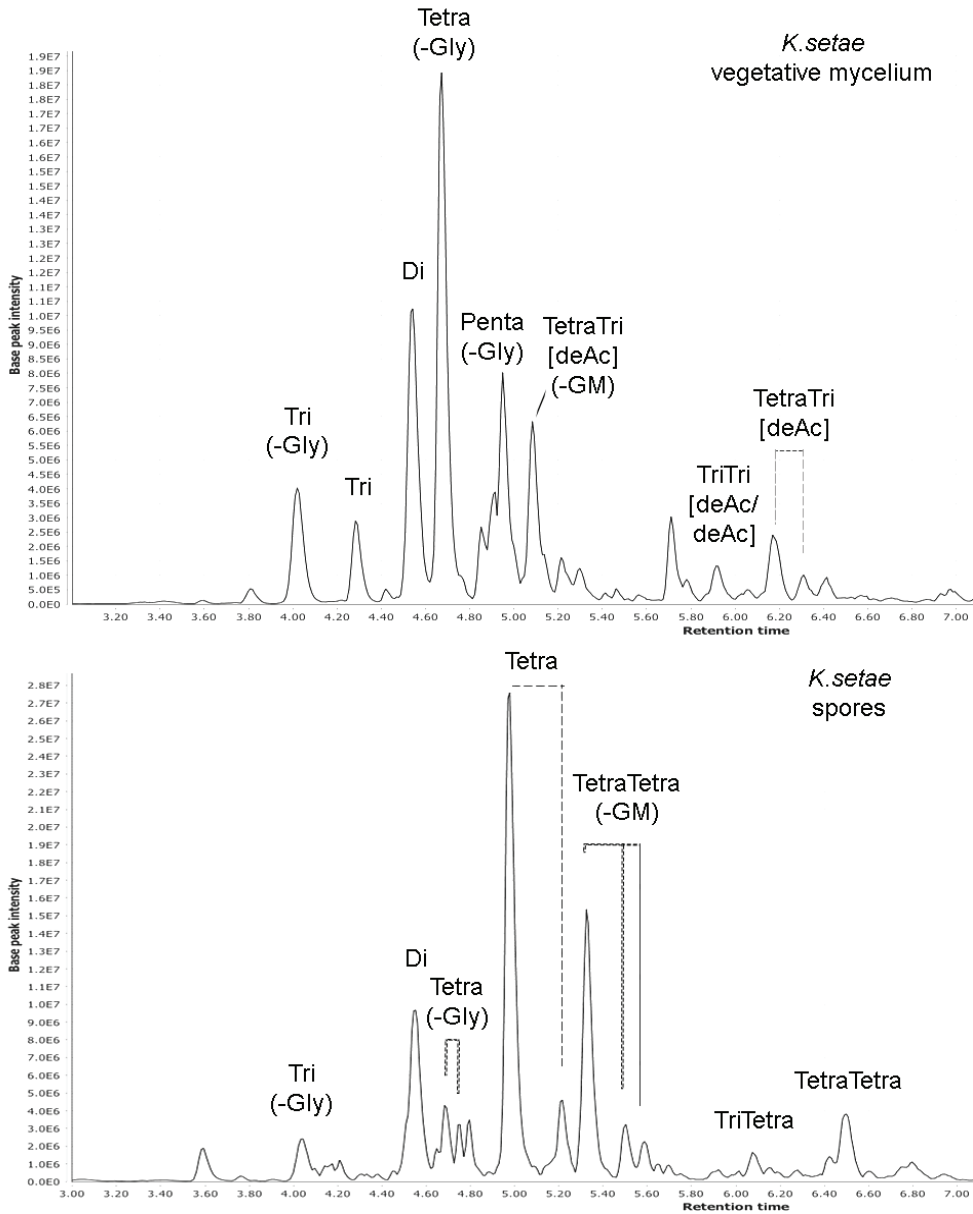


Figure 2. Separation of mucopeptides from vegetative cells (top) and spores (bottom) of *K. setae*. Major peaks are labeled and correspond to the labels in Table 1. In vegetative PG, the major peaks are tetrapeptides lacking Gly, Tetra(-Gly), and pentapeptides lacking Gly, Penta(-Gly) with a high amount of de-acetylated, [deAc], dimers. In spore PG, the major peaks are tetrapeptides (Tetra) and TetraTetra dimers lacking GlcNac-MurNac, TetraTetra(-GM). The x-axis shows the retention time in minutes, the y-axis the base peak intensity in arbitrary units.

Table 2. Relative abundance(%)^b of mucopeptides from *K. viridifaciens*

Muropeptides ^a	<i>K. viridifaciens</i>					
	16h	30h	42h	64h	spores	Δ <i>ssgB</i>
Monomers	1.4	1.3	1.8	1.8	2.3	0.5
Mono	0.1	0.2	0.3	0.3	0.2	0.1
Di [deAc]	8.4	11.6	14.6	13.7	7.5	8.5
Di	1.0	0.9	1.1	0.9	0.7	0.5
Tri (-Gly)	0.2	1.1	1.1	9.4	39.9	6.1
Tri [NH ₂]	0.3	2.4	0.1	0.6	0.1	14.1
Tri (-G) [deAc]	0.4	0.6	0.7	1.5	2.4	0.6
Tri	31.6	27.3	31.7	24.2	17.3	16.9
Tetra (-Gly)	0.8	0.7	0.7	0.9	0.7	0.4
Tetra [Gly ₄]	2.2	0.9	0.8	0.8	0.5	0.4
Tetra-X	0.2	2.6	0.1	0.5	0.3	14.8
Tetra	29.5	31.3	28.9	31.5	22.8	17.8
Penta [Gly ₅]	3.1	1.6	1.6	1.3	1.0	0.7
Penta -X	0.2	1.4	0.1	0.3	0.1	8.9
Penta	20.6	16.2	16.9	12.7	4.2	9.6
Deacetylation	0.4	0.8	1.0	1.8	2.7	0.7
amidation DAP	0.2	1.1	1.1	9.4	39.9	6.1
Modification 'X' ^c	0.8	6.4	0.2	1.4	0.5	37.8
	<i>K. viridifaciens</i>					
	16h	30h	42h	64h	spores	Δ <i>ssgB</i>
Dimers	1.4	1.2	2.9	1.1	3.4	1.5
TriTri	6.1	4.6	8.1	6.3	3.2	7.8
TriTri (-GM)	35.1	33.0	31.5	31.5	45.0	25.5
TriTetra	2.8	3.2	3.3	2.3	0.7	2.5
TriTetra (-GM) (-Gly)	5.5	16.4	16.0	15.0	8.0	22.4
TetraTetra	19.9	18.1	18.3	20.4	13.7	12.9
TetraTetra [Gly]	1.2	3.0	0.5	1.3	12.9	2.3
TetraTetra (-GM)	16.6	11.9	7.4	10.5	7.3	15.7
TetraPenta	9.7	6.1	9.6	8.8	2.9	7.9
missing MurNAcGlcNAc	31.0	36.1	34.9	34.0	19.3	48.4
3-3 cross links	50.9	58.4	61.9	56.1	55.8	56.5

^a The labels correspond to the labels in Figure 3. (-Gly) misses the DAP-linked Gly, [Gly₄] or [Gly₅] has Gly instead of the 4th or 5th D-Ala, [deAc] carries MurN instead of MurNAc, (-G) lacks GlcNAc, (-GM) lacks GlcNAcMurNAc.

^bRelative abundance is calculated as the ratio of the peak area over the sum of all peak areas recognized in the chromatogram.

^cThe molecular mass assumed with '-X' is 2.01 Da.

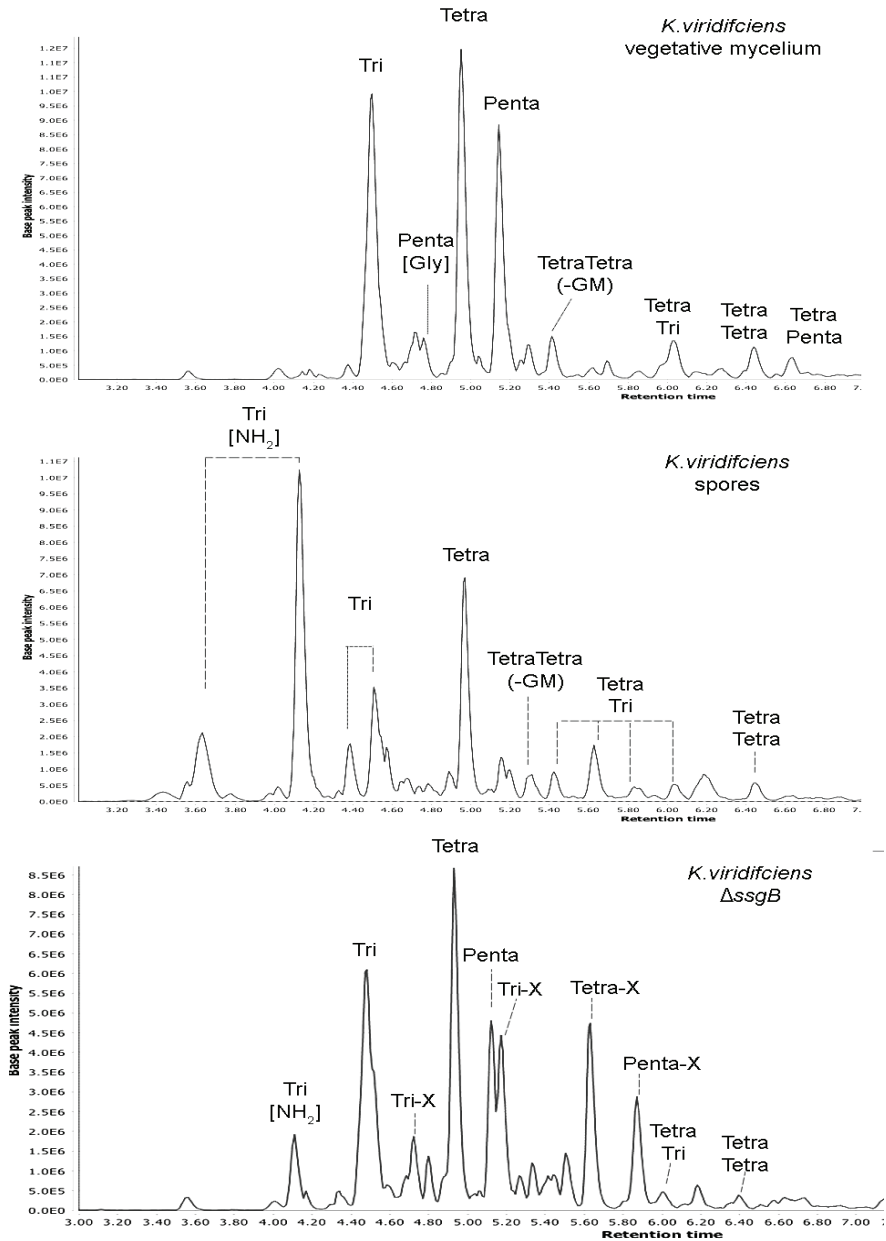


Figure 3. separation of muropeptides from *K. viridifaciens* vegetative mycelium (top), spores (middle) and the Δ ssgB deletion mutant (bottom). Major peaks are labeled and correspond to the labels in Table 2. Major peaks in vegetative mycelium are tripeptides, tetrapeptides and pentapeptides, Tri, Tetra and Penta. In spores, the major peaks are tripeptides with amidated DAP, Tri [NH₂] Tetra and the dimer consisting of a tetrapeptide and tripeptide, TetraTri. The muropeptide profile of the *ssgB* deletion mutant shows major amounts of muropeptides with modification 'X'. The x-axis shows the retention time in minutes, the y-axis the base peak intensity in arbitrary units.

In *K. setae*, the primary modifications in vegetative cells are the loss of the DAP-bound Gly and the de-acetylation of MurNAc, giving MurN, as shown in Figure 2 and Table 1. The major muropeptides seen in vegetative cells after 16 h of growth were tetrapeptides lacking Gly (Tetra (-Gly)) and dipeptides (Di), making up 37.2% and 24.5% of the total monomer content, respectively. This switches to tetrapeptides with Gly (tetra) and dipeptides (Di) at 51.2% and 22.6% of the monomers in spores. The amount of pentapeptides (-Gly) is higher in vegetative cells (14.5% of monomers) than in spores (3% of monomers).

The PG profile of *K. viridifaciens* is shown in Figure 3 and Table 2. The main difference between vegetative cells and spores was the amidation of DAP in spores. Vegetative hyphae of *K. viridifaciens* grown for 16 h had large amounts of tri-, tetra- and pentapeptides, 31.6%, 29.5% and 20.6% of the total content, respectively. In spores, this changed to tripeptides with an amidated DAP (Tri [NH₂]) and tetrapeptides (tetra), making up 39.9% and 22.8% of the total, respectively. The total monomer fraction with an amidated DAP was 40% in spores, whereas this modification was present only in trace amounts in vegetative mycelia (0.2 and 1.1% after 16 and 42 h, respectively). After 64 h, 9.4% of the muropeptides carried an amidated DAP, consistent with the formation of spores. Spore monomers carry a low amount of de-acetylated monomers, though a specific muropeptide contributed to this amount, MurN-tripeptides as have been found in *S. coelicolor*, mostly as LL-DAP (1.9% LL-DAP, 0.5% meso-DAP).

Modifications to dimers

Dimers are cross-linked via the DAP-bound Gly and, like in *Streptomyces*, *Kitasatospora* PG contains both 3-3 and 3-4 cross-links. Penicillin Binding Proteins (PBPs) recognize a pentapeptide as a donor strand, catalyze the cross-link of an DAP-bound Gly to D-Ala(4) on the opposite strand and cleave off the terminal D-Ala from the pentapeptide donor strand. L,D-transpeptidases recognize tetrapeptides and catalyze a cross-link between DAP-bound Gly and DAP, this way generating a 3-3 cross-link, and finally remove the terminal D-Ala from the tetrapeptide donor strand. TetraTetra dimers are cross-linked by a 3-4 cross-link, while TriTri dimers are cross-linked by a 3-3 cross-link. However, TetraTri dimers can be cross-linked by either 3-3 or 3-4 bonds; these two isomers have the same mass but they can be discriminated based on the difference in retention times. The cross-linking pattern was resolved by MS/MS (data not shown). In addition, cleavage of the glycan strand at the lactyl bond between MurNAc and L-Ala will give rise to dimers lacking one set of glycans.

Analysis of the PG dimers of *K. setae* showed that deacetylation of the glycan strands occurred mostly in vegetative cells (86.8% at 16 h) and far less frequently in spores (3.8%). In vegetative cells, both dimers with a double and a single set of glycans shows de-acetylated MurNAc, where 80% of the TetraTetra dimers lacking a set of glycans still carries MurN, suggesting that amidases are more likely to cleave off the dimers containing MurNAc than those containing MurN. Conversely, *K. setae* has an exceptionally high amount of dimers that have lost a set of glycans, representing 56-68% of the dimers throughout growth. The amount of 3-3 cross-links is higher in vegetative mycelium than in spores, at 92.4% at 16 h, 90.7 % at 30 h, 83.8 at 42 h, 47.1 at 64 h and 28.8% in spores. The PG dimers of *K. viridifaciens* had undergone less extensive hydrolysis as compared to those of *K. setae*, whereby 31-36% of the dimers of 16-64 h old cultures lacked a set of glycans, compared to

50-68% in *K. setae*. The amount of 3-3 cross-links in *K. viridifaciens* was relatively stable over time, between 50 and 62%.

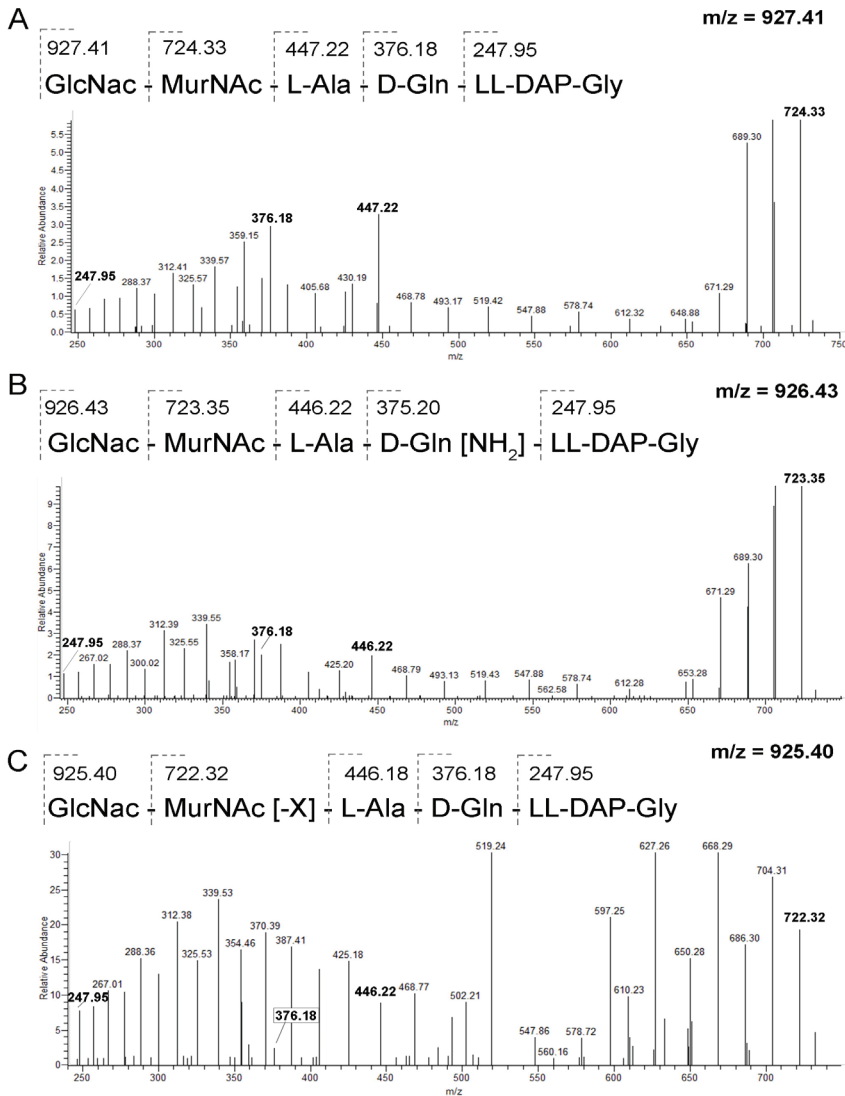


Figure 4. MS/MS fragmentations of (A), a tripeptide (Tri), which has a m/z of 927.41, (B) a tripeptide with an amidated DAP (Tri [NH₂]), with an m/z of 926.43, and (C) a tripeptide with a 'X' modification (Tri [-X]) with an m/z of 925.40. The base structure shows the major fragment masses, which are given in bold in the mass spectrum.

Transition from mycelium to spores

The *ssgB* deletion mutant of *K. viridifaciens* forms normal vegetative and aerial mycelia but does not form spores. Studying this mutant therefore allows us to observe modifications specific for older aerial mycelia even after prolonged incubation, without having to take spores into account. Interestingly, the muropeptide profile of the *ssgB* null mutant contained many muropeptides with an unknown modification, here named 'X'. Canonical tripeptides have a mass of (M+H) 927.41, while the Tri [-X] peptides from *ssgB* mutants had a mass of (M+H) 925.40. Therefore, the 'X' modification represents a 2.01 Da mass reduction as compared to other muropeptides. This suggests that a double bond is present in the Tri [-X] while the bond is reduced in canonical tripeptides. After recognizing this modification in the *ssgB* mutant, we revisited the PG profiles of *K. viridifaciens* and scrutiny of these samples also identified minor amounts of modification 'X' in 30 h old samples, namely 5.7% of the monomers. Suggestively, this is the moment the strain has produced aerial hyphae but does not yet form spores. Modification 'X' most likely occurs at the MurNAc moiety, as MS/MS analysis showed the initial loss of GlcNAc, and this still showed the mass difference, while the mass difference was resolved at the pentapeptide chain (see Figure 4).

DISCUSSION

Kitasatosporae are characterized by the striking difference in stereochemistry of DAP between vegetative and spore PG (Takahashi, 2017). We show that besides the DAP stereochemistry, the entire PG composition changes between these two growth phases in their life cycle. Despite the similarity in their life cycles, this has not been seen in *Streptomyces* (van der Aart *et al.*, 2018). Vegetative mycelia of *K. setae* lack the DAP-bound Gly and has heavily de-acetylated MurNAc, whereas spore PG carries the DAP-bound Gly and shows less de-acetylation. *K. viridifaciens* vegetative mycelium carries no modifications, whereas spores carry *N*-deacetylated MurN lacking GlcNAc, called MurN-Tri, and a large amount of amidated DAP. The amidation of DAP in *K. viridifaciens* occurs mostly in the spore wall, where 40% of all monomers carry an amidated version of DAP, in contrast to 0.2% in the 16 h old vegetative mycelium. Interestingly, 6.1% of the DAP residues in the cell wall of the non-sporulating *ssgB* mutant was amidated. Amidation of DAP contributes to lysozyme resistance by slightly decreasing the negative charge of the PG, that way reducing affinity of the positively charged lysozyme (Levefaudes *et al.*, 2015). However, this modification was not found in *K. setae*, and is therefore not a trait that is typical of all members of the genus *kitasatospora*.

PG cross-linking is performed by two different types of proteins, penicillin binding proteins (PBPs) and L, D-transpeptidases (LDTs). PBPs produce canonical 3-4 cross-links between the DAP-bound Gly and the 4th amino acid of the next strand, D-Ala. LDTs produce 3-3 cross-links between the DAP-bound Gly and the 3rd amino acid of the next strand, DAP. Tip growing bacteria have a relatively high amount of 3-3 cross-links due to the remodeling of the lateral wall by LDTs (Baranowski *et al.*, 2018). We have shown that in *Kitasatospora* the cross-linking is similar as in *Streptomyces*, as was apparent from the MS/MS patterns. In *K. setae*, the amount of 3-3 cross-links is high in vegetative (92% at 16 h) and lower during sporulation (47% at 64 h) and in spore preparations (29%). In *K. setae* and in *S. coelicolor* the proportion of 3-3 cross-links is higher in vegetative mycelium than in spores, which makes a correlation to specific DAP-isomers unlikely. In *K. viridifaciens*, the amount of 3-3 cross-links remained stable throughout growth at 50-62%, in contrast to what was observed for the PG of *K. setae*, where the amount of 3-3 cross-links was growth phase-dependent. The high amount of dimers lacking a set of glycans in *K. setae* is striking, as this type of dimer does not contribute to strengthening the PG structure (Vollmer *et al.*, 2008). Even of the dimers found in spores 61% lacked glycans, whereby a TetraTetra dimer lacking GlcNAc-MurNAc (TetraTetra(-GM)) prevailed (38.1%). In *K. viridifaciens*, the amount of dimers lacking glycans was lower, namely 31%- 36% in vegetative mycelium and 19.3% in spores.

The cell wall of the *ssgB* null mutant of *K. viridifaciens* showed a mass that could not be explained, and may therefore represent a unique modification. Ms/Ms analysis showed that the loss of 2.01 Da took place at the MurNAc moiety, and could be accounted for by formaitn of a double bond and hence loss of two hydrogens, such as in non-reduced MurNAc. The modification is highly abundant in the peptidoglycan of the *ssgB* mutant, but also occurred in small amounts over the course of growth, especially after 30 h of growth, coinciding with the onset of aerial mycelium formation by *K. viridifaciens*. This is precisely the stage where *ssgB* mutants are blocked in development, and we may therefore see the consequence of a specific cell-cycle arrest. Modification "X" may be part of a hydrolytic event. Peptidoglycan amidases

recognize tri-, tetra- and pentapeptides and targets the site between MurNac and L-Ala, then the mucopeptide is cleaved between the MurNac-associated D-Lac and L-Ala (Rocaboy *et al.*, 2013; Wang *et al.*, 2003). The exact nature of the ‘-X’ modification requires further investigation.

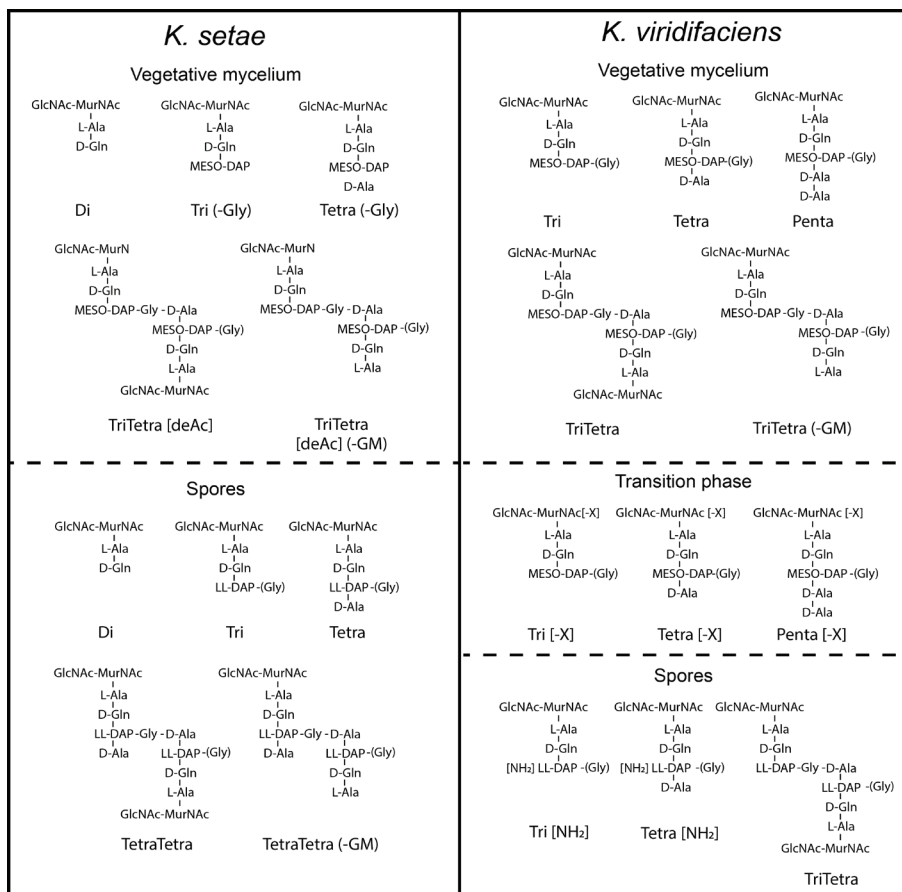


Figure 5. summary of mucopeptides found in *K. setae* and *K. viridifaciens* vegetative mycelium and spores. Vegetative mycelium of *K. setae* shows mucopeptides with Meso-DAP, lacking Gly (-Gly) and with de-Acetylated MurNac [deAc], spore cell walls carry mucopeptides with LL-DAP, Gly and less deacetylation. *K. viridifaciens* carries Meso-DAP in vegetative mycelium, in transition phase, modification X occurs at the site of MurNac. Spore mycelium shows LL-DAP and amidated DAP [NH₂]. In all life stages, some dimers lack a set of glycans (-GM).

Cell wall construction

DapF is responsible for the isomerization of LL-DAP into *meso*-DAP, while *K. setae* has 3 copies of this gene, other species of *Kitasatospora* have a single copy (Girard *et al.*, 2014). *Streptomyces* species, which only have LL-DAP, also carry DapF but *meso*-DAP can be an intermediate in the production of Lysine. During the process of cell wall construction, the well-conserved MurE adds LL- or *meso*-DAP to

UDP-MurNac-L-Ala-D-Glu (Smith, 2006). The only other bacterium that carries both LL- and *meso*-DAP, the Gram-negative *Myxococcus xanthus*, has a single version of MurE (Bui *et al.*, 2009). *Kitasatosporae* apparently carry two versions of MurE, one of which is encoded by a gene in the *dcw* (division of cell wall) cluster and one by a gene elsewhere on the genome. It needs to be analyzed whether the second MurE paralogue is functional and if so, whether it has similar bioactivity as the canonical MurE. In any case, the *murE* genes of *Kitasatosporae* (LL- and *meso*-DAP) are placed in a separate clade from *Streptomyces* (LL-DAP) and *Mycobacterium* (*meso*-DAP), suggesting that the canonical MurE could be adapted to ligate both LL- and *meso*-DAP (Hwang *et al.*, 2015).

Implications for taxonomy

The switch from incorporation of *meso*-DAP to incorporating LL-DAP in the PG allows us to recognize the difference between these different types of mycelia, which is more elusive in *Streptomyces*. Notably, *Kitasatosporae* appear to hydrolyze most of the mycelia with *meso*-DAP at the switch to spore formation, and although the concept of programmed cell death is not novel, the hydrolysis of practically all PG with *meso*-DAP comes as a surprise. After 64 h, the cell wall of both *Kitasatosporae* mostly contains LL-DAP, indicating that extensive hydrolysis of the vegetative mycelium has taken place. This implies that if chemotaxonomy is performed on older cultures of *Kitasatosporae*, the data could be confused with those obtained for *Streptomyces*. Previous amino acid composition analyses had already shown that *K. setae* carries very little glycine in the vegetative mycelium, but an equal amount of Gly per DAP in spores (Takahashi *et al.*, 1999). However, this shift in the amount of Gly is not specific for *Kitasatosporae*, as *K. viridifaciens* has equal amounts of Gly per DAP throughout its life cycle.

In summary, our data show that *Kitasatosporae* have different modifications in vegetative mycelium and in spores, besides just the switch from *meso*-DAP to LL-DAP. This switch requires different modifying and hydrolyzing proteins and emphasizes that tip growth and sporulation are regulated by two different systems. Mycelium of the *ssgB* contained a yet unidentified modification, which suggests loss of 2.01 Da in the MurNac moiety. The presence of only trace amounts of LL-DAP in this mutant indicates that the DAP stereochemistry of the *Kitasatospora* cell wall changes at a time prior to the onset of septation. It is difficult to say whether the difference in stereochemistry is a consequence or a cause of the switch in regulation between vegetative- and reproductive growth.

Acknowledgements

The *ssgB* mutant of *K. viridifaciens* was a kind gift from Karina Ramijan and Dennis Claessen.

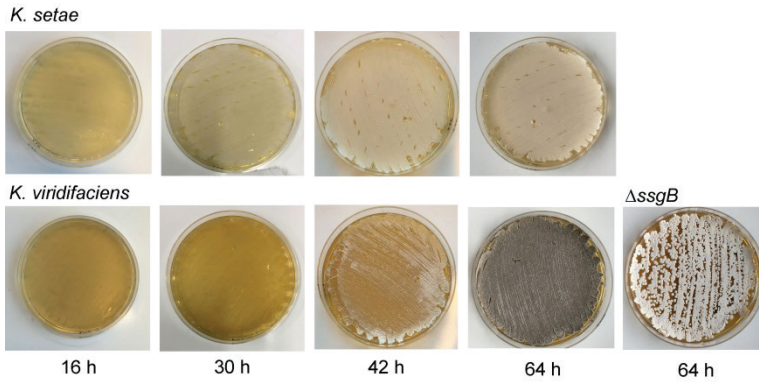
Appendix 1. Supplemental information belonging to Chapter 4

Figure S1. Development of *K. setae* and *K. viridifaciens* grown on SFM agar plates. After 42 h, *K. setae* had developed white spores, as seen with an impression print, while *K. viridifaciens* developed white aerial mycelium at 42 h and grey spores after 64 h. The *ssgB* mutant of *K. viridifaciens* only formed aerial hyphae and did not develop spores.

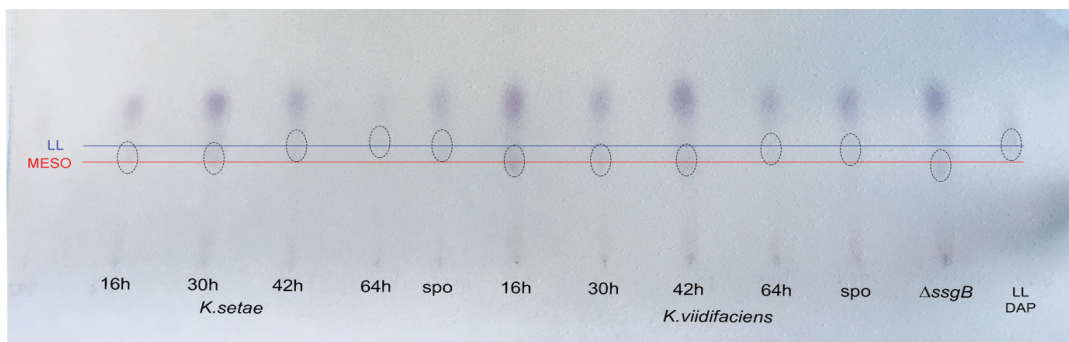


Figure S2. DAP analysis of *K.setae* and *K.viridifaciens* over growth. At 16 h, both strains only carry *meso*-DAP in the PG, after 42 hours this shifts to LL-DAP. At 64 h both strains carry mostly LL-DAP. The *ssgB*-mutant consists mostly of *meso*-DAP but has trace amounts of LL-DAP.

Table S1. Muropeptides identified in *K. setae* peptidoglycan

Monomers	Observed mass		<i>K. setae</i>				
	[M+H]	rt	16 h	30 h	42 h	64 h	spores
Mono	570.25	4.68	2.1%	2.3%	2.4%	0.2%	0.0%
Di [deAc]	656.30	4.08	0.3%	0.8%	1.2%	1.0%	0.9%
Di	698.31	4.54	20.2%	22.5%	21.6%	22.9%	17.5%
Di [Glu]	699.30	4.99	4.0%	4.4%	4.6%	4.9%	4.2%
Tri (-Gly)	870.40	4.02	8.5%	9.5%	10.9%	8.9%	4.7%
Tri (-Gly) [Glu]	871.38	4.29	1.3%	1.4%	2.1%	1.5%	0.6%
Tri	927.42	4.28	5.1%	7.6%	4.2%	2.5%	0.0%
Tri	927.42	4.52	0.0%	0.3%	1.5%	3.0%	6.2%
Tri [Glu]	928.40	4.76	0.0%	0.0%	0.1%	0.3%	0.7%
Tri [Glu]	928.40	4.51	0.9%	1.2%	0.7%	0.0%	0.0%
Tetra (-Gly)	941.43	4.67	32.8%	28.4%	25.1%	17.8%	6.4%
Tetra (-Gly) [Glu]	942.42	4.92	4.4%	5.9%	5.8%	3.6%	0.9%
Tetra	998.46	4.53	3.5%	3.2%	2.0%	0.0%	0.0%
Tetra	998.46	4.97	0.7%	3.2%	8.8%	23.4%	44.0%
Tetra [Glu]	999.44	4.76	0.7%	0.4%	0.0%	0.0%	0.0%
Tetra [Glu]	999.44	5.19	0.7%	0.6%	2.1%	4.1%	7.2%
Penta [deAc]	1012.47	4.95	13.8%	6.7%	5.2%	3.0%	0.4%
Penta [Glu/ deAc]	1013.46	5.21	0.1%	1.1%	0.9%	0.5%	0.1%
Penta [Gly5]	1055.48	4.78	0.1%	0.1%	0.1%	0.9%	2.2%
Penta [Gly5]	1055.48	4.29	0.0%	0.1%	0.1%	0.0%	0.0%
Penta [Glu /Gly5]	1056.46	4.61	0.3%	0.0%	0.0%	0.0%	0.0%
Penta	1069.49	5.18	0.0%	0.2%	0.4%	1.1%	2.2%
Penta [Glu]	1070.48	5.44	0.3%	0.0%	0.1%	0.1%	0.3%
Dimers							
	[M+H]	rt	16 h	30 h	42 h	64 h	spores
TriTri (-GM /-Gly)	1298.60	4.59	2.1%	4.0%	1.7%	1.1%	1.8%
TriTri (-GM /-Gly) [Glu]	1299.60	4.60	1.9%	2.0%	2.2%	0.6%	0.3%
GnacMN-tritri	1313.60	5.06	1.8%	4.2%	3.7%	1.9%	0.6%
GnacMN-tritri	1313.60	5.61	3.7%	8.9%	7.8%	3.1%	0.5%
GnacMN-tritri	1314.60	5.60	1.8%	0.7%	3.3%	2.2%	0.4%
GnacMN-tritri	1314.62	4.91	4.8%	8.9%	6.4%	2.8%	0.4%
TetraTri (-GM) (-Gly)	1369.64	4.63	1.9%	5.8%	2.9%	1.9%	0.9%

Supplemental information belonging to Chapter 4

TetraTri (-GM) (-Gly)	1370.63	4.80	1.8%	0.7%	1.8%	0.9%	0.8%
GMN-TetraTri	1383.65	5.08	27.3%	26.0%	20.0%	9.8%	0.4%
GMN-TetraTri	1384.64	5.27	6.8%	6.2%	5.6%	2.6%	0.0%
TetraTri (-GM)	1426.66	5.01	0.0%	0.1%	0.5%	4.9%	12.0%
TetraTri (-GM) [Glu]	1427.66	4.95	1.8%	0.0%	0.7%	1.7%	2.5%
TetraTri (-GM) [Glu,- Glu]	1497.68	4.97	0.0%	0.0%	0.0%	0.0%	2.0%
GM-tetratetra	1497.70	5.32	0.3%	0.6%	3.2%	15.5%	30.8%
GM-tetratetra	1498.68	5.48	0.2%	0.2%	2.6%	1.5%	5.2%
TriTri [deAc,deAc] (3-3)	1792.81	5.94	8.6%	8.3%	7.0%	2.3%	0.7%
TriTri [deAc,deAc] (3-3)	1793.80	6.13	2.5%	0.5%	5.3%	2.1%	0.4%
TriTri [deAc,deAc] (3-3)	1794.82	5.92	2.5%	3.0%	3.2%	0.9%	0.3%
TetraTri [deAc] (3-3)	1863.85	6.18	22.2%	9.5%	5.9%	1.8%	0.1%
GnacMN-tritetraGM (3-3)	1864.84	6.41	0.8%	1.8%	5.7%	2.8%	0.1%
GnacMnac-AEm(G) A-(G)mEA-GM	1906.86	6.08	0.0%	0.0%	0.0%	1.8%	3.9%
GnacMnac-AEm(G) A-(G)mEA-GM	1906.86	6.02	0.0%	0.0%	0.0%	0.5%	0.7%
GM-tri-tetra-MG	1907.84	6.25	0.0%	0.0%	0.0%	0.1%	0.2%
GM-tri-tetra-MG	1907.86	6.03	0.0%	0.0%	0.0%	1.2%	1.7%
TetraTetra [Gly4 / deAc]	1934.89	6.31	3.9%	1.3%	0.6%	0.1%	0.0%
TetraTetra [Gly4 / Glu]	1964.76	4.54	0.8%	2.1%	4.4%	3.7%	2.2%
TetraTetra [Gly4 / Glu]	1964.76	4.96	1.3%	2.3%	0.8%	5.5%	4.9%
TetraTetra [Gly4 / Glu]	1964.76	6.08	0.3%	1.2%	0.8%	3.7%	0.3%
TetraTetra [Gly4 / Glu]	1964.78	6.41	0.3%	1.2%	1.2%	5.2%	0.3%
GM-tetra-tetra-MG	1977.90	6.50	0.2%	0.3%	1.2%	5.4%	11.1%
GM-tetra-tetra-MG	1978.88	6.76	0.2%	0.1%	0.7%	6.1%	2.7%
GM-tetra-tetra-MG	1978.90	6.49	0.2%	0.1%	0.7%	6.3%	11.4%
GM-tetra-tetra-MG	1979.39	6.50	0.0%	0.0%	0.0%	0.0%	0.3%

Table S2. Muropeptides identified in *K. viridifaciens* peptidoglycan

m/z	Monomers ID	observed mass		<i>K. viridifaciens</i>						
		[M+H]	rt (min)	16 h	30 h	42 h	64 h	spores	Δ ssgB	
570.25	Mono	570.25	4.67	1.4%	1.3%	1.8%	1.8%	2.3%	0.5%	
656.30	Di [deAc]	656.30	4.07	0.1%	0.2%	0.3%	0.3%	0.2%	0.1%	
682.27	Tri [deAc] (-G)	682.27	4.99	0.0%	0.0%	0.1%	1.0%	1.9%	0.0%	
682.30	Tri [deAc] (-G)	682.30	4.58	0.4%	0.6%	0.6%	0.5%	0.5%	0.6%	
698.31	Di	698.31	4.52	7.0%	10.1%	12.3%	11.5%	6.3%	7.3%	
699.30	Di [Glu]	699.30	4.98	1.4%	1.3%	2.0%	1.9%	0.9%	1.1%	
724.34	Tri (-G)	724.34	4.49	2.1%	1.9%	2.1%	1.6%	0.7%	1.1%	
725.32	Tri (-G) [Glu]	725.32	4.71	0.3%	0.1%	0.2%	0.2%	0.0%	0.1%	
781.36	Tetra (-G) [Gly4]	781.36	4.55	0.1%	0.1%	0.0%	0.0%	0.0%	0.0%	
795.38	Tetra (-G)	795.38	4.95	1.7%	2.0%	1.8%	2.1%	1.4%	1.2%	
796.36	Tetra (-G) [Glu]	796.36	5.18	0.2%	0.1%	0.2%	0.2%	0.1%	0.1%	
870.40	Tri (-Gly)	870.40	4.02	0.9%	0.9%	1.0%	0.9%	0.7%	0.5%	
871.38	Tri (-Gly) [Glu]	871.38	4.28	0.1%	0.1%	0.1%	0.1%	0.1%	0.0%	
925.40	Tri-X	925.40	4.72	0.1%	0.7%	0.0%	0.2%	0.1%	3.8%	
925.40	Tri-X	925.40	5.17	0.2%	1.7%	0.0%	0.4%	0.1%	10.3%	
926.43	Tri [NH2]	926.43	3.63	0.0%	0.0%	0.0%	0.4%	9.9%	2.7%	
926.43	Tri [NH2]	926.43	4.12	0.2%	1.1%	1.1%	9.0%	30.1%	3.4%	
927.42	Tri	927.42	4.39	0.0%	0.0%	0.0%	0.0%	5.0%	0.0%	
927.42	Tri	927.42	4.50	25.0%	22.8%	26.2%	19.9%	10.2%	13.9%	
928.40	Tri [Glu]	928.40	4.71	4.2%	2.4%	3.2%	2.5%	1.4%	1.8%	
941.43	Tetra (-Gly)	941.43	4.67	0.8%	0.7%	0.7%	0.9%	0.7%	0.4%	
984.44	Tetra [Gly4]	984.44	4.55	1.9%	0.9%	0.7%	0.7%	0.5%	0.4%	
985.42	Tetra [Glu/Gly4]	985.42	4.75	0.2%	0.0%	0.0%	0.0%	0.1%	0.0%	
996.44	Tetra -X	996.44	5.22	0.0%	0.6%	0.0%	0.0%	0.0%	3.8%	
996.44	Tetra -X	996.44	5.69	0.2%	1.4%	0.0%	0.4%	0.2%	8.3%	
997.43	Tetra [Glu/ -X]	997.43	5.89	0.0%	0.3%	0.0%	0.1%	0.0%	2.0%	
997.43	Tetra [Glu / -X]	997.43	5.39	0.0%	0.3%	0.0%	0.0%	0.0%	0.8%	
998.46	Tetra	998.46	4.95	23.4%	26.0%	24.2%	25.9%	18.6%	14.6%	
999.44	Tetra [Glu]	999.44	5.18	4.1%	3.1%	2.7%	3.4%	2.7%	2.0%	
1055.48	Penta [Gly5]	1055.48	4.76	2.7%	1.5%	1.4%	1.2%	1.0%	0.6%	
1056.46	Penta [Glu /Gly5]	1056.46	4.98	0.4%	0.1%	0.1%	0.1%	0.0%	0.0%	
1067.48	Penta -X	1067.48	5.87	0.1%	0.4%	0.0%	0.2%	0.0%	5.2%	
1067.48	Penta -X	1067.48	5.33	0.1%	0.9%	0.0%	0.0%	0.0%	2.0%	

Supplemental information belonging to Chapter 4

1068.46	Penta [Glu / -X]	1068.46	6.18	0.0%	0.1%	0.0%	0.0%	0.0%	1.2%
1068.46	Penta [Glu / -X]	1068.46	5.62	0.0%	0.0%	0.0%	0.0%	0.0%	0.5%
1069.49	Penta	1069.49	5.14	17.5%	14.5%	14.9%	11.2%	3.7%	8.4%
1070.48	Penta [Glu]	1070.48	5.41	3.2%	1.8%	2.0%	1.5%	0.5%	1.3%
Dimers	Dimers								
m/z	ID	[M+H]	rt(min)	16 h	30 h	42 h	64 h	spores	Δ ssgB
1298.60	TriTri (-GM /-Gly)	1298.60	5.07	2.9%	1.2%	2.9%	2.1%	2.0%	0.9%
1355.62	TriTri (-GM)	1355.62	4.60	3.2%	3.4%	5.2%	4.2%	1.2%	6.9%
1369.64	TetraTri (-GM) (-Gly)	1369.64	5.25	2.8%	3.2%	3.3%	2.3%	0.7%	2.5%
1426.66	TetraTri (-GM)	1426.66	4.93	5.5%	16.4%	16.0%	15.0%	8.0%	22.4%
1497.70	TetraTetra (-GM)	1497.70	5.30	5.0%	5.2%	4.4%	6.8%	3.9%	4.7%
1498.68	TetraTetra (-GM) [Glu]	1498.68	6.18	7.8%	4.5%	2.5%	3.1%	2.5%	8.5%
1499.68	TetraTetra (-GM) [Glu/Glu]	1499.68	6.16	3.7%	2.2%	0.6%	0.6%	0.9%	2.4%
1835.82	TriTri (3-3)	1835.82	5.62	1.4%	1.2%	2.9%	1.1%	3.4%	1.5%
1904.84	TetraTri [-X]	1904.84	6.62	0.0%	0.0%	0.0%	0.0%	0.0%	3.2%
1906.87	TetraTri (3-4)	1906.87	5.42	0.0%	0.0%	0.0%	0.0%	4.5%	0.0%
1906.87	TetraTri (3-3)	1906.87	5.63	0.7%	0.9%	0.4%	2.9%	20.1%	0.0%
1906.86	TetraTri (3-3)	1906.86	5.83	0.0%	0.0%	0.0%	0.0%	3.4%	0.0%
1906.86	TetraTri (3-3)	1906.86	6.04	17.4%	17.0%	16.3%	14.6%	9.4%	11.7%
1907.86	TetraTri [Glu] (3-3)	1907.86	6.03	17.0%	15.0%	14.8%	14.0%	7.6%	10.6%
1907.84	TetraTri [Glu] (3-4)	1907.84	6.25	1.9%	2.5%	2.3%	3.0%	2.8%	1.5%
1964.75	TetraTetra[Gly4]	1964.75	5.15	1.2%	3.0%	0.5%	1.3%	12.9%	2.3%
1977.89	TetraTetra	1977.89	6.45	8.6%	9.2%	9.1%	10.2%	8.8%	6.6%
1978.90	TetraTetra [Glu]	1978.90	6.37	11.2%	9.0%	9.2%	10.2%	4.9%	6.3%
2048.93	PentaTetra	2048.93	6.63	5.3%	2.3%	4.3%	3.4%	1.7%	3.8%
2049.93	PentaTetra [Glu]	2049.93	6.57	4.3%	3.8%	5.2%	5.4%	1.2%	4.1%

Supplementary table 3

The amino acid composition in the cell wall of *K.setae* was previously assessed to be:

Cell type	DAP	Ala	Glu	Gly
Aerial spores	1.0 (<i>LL</i>)	1.6	0.5	1.0
Vegetative mycelium	1.0 (<i>meso</i>)	1.6	0.7	0.2

Amino acid composition in the cell walls of *K.setae* (Molar ratio). Table adapted from (Takahashi *et al.*, 1999)

CHAPTER 5

Substrate inhibition of VanA by D-alanine reduces vancomycin resistance in a VanX-dependent manner

Lizah T. van der Aart, Nicole Lemmens, Willem J. van Wamel and Gilles P. van Wezel

Adapted from: *Antimicrobial Agents and Chemotherapy* (2016)
vol. 60 no. 8 4930-4939

Supplementary material available at:
<https://aac.asm.org/content/early/2016/06/01/AAC.00276-16>

ABSTRACT

The increasing resistance of clinical pathogens against the glycopeptide antibiotic vancomycin, a last resort drug against infections with Gram-positive pathogens, is a major problem in the nosocomial environment. Vancomycin inhibits peptidoglycan synthesis by binding to the D-Ala-D-Ala terminal dipeptide moiety of the cell-wall precursor Lipid II. Plasmid-transferable resistance is conferred by modification of the terminal dipeptide into the vancomycin-insensitive variant D-Ala-D-Lac which is produced by VanA. Here we show that exogenous D-Ala competes with D-Lac as a substrate for VanA, increasing the ratio of wild-type over mutant dipeptide, an effect that was augmented by several orders of magnitude in the absence of the D-Ala-D-Ala peptidase VanX. LC-MS analysis showed that high concentrations of D-Ala led to the production of a significant amount of wild-type cell-wall precursors, while *vanX* null mutants produced primarily wild-type precursors. This enhanced the efficacy of vancomycin in the vancomycin-resistant model organism *Streptomyces coelicolor*, and the susceptibility of vancomycin-resistant clinical isolates of *Enterococcus faecium* (VRE) increased by up to 100-fold. The enhanced vancomycin sensitivity of *S. coelicolor* cells correlated directly to increased binding of the antibiotic to the cell wall. We isolated the VanX protein from *E. faecium* (VanB-type) and developed an assay with a fluorescent readout which can easily be adapted to a high throughput system for a potential inhibitor screen. Our work offers new perspectives for the treatment of diseases associated with vancomycin-resistant pathogens and for the development of drugs that target vancomycin resistance.

INTRODUCTION

Infectious diseases caused by multi-drug-resistant (MDR) pathogens are spreading rapidly and are among the biggest threats to human health (Arias & Murray, 2009, Boucher *et al.*, 2009, Laxminarayan *et al.*, 2013, WHO, 2014). To deal with the increasing antibiotic resistance, novel antibiotics are called for, or alternatively the lifespan of the current drugs must be prolonged by compounds counteracting resistance. Exemplary is amoxicillin-clavulanic acid (Augmentin), which is a combination of a β -lactam antibiotic (amoxicillin), and a β -lactamase inhibitor (clavulanic acid) (Reading & Cole, 1977).

The cell wall and its biosynthetic machinery are a major target of the action of clinical antibiotics, including fosfomicin, bacitracin, cycloserine, β -lactam antibiotics (penicillins, cephalosporins) and glycopeptide antibiotics (vancomycin and teicoplanin) (Breukink & de Kruijff, 2006, Bugg *et al.*, 2011, Silver, 2013). Enterococci and many other Gram-positive pathogenic bacteria are resistant to a wide spectrum of antibiotics and can often only be treated with specific β -lactam antibiotics or with vancomycin (Rice, 2001, Frieden *et al.*, 1993, Bell *et al.*, 1998). Vancomycin resistance was first discovered in the 1950s (Walsh *et al.*, 1996). Vancomycin resistance is exchanged between bacteria via movable elements such as transposon *Tn1546*, which is carried by many vancomycin-resistant enterococci (VRE) (Courvalin, 2006). The most common forms of transferable vancomycin resistance are the VanA- and VanB-type resistance, the expression of which is inducible by vancomycin. VanA-type strains are resistant to high levels of vancomycin as well as to another glycopeptide antibiotic, teicoplanin, while VanB-type strains only show inducible resistance to vancomycin but retain susceptibility to teicoplanin (Aslangul *et al.*, 1997). While vancomycin resistance is most prevalent in enterococci (Murray, 2000), resistance has spread to methicillin-resistant *Staphylococcus aureus* (MRSA) (Howden *et al.*, 2010).

Vancomycin targets the cell wall and prevents cell growth by specifically binding to the D-alanyl-D-alanine (D-Ala-D-Ala) termini of the peptidoglycan (PG) precursor Lipid II, prior to its incorporation (Reynolds, 1989, Fischer *et al.*, 2013). The terminal D-Ala-D-Ala dipeptide is almost universally conserved in bacteria, the only exceptions being D-Ala-D-Lac or D-Alanyl-D-Serine in strains with either natural or acquired resistance to vancomycin (Vollmer *et al.*, 2008a). The VanA-type vancomycin resistance gene cluster in *S. coelicolor* consists of seven genes in four different operons: VanRS, VanJ, VanK and VanHAX that together mediate the substitution of the terminal D-alanine (D-Ala) by D-lactate (D-Lac), thereby decreasing the affinity of vancomycin for lipid II by three orders of magnitude (Walsh *et al.*, 1996, Smith *et al.*, 1999). The vancomycin resistance gene cluster provides resistance to both vancomycin and to teicoplanin and is located on the genome of the vancomycin producer *Amycolatopsis mediterranei* (Marshall *et al.*, 1998, van Wageningen *et al.*, 1998) as well as that of other actinomycetes, including the model species *Streptomyces coelicolor* A3(2) (Hong *et al.*, 2004).

Streptomyces are Gram-positive soil bacteria with a complex multicellular life style (Claessen *et al.*, 2014, Flårdh & Buttner, 2009, Barka *et al.*, 2016). Streptomyces are a major source of antibiotics and many other natural products of medical and biotechnological importance, such as anticancer, antifungal or herbicidal compounds (Bérdy, 2005, Hopwood, 2007). Due to the competitive environment of the soil, these microorganisms readily exchange genetic material, including antibi-

Substrate inhibition of VanA by D-alanine reduces vancomycin resistance in a VanX-dependent manner

otic biosynthetic clusters and antibiotic resistance (Wiener *et al.*, 1998, Allen *et al.*, 2010). *S. coelicolor* is a non-pathogenic and genetically tractable model system for vancomycin resistance, with a well-annotated genome (Bentley *et al.*, 2002). The vancomycin resistance cluster of *S. coelicolor* consists of *vanRS*, a two-component regulatory system (TCS) consisting of sensory kinase VanS, and response regulator VanR that together ensure the transcription of the resistance genes in response to vancomycin challenge, and five resistance genes in the order *vanJKHAX*, with *vanHAX* forming a single transcription unit. Vancomycin resistant enterococci classically carry *vanRSHAX*, the function of which is highly similar to that in *S. coelicolor*, with the gene products VanH, VanA, VanX sharing 61%, 63% and, 64% aa identity, respectively, while the TCS components VanR and VanS share 31% and 25% aa identity, respectively (Hong *et al.*, 2004, Reynolds *et al.*, 1994). In response to vancomycin at the cell membrane, VanRS ensure the induction of the expression of *vanHAX*, and in the case of *S. coelicolor* also *vanK* and *vanJ* (Hutchings *et al.*, 2006). VanH produces D-Lac from pyruvate (Bugg *et al.*, 1991b), VanA is a D-alanyl-D-lactate (D-Ala-D-Lac) ligase (Wright & Walsh, 1992, Marshall *et al.*, 1997), VanX hydrolyses the D-Ala-D-Ala dipeptide and has been the target of previous studies assessing vancomycin sensitivity and resistance (Reynolds *et al.*, 1994, Wu *et al.*, 1995). VanX acts highly specific, it cleaves D-Ala-D-Ala, D-Ala-Gly, D-Ala-D-Ser, D-Ala-D-Val and D-Ala-D-Asn, but does not cleave D-Ala-L-Ala, L-Ala-D-Ala, L-Ala-L-Ala or the tripeptide D-Ala-D-Ala-D-Ala (Wu *et al.*, 1995). VanK attaches glycine to lipid II with D-Lac as the terminal residue (Hong *et al.*, 2004, Hong *et al.*, 2005). VanJ is not required for vancomycin resistance but is instead involved in the resistance to teicoplanin (Novotna *et al.*, 2012). Importantly, VanA is a bifunctional enzyme, which besides D-Ala-D-Lac can also produce the wild-type D-Ala-D-Ala dipeptide, although this is negligible during vancomycin challenge. (Hong *et al.*, 2005, Hong *et al.*, 2004, Verkade, 2008, Bugg *et al.*, 1991a). In this work, we show that D-Ala, but not L-alanine (L-Ala), acts as an inhibitor of the D-Ala-D-Lac ligase activity of VanA, an effect which is visible in the presence of vancomycin sensitive and resistant PG precursors. This effect was augmented by several orders of magnitude in *vanX* null mutants, effectively sensitizing the strains to vancomycin. We propose that a combination of D-Ala with a VanX inhibitor could resensitize clinical strains of VRE to vancomycin.

MATERIALS AND METHODS

Bacterial strains, culturing conditions and minimal inhibitory concentration (MIC)

Escherichia coli strains JM109 (Sambrook *et al.*, 1989) and ET12567 (Kieser *et al.*, 2000) were used for routine cloning procedures and for extracting non-methylated DNA, respectively. Cells of *E. coli* were grown in Luria-Bertani broth (LB) at 37°C. *Streptomyces coelicolor* A3(2) M145 was the parent of all mutants described in this work. All media and routine *Streptomyces* techniques were carried out as described (Kieser *et al.*, 2000). SFM (soy flour mannitol) agar plates were used for propagating *S. coelicolor* strains and to prepare spore suspensions. For liquid-grown cultures, *S. coelicolor* mycelia were grown in normal minimal media with phosphate (NMMP) supplemented with 1% (w/v) mannitol as the sole carbon source. The MIC of vancomycin against *S. coelicolor* M145 and its mutant derivatives were determined by growth on minimal media (MM) agar plates supplemented with 1% mannitol as the sole carbon source, and 0, 2, 4, 8, 16, 32, 64, 128, 256 or 512 $\mu\text{g}\cdot\text{ml}^{-1}$ vancomycin, in combination with 0, 1, 5, 10 or 50 mM of D-Ala or L-Ala. Due to their much higher vancomycin sensitivity, *vanX* mutants were tested with 1, 5, 10, 50 and 100 μM D-Ala and L-Ala.

Five *vanA*-positive *Enterococcus faecium* (*E. faecium*) strains collected in 2011 and 2014 from patients in the Erasmus University Medical Centre, Rotterdam, The Netherlands were used. Presence of the *vanA* gene was confirmed by real-time PCR with the Light Cycler® 480 instrument (Roche Diagnostics, Almere, The Netherlands) with primers *vanA* F1 and *vanA* R1, and a *vanA*-specific probe labeled with 6-fluorescein amidite (FAM) at the 5' end and with black hole quencher (BHQ1) at the 3' end. The resistance profile of these isolates (Supplemental Table S2) was determined using the VITEK II (BioMerieux) system AST-P586. To determine the MIC of vancomycin against *E. faecium*, cells were grown overnight on Tryptic Soy Agar (TSA) blood agar plates (Becton Dickinson, Breda, The Netherlands) and suspended in 0.9% NaCl until OD₆₀₀ 0.5 (\pm 0.05). Of this suspension, 10 μl was dispensed into wells of sterile flat-bottom 96-well polystyrene tissue culture plates (Greiner Bio-One, Alphen a/d Rijn, The Netherlands) containing serial dilutions of vancomycin in 190 μl of a 1:1 mixture of Fetal Bovine Serum (FBS) (Gibco, Bleiswijk, The Netherlands) and Iscove's Modified Dulbecco's Medium (IMDM) (without phenolred, Gibco, Bleiswijk, The Netherlands), and in the presence or absence of 50 mM D-alanine (Alfa Aesar, Ward Hill, MA, USA). Plates were incubated for 18-24 h at 37°C and MIC values determined visually following the CLSI guidelines, or by absorbance at 600 nm.

VanX overexpression and isolation:

VanX was amplified from the genome of *Enterococcus faecium* (*vanB*-type) with primers pVanX_FW and pVanX_RV. The resulting product was inserted as a NdeI/BamHI fragment into pET28a resulting in vector: VanX-Pet28a. VanX-Pet28a was transformed to expression strain BL21(DE3) (fermentas) for protein expression. BL21(DE3) carrying VanX-Pet28a was grown in LB medium with 200 μM ZnSO₄ and 50 $\mu\text{g}/\text{ml}$ kanamycin. For protein expression, the strain was grown at 30°C to an OD of 1.8, at this point 1mM IPTG was added, biomass was harvested after 75 minutes (Wu *et al.*, 1995). The medium was centrifuged and the supernatant discarded. The pellet was frozen at -80°C overnight. The following day the sample

Substrate inhibition of VanA by D-alanine reduces vancomycin resistance in a VanX-dependent manner

was sonicated for 7.5 minutes in total. Cell debris was removed by several rounds of centrifugation (10.000g, 10 minutes ; 30.000g, 30 minutes ; 100.000g for 90 minutes). The supernatant was incubated overnight with Ni-column resin and purified the following day.

Buffer: PBS pH 7.4 + 200mM NaCl. Wash buffer: 20mM imidazole. Elution buffer: 200mM imidazole. The fractions were tested for activity by adding 5 μ L of each respective fraction to a reaction mix with 10mM Tris-HCl Ph7.0 with 100 μ M D-Ala-D-Ala. After an hour, 1 μ L from the reaction mix is spotted on a TLC.

TLC conditions for separation of D-Ala-D-Ala and D-Ala.

Samples were spotted on a silica TLC with D-Ala and D-Ala-D-Ala as controls. The running buffer was: n-butanol:acetic acid:water, 3:1:1. After the running buffer reached the top of the TLC plate, this was dried and afterwards stained with a Ninhydrin solution of: 0.1g Ninhydrin, 0.5mL acetic acid and 100mL acetone. After staining with ninhydrin, the plate was developed at 100 degrees for 5 minutes.

Conditions VanX activity assay.

The activity of VanX was measured by quantifying the amount of D-Ala generated by the dipeptidase activity. Each reaction contained: 20 μ M Amplex Red, 1 μ g/mL D-amino acid oxidase, 10 μ g/mL peroxidase and 100 μ M D-Ala-D-Ala (Arthur *et al.*, 1998). The reaction was read out in a TECAN Spark 10M plate reader with an excitation wavelength of 550 nm and a bandwidth of 20nm. The emission was measured at 590nm with a bandwidth of 20nm. The reaction needs to be prepared in the dark, UV light can catalyze the reaction from Amplex Red to resorufin.

Constructs for gene disruption and complementation

Deletion mutants were constructed according to a method described previously (Braun *et al.*, 2015). For deletion of *ddl*, the -948/+20 and +1173/+2638 regions relative to the translational start of *ddl* were amplified by PCR using primer pairs *ddl_LF* and *ddl_LR*, and *ddl_RF* and *ddl_RR*, using PCR conditions as described (Colson *et al.*, 2007). The left and right flanks were cloned into the multi-copy vector pWHM3 (Vara *et al.*, 1989), which is highly unstable in *Streptomyces* and therefore allows efficient gene disruption (van Wezel *et al.*, 2005). Subsequently, the apramycin resistance cassette *aac(3)IV* flanked by *loxP* sites was cloned into the engineered XbaI site to create deletion construct pGWS1152. The same strategy was used to create a construct for the deletion of *vanX*. In this case, the -1477/+30 and +572/+2035 regions relative to the start of *vanX* (SCO3596) were PCR-amplified using primer pairs *vanX_LF* and *vanX_LR*, and *vanX_RF* and *vanX_RR* (Supplemental table S3). Insertion of *aac(3)IV-loxP* site in the engineered XbaI site generated deletion construct pGWS1164. The presence of *loxP* sites allows the efficient removal of the apramycin resistance cassette from the chromosome following the introduction of plasmid pUWLCRE that expresses the Cre recombinase (Fedoryshyn *et al.*, 2008).

Complementation constructs

A construct for the genetic complementation of *ddl* was made by amplifying the promoter- and coding region of *ddl* using primers *ddlcomp_F* and *ddlcomp_R* (nt positions: -573/+1184 relative to the start of *ddl* (Supplemental table S3), and inserted as an EcoRI/BamHI fragment in the low copy vector pHJL401 (Larson & Hershberger, 1986), a highly stable low-copy number vector that is well suited for genetic

complementation (van Wezel *et al.*, 2000b), resulting in pGWS1159.

Fluorescence microscopy

Samples were grown for 18 h in liquid NMMP after which a sample was taken from the culture to stain with BODIPY FL vancomycin (Vanco-FL) as described (Daniel & Errington, 2003). Equal amounts of unlabeled vancomycin and Van-FL were added to the sample to a final concentration of 1 $\mu\text{g/ml}$ and was incubated for 10-20 min at 30°C. Directly after taking the first sample, 50 mM D-Ala was added to the medium and was left to grow for another hour before imaging the effect of added D-Ala. Imaging was done as described previously (Willemse & van Wezel, 2009). A Zeiss observer with a Plan-Neofluar 40x/0.9 lens was used, and GFP was excited with a wavelength of 488 nm and observed at 515 nm with filter BP505-550, with illumination power set to 7.5%. The images were analyzed with ImageJ, all the fluorescent images were processed identically. The final figure was made with Adobe Photoshop CS6.

Isolation of cytoplasmic peptidoglycan precursors

For the cytoplasmic PG precursor isolation and identification we used a modification of the method described previously by Hong and colleagues (Hong *et al.*, 2004). Where applicable, 10 μg vancomycin was added to the strains at the moment of inoculation. The strains were grown in NMMP (1% (w/v) Mannitol, 50 mM MgCl_2) until mid-log phase (OD-0.3-0.4) and mycelia were harvested by centrifugation at 4°C and washed in 0,9% NaCl. Mycelia was extracted with 5% cold trichloric acid (TCA) for 30 minutes at 4°C. This was centrifuged and the supernatant desalted on a Sephadex G-25 column (Illustra NAP-10 Columns, GE Healthcare, Pittsburgh), and concentrated by rotary evaporation. The concentrated precursors were dissolved in HPLC-grade water and separated by LC-MS using a gradient of 0-20% acetonitrile in water with 0,1% TFA. The elution was monitored at absorbance 254 nm and by the sizes eluted (1193.8 - 1195.3 m/z).

For the measurement over time, the protocol was adjusted in the following way: 300 ml NMMP cultures were grown until exponential phase (OD 0.3-0.4), at which point a 10 ml sample was taken (sample t=0) and 50 mM of D-Ala or L-Ala was added to the original culture, followed by further sampling after 1, 5, 15, 30, 60, 120 and 180 minutes. Samples were rapidly filtered with a vacuum pump and washed with 0.9% (w/v) NaCl, mycelia scraped off the filter and transferred to 5% TCA.

RESULTS

D-Ala reduces vancomycin resistance

The bifunctional activity and structural analysis of the VanA enzyme implies that it can use both D-Lac and D-Ala as a substrate (Roper *et al.*, 2000, Wright & Walsh, 1992), suggesting that D-Ala might be able to compete with D-Lac in the active site of the enzyme. To test the applicability of this concept, we used the naturally vancomycin-resistant *S. coelicolor* M145 as a model system. The strain was grown on minimal media (MM) agar plates with increasing concentrations of D-Ala and vancomycin. D-Ala was thereby added in concentrations of 5, 10 or 50 mM and the effect on the MIC of vancomycin assessed. As controls we added either L-Ala or neither alanine stereoisomer. In the absence of added amino acids, the MIC of vancomycin against *S. coelicolor* was 128 µg/ml. Supplementing the media with up to 50 mM L-Ala did not have any effect on the susceptibility to vancomycin (Table 1 and Fig S1). Sensitivity to vancomycin increased significantly when D-Ala was added; at 10 mM D-Ala, the MIC decreased to 32 µg/ml (4-fold reduction), while at 50 mM D-Ala the MIC was reduced to 4 µg/ml (32-fold reduction) (Table 1 and Fig S1). This supports the concept that D-Ala can reduce VanA-based vancomycin resistance, presumably by competing with the substrate D-Lac at the active site of the VanA enzyme (Arthur *et al.*, 1994, Zarlenga *et al.*, 1992).

Table 1. Effect of D-Ala on the MIC of vancomycin (in µg/ml) against *S. coelicolor* M145 and its mutant LAG2.

Strain	No AA	D-Ala			L-Ala		
		5 mM	10 mM	50 mM	5 mM	10 mM	50 mM
M145	128	32	32	4	128	128	128
Δddl^a	128	32	32	4	128	128	128
LAG2	128	64	32	4	128	128	128

^a. The *ddl* null mutant is not viable on medium without vancomycin but furthermore had an identical MIC value to M145.

Creation of a vancomycin-independent *ddl* mutant

To study the molecular basis of this effect in more detail, a strain was required that depends on *vanA* for the synthesis of the D-Ala-D-Ala dipeptide and thus for cell-wall synthesis. The wild-type gene for D-Ala-D-Ala ligase is *ddl* (SCO5560 in *S. coelicolor*), which is essential for normal growth, but its absence can be rescued by the vancomycin-inducible expression of *vanA*, the only other paralogue of *ddl* on the *S.coelicolor* genome (Wright & Walsh, 1992, Kwun *et al.*, 2013). To allow direct comparison with other mutants related to GlcNAc and cell-wall metabolism previously made in our laboratory (Nothaft *et al.*, 2010, Rigali *et al.*, 2008, Swiatek *et al.*, 2012), a *ddl* (SCO5560) null mutant was created in our specific *S. coelicolor* M145 laboratory host, thereby ensuring that all of the mutants have the same isogenic background. This was done by replacing the entire *ddl* coding region by the apramycin resistance cassette (*aacC4*) via homologous recombination and subsequent removal to leave an in-frame deletion of *ddl* in the genome. The *aacC4* gene was flanked by *loxP* sites, allowing the subsequent removal by expression of the Cre recombinase, resulting in a markerless deletion mutant of *ddl* (see Materials and

Methods section). To compensate for the absence of D-Ala-D-Ala, the *ddl* mutant was created in the presence of vancomycin, so as to elicit the production of the alternative precursor dipeptide D-Ala-D-Lac by VanA (Hong *et al.*, 2005). Many candidate *ddl* null mutants were obtained, all of which failed to grow in the absence of vancomycin and showed normal sporulation. One of these strains was selected for further characterization. The absence of *ddl* in this mutant was confirmed by PCR (data not illustrated). Expectedly, the *ddl* mutant could only grow on agar plates with vancomycin (Fig. 1). Introduction of plasmid pGWS1159, which expresses the *ddl* gene from its own promoter, into the *ddl* null mutant restored normal development and growth in the absence of D-Ala (data not illustrated).

To allow studying the sensitivity of VanA to inhibitory molecules regardless of the presence or absence of vancomycin, we selected for suppressor mutants by plating spores (10^7 cfu) of the *ddl* null mutant onto SFM agar plates lacking vancomycin, so as to select for suppressors with constitutive expression of the vancomycin resistance cluster. This yielded a small number of spontaneous suppressor mutants, which occurred at a frequency of around 10^{-6} . One of these mutants has been selected and designated LAG2. These constitutively expressed the vancomycin resistance cluster, as this is a requirement to compensate for the absence of *ddl*. One of the suppressor mutants was selected and designated LAG2 (Fig. 1)

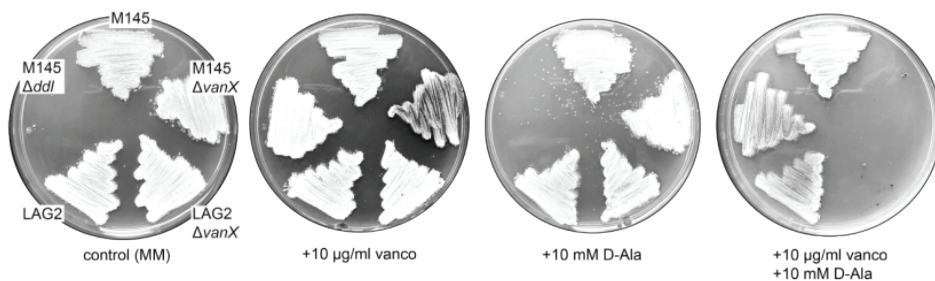


Figure 1. Effect of D-Ala on growth of *S. coelicolor* M145 and derivatives. Strains are *S. coelicolor* M145 (parental strain), its *vanX* mutant, suppressor mutant LAG2, LAG2 Δ *vanX* and M145 Δ *ddl*. Strains were streaked on MM with from left to right, no additives (control); MM with 10 μ g/ml vancomycin; 10 mM D-Ala; 10 μ g/ml vancomycin + 10 mM D-Ala. The *ddl* mutant fails to grow in the absence of vancomycin, a phenotype that is suppressed in LAG2 due to constitutive expression of the *van* resistance cluster. Note the high sensitivity of the *vanX* null mutants of M145 and LAG2 to the combination of vancomycin and D-Ala. Plates were incubated for 3 days at 30°C.

DNA sequencing of the vancomycin resistance genes *vanRSJKHAX* of strain LAG2 revealed that the insertion element IS466A (SCO3469) (Yamasaki *et al.*, 2000, Hong *et al.*, 2008, Courvalin, 2006) had inserted at nt position 55 relative to the translational start of *vanS*, causing loss-of-function. This spontaneous integration event in *vanS* had been observed before in both *Streptomyces* and in strains of *Enterococcus*, and results in constitutive upregulation of the vancomycin resistance cluster (Hutchings *et al.*, 2006, Thaker *et al.*, 2015, Arthur *et al.*, 1997). The *ddl* suppressor mutant LAG2 had a similar level of vancomycin resistance as the parental strain, with an MIC of 128 μ g/ml (Table 1). Similar as seen for wild-type cells, addition

Substrate inhibition of VanA by D-alanine reduces vancomycin resistance in a VanX-dependent manner

of L-Ala did not affect the MIC for vancomycin, while addition of D-Ala decreased the MIC to 4 $\mu\text{g/ml}$ when 50 mM D-Ala was added to the agar plates (Table 1). Thus, while LAG2 constitutively expresses the vancomycin resistance cluster, it has a comparable MIC to vancomycin as wild-type cells, which in both cases could be strongly reduced by the addition of D-Ala.

Deletion of *vanX* amplifies the effect of D-Ala on vancomycin sensitivity

We then wondered if targeting *vanX* could further potentiate the effect of D-Ala as inhibitor of vancomycin resistance. VanX hydrolyzes D-Ala-D-Ala, thereby counteracting the accumulation of wild-type precursors and supporting vancomycin resistance (Lessard & Walsh, 1999, Tan *et al.*, 2002). A *vanX* null mutant was created using a similar strategy as for *ddl*, replacing the coding region of *vanX* by the apramycin resistance cassette *aacC4*. The mutant was created in both the parental strain *S. coelicolor* M145 and in its *ddl* suppressor mutant LAG2, generating M145 ΔvanX and LAG4 (LAG2 ΔvanX), respectively.

The respective *vanX* mutants of M145 and LAG2 grew on medium supplemented with 10 $\mu\text{g/ml}$ vancomycin, and 10 mM D-Alanine but failed to grow on media containing both vancomycin and D-Alanine at a concentration where M145 and LAG2 did not show sensitivity to vancomycin (Figure 1). LAG2 ΔvanX produced 20% wild-type precursors prior to the addition of D-Ala. This strongly suggests that VanA produces a significant amount of D-Ala-D-Ala *in vivo*, which accumulates in the absence of VanX. Consistent with this idea, the MIC of vancomycin was lower for the *vanX* mutant, namely 32 $\mu\text{g/ml}$ for the *vanX* mutant, and 64 $\mu\text{g/ml}$ for LAG2 ΔvanX , as compared to 128 $\mu\text{g/ml}$ for the parental strain M145 (Table 2)

In wild-type cells, 50 mM D-Ala was required to reduce the MIC for vancomycin to 4 $\mu\text{g/ml}$. However, only 50 μM D-Ala was required to reduce the MIC of vancomycin for the *vanX* mutant to 1 $\mu\text{g/ml}$. This spectacular difference means that D-Ala is around 4000 times more effective in the absence of the D-Ala-D-Ala peptidase activity of VanX. This is consistent with the very strong accumulation of wild-type precursors in *vanX* null mutants as compared to the *vanX*-positive parental strain.

Table2. The MIC of vancomycin ($\mu\text{g/ml}$) on *S.coelicolor* *vanX*-mutants with D-Ala.

Strain	No AA	D-Ala			L-Ala		
		10 μM	50 μM	100 μM	10 μM	50 μM	100 μM
M145 ΔvanX	32	16	1	1	32	32	32
LAG2 ΔvanX	64	32	8	2	32	32	32

Analysis of peptidoglycan precursors

In order to get more insight into the synthesis of vancomycin-sensitive (*i.e.* wild-type) or vancomycin-resistant PG, the pool of PG precursors was analyzed by Liquid Chromatography coupled to Mass Spectrometry (LC-MS) (Arthur *et al.*, 1994, Arthur *et al.*, 1998, Kwun *et al.*, 2013) When cells produce wild-type PG, only MurNAC-pentapeptides with a D-Ala-D-Ala terminus are detected, while vancomycin-resistant PG precursors have a D-Ala-D-Lac terminus. Wild-type precursors ending with D-Ala-D-Ala are characterized by a peak with a monoisotopic mass of 1994 Da and a retention time of around 7.2 minutes, while vancomycin-insensitive precursors ending with D-Ala-D-Lac are characterized by a peak of a monoisotopic mass of 1995 Da and a significantly higher retention time of around 8.2 minutes (Fig. 3A).

In extracts from the parental strain grown in the absence of vancomycin, only wild-type precursors were observed (Fig. 3B). Expectedly, when *S. coelicolor* M145 was grown in the presence of 10 $\mu\text{g/ml}$ vancomycin, the vast majority of the precursors (91.5%) represented the vancomycin-insensitive variant. Similarly, 95.7% of the precursors from the *ddl* null mutant grown in the presence of vancomycin contained the terminal D-Ala-D-Lac dipeptide (Fig. 3B). This indicates that VanA produces a low level of the D-Ala-D-Ala dipeptide. In the *ddl* suppressor mutant LAG2, which constitutively expresses the vancomycin resistance gene cluster, nearly all PG precursors terminated with D-Ala-D-Lac (99.8% and 99.7% for cultures grown with and without vancomycin, respectively) (Fig. 3B). We then wondered how D-Ala would affect the accumulation of wild-type precursors over time in the suppressor mutant. The constitutive expression of the vancomycin resistance cluster in the suppressor mutant allows growth of *ddl* null mutants without the need for vancomycin and ensures that the result is caused by substrate competition, not a difference in the expression of the vancomycin resistance cluster. For the time-lapse experiment, 300 ml NMMP cultures were supplemented with either D-Ala or L-Ala (control) at 50 mM end concentration, and 10 ml samples were collected prior to and 1, 5, 15, 30, 60, 120 and 180 min after the addition of either alanine stereoisomer. Prior to the addition of D-Ala or L-Ala ($t=0$), LAG2 did not accumulate any wild-type precursors. However, addition of 50 mM D-Ala resulted in the production of small amounts of wild-type precursor (1%) within 1 min. After 15 min this amount had increased to 4%, which appeared to be close to the maximum, with levels of wild-type precursors never exceeding 5%. L-Ala did not result in detectable levels of wild-type precursors in LAG2.

Strikingly, analysis of PG precursors in *vanX* null mutants revealed that the addition of even low levels of D-Ala facilitated the accumulation of high levels of wild-type precursors, up to as much as 80% wild-type precursors 3 h after the addition of D-Ala (Figure 3). This supports the notion that in the absence of VanX, wild-type precursors are incorporated much more frequently into the cell wall, with increased sensitivity to vancomycin as a consequence.

Substrate inhibition of VanA by D-alanine reduces vancomycin resistance in a VanX-dependent manner

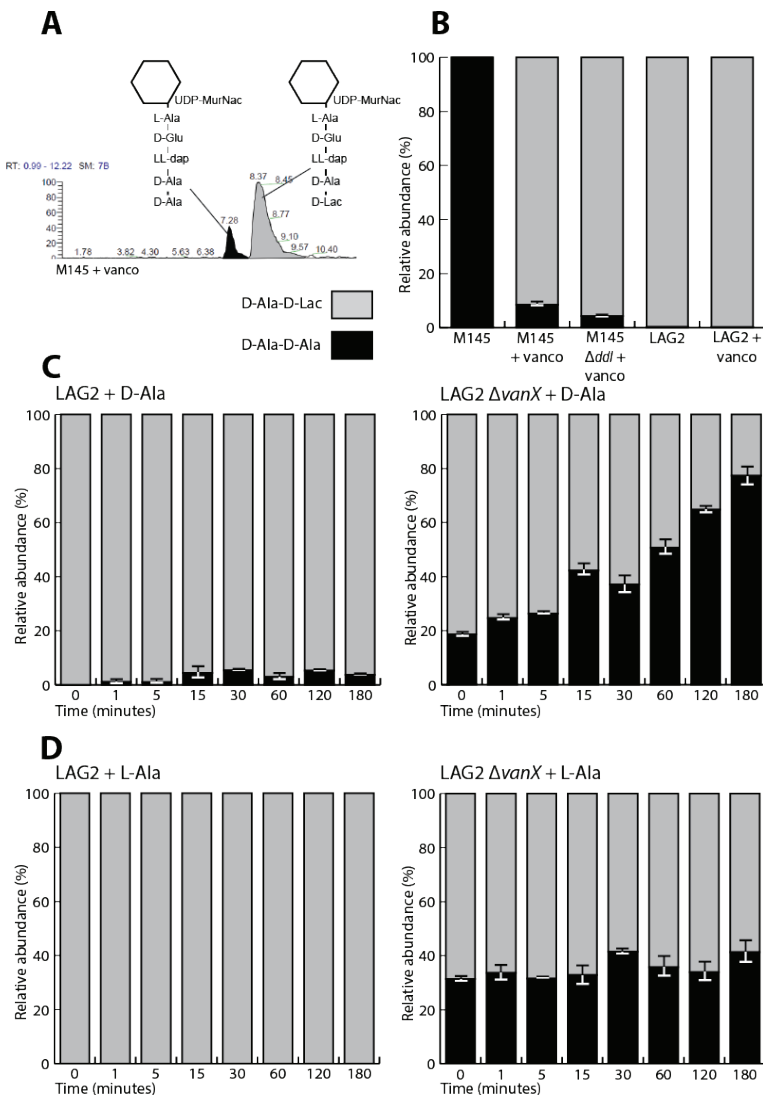


Figure 2. LC-MS analysis of peptidoglycan precursors. (A) Example peak profile and corresponding precursors of *S. coelicolor* M145 grown with vancomycin, with the peak area corresponding to a precursor terminating in D-Ala-D-Ala shown in black, and the peak corresponding to a precursor terminating in D-Ala-D-Lac in grey. (B) Ratio (in %) of wild-type (black) and vancomycin-resistant (grey) precursors in *S. coelicolor* M145, its *ddl* null mutant and suppressor mutant LAG2, grown with or without vancomycin (10 μ g/ml). The *ddl* mutant is only shown with vancomycin as it fails to grow in its absence. LAG2 with and without vancomycin have less than 1% wild-type (vancomycin-sensitive) peptidoglycan. Strains were grown with or without vancomycin until OD 0.3-0.4 before harvesting. (C) Accumulation of wild-type and vancomycin-resistant precursors over time in LAG2 and LAG2 Δ vanX. The samples were grown until OD 0.3-0.4 prior to the addition of 50 mM D-Ala. Samples were taken prior to (0) or 1, 5, 15, 30, 60, 120 or 180 minutes after the addition of D-Ala. (D) Same as (C), but with L-Ala instead of D-Ala. Bars representing the precursors shown as percentages (total set to 100%).

Visualization of vancomycin binding by fluorescence microscopy

To qualitatively determine the ability of vancomycin to bind to the cell walls of different *Streptomyces* strains and also visualize the effect of D-Ala, mycelia of *S. coelicolor* were fluorescently stained with BODIPY-FL vancomycin (Vanco-FL). In vancomycin-sensitive bacteria, vancomycin localizes in foci at sites of *de novo* cell wall synthesis (Daniel & Errington, 2003). In *S. coelicolor*, which grows by tip extension (Gray *et al.*, 1990), these sites are in particular the hyphal tips and cell division septa.

While hyphae of *S. coelicolor* M145 were stained well by Vanco-FL, hardly any Vanco-FL bound to the hyphae of strains constitutively expressing vancomycin resistance (LAG2 or LAG2 Δ *vanX*) (Fig. 4A). However, addition of D-Ala resulted in marginal staining by Vanco-FL of the LAG2 hyphal tips (Fig. 4B); in contrast, its *vanX* mutant derivative LAG4 was stained very well, in line with the strongly enhanced vancomycin sensitivity of the mutant (Fig. 4).

Taken together, our mutational, microscopy and LC-MS experiments show that D-Ala effectively and specifically enhances the sensitivity of vancomycin resistant *S. coelicolor* to vancomycin, by allowing accumulation of wild-type cell-wall precursors and thus binding of vancomycin to sites of active cell-wall biosynthesis. This effect was strongly enhanced in *vanX* mutants (which lack D-Ala-D-Ala peptidase activity).

Substrate inhibition of VanA by D-alanine reduces vancomycin resistance in a VanX-dependent manner

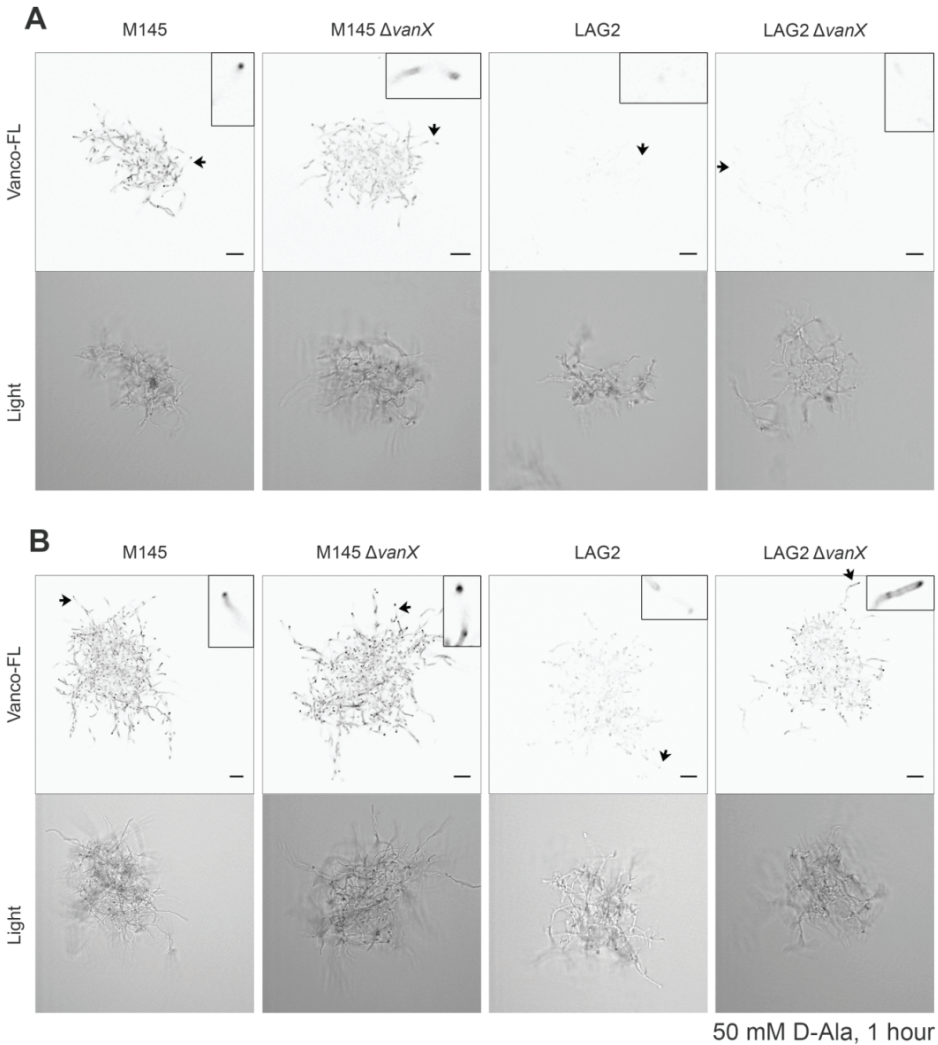


Figure 3. Fluorescence micrographs of Vanco-FL stained hyphae. To analyze vancomycin binding, *S. coelicolor* strains M145, M145 Δ vanX, LAG2 and LAG2 Δ vanX, were grown in liquid NMMP for 12 h, and continued to grow for 1 h in the absence (A) or presence (B) of 50 mM D-Ala. Mycelia were then stained with Vanco-FL and imaged. Top, fluorescence micrographs (inverted greyscale); bottom, corresponding light images. *S. coelicolor* M145 and its *vanX* mutant were readily stained by Vanco-FL. Constitutively vancomycin resistant strain LAG2 was not stained by Vanco-FL in the absence of D-Ala, and showed some binding after the addition of D-Ala. Extensive Vanco_FL staining was seen for LAG2 Δ vanX only after the addition of D-Ala. Inserts are magnifications of the areas indicated by arrows in the respective image. Scale bar, 10 μ m.

Analysis of the effect of D-Ala on the MIC of clinical isolates of VRE

Having established that D-Ala enhances the efficacy of vancomycin against vancomycin-resistant *S. coelicolor*, we then assessed its effect on the resistance of *vanA*-positive clinical isolates of *E. faecium*. MIC values were calculated by testing a serial (two-fold) dilution of vancomycin in the presence or absence of D-Ala in triplicate (Table 3). [Similar as seen for *S. coelicolor*, addition of 50 mM D-Ala to the growth media resulted in a strong increase in the efficacy of vancomycin against all clinical isolates, with reduction of 4-7 dilution steps. Even in the worst cases, the MIC of vancomycin was still reduced 16-32 fold (from 4096 $\mu\text{g/ml}$ to 256 $\mu\text{g/ml}$ or 128 $\mu\text{g/ml}$), while we also noted a further decrease to values as low as 16 $\mu\text{g/ml}$ for strain *vanA10*. This value corresponds to intermediate resistance.

Table 3. MIC of vancomycin ($\mu\text{g/ml}$) against VRE in the presence or absence of D-Ala.

Strain	0 mM D-Ala	50 mM D-Ala	steps down
<i>vanA1</i>	4096	256	4
<i>vanA2</i>	4096	256	4
<i>vanA3</i>	4096	128	5
<i>vanA4</i>	4096	128	5
<i>vanA10</i>	2048	16	7

VanX isolation and characterization.

Here, we have found that VanX is an essential protein in the vancomycin resistant complex, a knockout of the *vanX* gene in *S.coelicolor* causes it to become a thousand fold more sensitive to vancomycin when combined with D-Ala. For this reason, we expressed and isolated the VanX protein from *Enterococcus faecium* and developed an assay with a fluorescent readout. VanX is a 23.35Da protein with dipeptidase activity which is highly specific for D-Ala-D-Ala, it does not cleave the stereoisomer L-Ala-D-Ala or L-Ala-L-Ala. The binding pocket for D-Ala-D-Ala is located in the center of the protein and requires a Zn^{2+} cofactor (Figure 5). The protein was amplified from the genome of a VanB-type *Enterococcus faecium*, this was cloned into pET-28a, which carries a HIS-tag at the N-terminus and expressed in *E.coli* BL21 (DE3). The protein was purified using a nickel column and the activity was initially tested by adding 5 μ L of the fraction to a 20 μ L reaction mix in 10mMTris-HCl, pH 7.0 and 100 μ M D-Ala-D-Ala. After an hour incubation, the mix is spotted on a silica TLC with running buffer n-butanol:acetic acid:water, 3:1:1, until the solution almost hit the top of the TLC plate. The plate was developed with a ninhydrin stain. this showed that the protein was still active after purification.

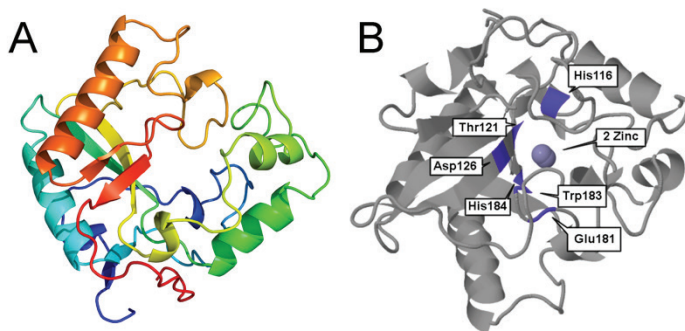


Figure 5. (A) Structural model of VanX. PHYRE²(Kelley *et al.*, 2015) model of VanX, The N- to C-terminus is rainbow-coloured. (B) The D-Ala-D-Ala binding site prediction, a small pocket of amino acids makes up the active site, associated with a Zn^{2+} cofactor.

To measure the activity of VanX, it is necessary to differentiate between D-Ala and D-Ala-D-Ala. Although this is straightforward by TLC, this method would not be feasible for a high-throughput assay. An assay with a fluorescent output was developed based on the activity of a D-amino acid oxidase (DAO), this protein oxidases D-Ala, but not D-Ala-D-Ala. CAO converts D-Ala to pyruvate, ammonia and hydrogen peroxide, after which Horseradish peroxidase catalyzes the reaction of hydrogen peroxide and Amplex Red to the fluorescent Resorufin and oxygen, as shown in Figure 6. The reaction without VanX (0 VanX) showed a flat slope, the reaction with D-Ala instead of D-Ala-D-Ala showed high initial fluorescence and bleached afterwards. An increasing amount of VanX (5-50 μ g/ mL) increased the primary reaction speed, from 10 μ g/mL on, the slope was the same, indicating that another protein is the limiting step. With these concentrations, 5-10 μ g VanX would be ideal for a high-throughput set up.

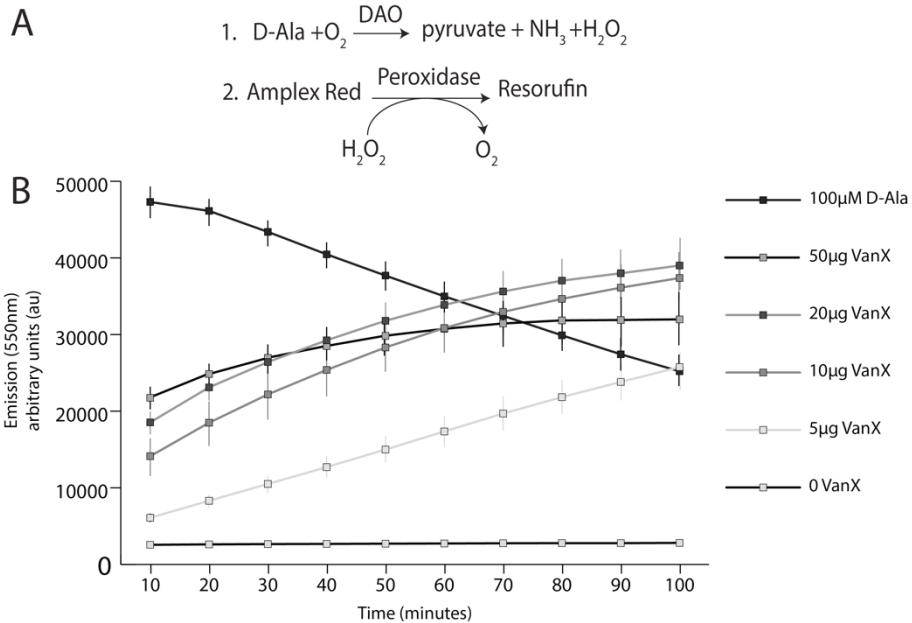


Figure 6. A: The fluorescence assay is based on two reactions: 1. The oxidation of D-Ala by DAO which gives pyruvate, ammonia and hydrogen peroxide. 2. Hydrogen peroxide is then converted to oxygen by horseradish peroxidase for which Amplex red is the electron donor converting that into Resorufin which gives a strong fluorescent signal. B: Fluorescence assay to measure D-Ala, the plate was measured every ten minutes, 5 wells are averaged for every data point. The y-axis shows the emission at 550 nm, measured in arbitrary units (au). The x-axis shows time in minutes. The reaction was performed with 0, 5, 10, 20 and 50 μg/mL VanX protein and with 100 μM D-Ala as a control.

DISCUSSION

With the rapid spread of vancomycin resistance, new efforts are needed to maintain this last resort antibiotic as a clinical drug against multi-drug resistant bacterial infectious diseases. So far, attempts included engineering VanX-inhibitors (Muthyala *et al.*, 2014, Wu *et al.*, 1995, Aráoz *et al.*, 2000), or re-engineering vancomycin itself to target not only the cell-wall precursors with D-Ala-D-Ala termini, but also those ending with D-Ala-D-Lac (Xie *et al.*, 2011). As a basis to develop new approaches to target vancomycin resistance, we studied the model organism *S. coelicolor*, which has a very similar set of vancomycin resistance genes as the pathogenic VRE (Wiener *et al.*, 1998).

VanA, a variant of Ddl that ligates D-Ala to D-Lac to form D-Ala-D-Lac, plays a key role in vancomycin resistance. VanA is a bifunctional enzyme which can produce both D-Ala-D-Lac and D-Ala-D-Ala, the affinity for either D-Lac or D-Ala as a substrate being highly dependent of substrate and pH (Verkade, 2008, Healy *et al.*, 2000, Lessard *et al.*, 1999). The extracellular addition of high concentrations D-Ala results in increased accumulation of wild-type cell-wall precursors and consequently the build-up of vancomycin-sensitive PG, due to competition with D-Lac at the active site of VanA, while supplementing D-Lac leads to a high abundance of precursors terminating in D-Ala-D-Lac (Kwun *et al.*, 2013, Arthur *et al.*, 1998, Arthur *et al.*, 1994) This effect is specific for vancomycin and did not work on A40926, the natural product of the novel glycopeptide dalbavancin, of which the mechanism is similar but different from vancomycin. We analyzed the accumulation of precursors, which revealed that supplementing cultures of a constitutively vancomycin-resistant variant of *S. coelicolor* M145 with excess D-Ala, resulted in accumulation of up to 5% wild-type precursors. While interesting, the effect is too low to be effective in treatment of vancomycin-resistant pathogens. However, we here show that the effect of D-Ala is massively enhanced in the absence of VanX, with up to 80% of the precursors accumulated in *vanX* null mutants containing the wild-type dipeptide. As support of the biochemical data, active incorporation of wild-type precursors at apical sites was visualized with Vanco-FL, which fluorescently stains all sites of active cell-wall synthesis, *i.e.* the hyphal tips and newly synthesized septa. While wild-type cells and *vanX* mutant cells were stained very well by Vanco-FL, derivatives with constitutive vancomycin resistance were hardly stained. However, addition of D-Ala recovered fluorescence even to cells with constitutive vancomycin resistance, indicative of the incorporation of wild-type cell-wall material concomitant with increased sensitivity to vancomycin. Other ways D-Ala could affect vancomycin sensitivity could be by D,D-transpeptidases in the periplasm substituting D-Lac for D-Ala on the precursors (Hugonnet *et al.*, 2014). The strong direct correlation between PG precursor accumulation and vancomycin binding (as determined by imaging fluorescent vancomycin) argues against a major influence of D,D-transpeptidases in this work. The fluorescence correlated with the level of wild-type cell-wall precursors in the various strains, and this method therefore offers rapid qualitative assessment of vancomycin sensitivity, which could be applied in high-throughput screening for compounds that potentiate vancomycin resistance. By combining the precursor analysis and staining with Vanco-FL it is also clear that D-Ala is not only incorporated in PG precursors but the pentapeptides terminating in D-Ala-D-Ala are displayed at the cell surface. A question which remains though is which amount of vancomycin sensitive PG would be sufficient to regain sensitivity against vancomycin.

Previous work indicated that the deletion of *vanX* increases the sensitivity to vancomycin (Arthur *et al.*, 1998). However, as our work shows, significant changes in the MIC are only brought about when D-Ala is added as competitive inhibitor for D-Lac. This change in response to the deletion of *vanX* may well depend on the target organism, which is underlined by the differential effect of added D-Ala on the MICs of independent clinical VRE isolates. Based on the findings presented in this work, we propose a model for vancomycin resistance in which the catalytic activity of VanA depends largely on the available substrate (Fig. 5). In the presence of excess of D-Ala, VanA is bifunctional and synthesizes both D-Ala-D-Ala and D-Ala-D-Lac, but the wild-type dipeptide is then cleaved by the VanX peptidase. However, excess of D-Ala will result in such large amounts of D-Ala-D-Ala that VanX cannot degrade the dipeptides sufficiently rapidly to avoid their use as substrate by VanA, thus resulting in low levels of wild-type lipid II. As a result, a small proportion of wild-type PG is produced, giving enhanced vancomycin sensitivity. In the absence of *vanX* the addition of even very small amounts of D-Ala (10-50 μ M instead of 10-50 mM) already led to strong accumulation of wild-type precursors and a drop in the MIC of vancomycin to values as low as 1 μ g/ml. This is well within the range of clinical sensitivity.

How can the concepts developed in this work be implemented into approaches to counteract vancomycin resistant Gram-positive pathogens like VRE and VRSA? The high sensitivity of *vanX* null mutants to the combination of vancomycin and D-Ala strongly suggests that the combined treatment with vancomycin and D-Ala will be particularly effective in combination with molecules that perturb the bioactivity of VanX. VanX inhibitors have been described in the literature, but their effect was limited (Muthyala *et al.*, 2014, Chang *et al.*, 2006, Aráoz *et al.*, 2000, Yang *et al.*, 2011b, Wu *et al.*, 1995). Based on the data presented here, this is likely explained by the fact that the effect of a *vanX* deletion without additional D-Ala is very limited, only decreasing the MIC by two-fold in this work. Similarly, the data also point out that VanX inhibitors that have been or will be developed in the future should be (re)tested in the presence of added D-Ala, as this largely augments their efficacy. Strains that depend on the vancomycin resistance cluster for growth thereby candidate as screening hosts for a high-throughput screen of small molecules that target vancomycin resistance. This may prove an important asset in the hunt for drugs that counteract vancomycin-resistant pathogens such as VRE and VRSA.

Substrate inhibition of VanA by D-alanine reduces vancomycin resistance in a VanX-dependent manner

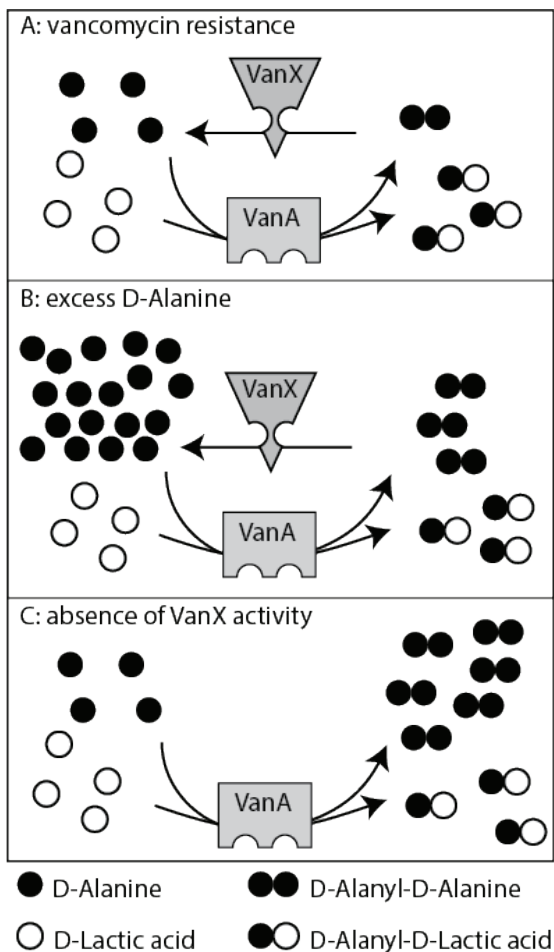


Figure 4. Model of how D-Ala influences the activity of VanA in the presence or absence of VanX. All drawings show the situation where VanA is constitutively expressed and in the absence of Ddl. (A) Normal situation. VanA produces both D-Ala-D-Ala and D-Ala-D-Lac, whereby D-Ala-D-Ala is broken down by VanX (resulting in a strong bias for D-Ala-D-Lac). (B) situation in the presence of excess D-Ala, which is then preferentially used as substrate by VanA to favor the formation of the D-Ala-D-Ala dipeptide, which is however still broken down by VanX. (C) situation in the absence of *vanX*. Because of the lack of VanX activity, D-Ala-D-Ala accumulates and the pool of D-Ala-D-Ala is dramatically increased when excess D-Ala is added. This then enhances the percentage of wild-type cell-wall precursors and strongly amplifies the efficacy of vancomycin.

Acknowledgements

We thank Gerry Wright for critically reading the manuscript, David Roper for the suggestion of using a D-amino acid oxidase-based assay and Hans van den Elst for assistance with LC-MS. We are grateful to Margherita Sosio (NAICONS, Milan, Italy) for providing A40926.

Authors contributions

LvdA: Conception and design, performed the work on *S.coelicolor*, wrote and revised the article. NL: performed the work on *E. faecium*. WvW designed the work on *E. faecium* and wrote the article. GvW: Conception and design, wrote and revised the article. All authors read and agreed on the final version of the article.

CHAPTER 6

Structural and functional characterization of the alanine racemase from *Streptomyces coelicolor* A3(2)

Raffaella Tassoni, Lizah T. van der Aart, Marcellus Ubbink, Gilles P. van Wezel, Navraj S. Pannu.

This Chapter is published as:
Biochemical and Biophysical Research Communications (2017) Vol. 483, Issue 1, 29 January 2017, Pages 122-128

Supplemental material available at:
<https://ars-els-cdn-com.ezproxy.leidenuniv.nl:2443/content/image/1-s2.0-S0006291X16322550-mmc1.pdf>

ABSTRACT

The conversion of L-alanine (L-Ala) into D-alanine (D-Ala) in bacteria is performed by pyridoxal phosphate-dependent enzymes called alanine racemases. D-Ala is an essential component of the bacterial peptidoglycan and hence required for survival. The Gram-positive bacterium *Streptomyces coelicolor* has at least one alanine racemase encoded by the putative gene *alr*. Here, we describe an *alr* deletion mutant of *S. coelicolor* which is completely dependent on D-Ala for growth and shows an increased sensitivity to the antibiotic D-cycloserine. The crystal structure of the alanine racemase (Alr) was solved with and without the inhibitors D-cycloserine and propionate. The crystal structures revealed that Alr is a homodimer with residues from both monomers contributing to the active site. The dimeric state of the enzyme in solution was confirmed by gel filtration chromatography, with and without L-Ala or D-cycloserine. Specificity of the enzyme was 66 ± 3 U mg^{-1} for the racemization of L- to D-Ala, and 104 ± 7 U mg^{-1} for the opposite direction. Comparison of Alr from *S. coelicolor* with orthologous enzymes from other bacteria, including the closely related D-cycloserine-resistant Alr from *S. lavendulae*, strongly suggests that structural features such as the hinge angle or the surface area between the monomers do not contribute to D-cycloserine resistance, and the molecular basis for resistance therefore remains elusive.

INTRODUCTION

All canonical, proteinogenic amino acids, with the exception of glycine, have a stereocenter at the C α and can exist either as the L- or D-enantiomer. While in the past it was generally accepted that only L-amino acids had a role in living organisms, studies revealed a variety of roles for free D-amino acids, for example in the regulation of bacterial spore germination and peptidoglycan structure (Cava *et al.*, 2011). Peptidoglycan is essential for cell shape and osmotic regulation and its biosynthesis is dependent on the availability of the less naturally abundant D-alanine (Lam *et al.*, 2009, Steen *et al.*, 2005, Vollmer *et al.*, 2008a). D-alanine (D-Ala) is generated through racemization of the abundant L-enantiomer (L-Ala) by the enzyme alanine racemase (Walsh, 1989).

Alanine racemases (Alr; E.C. 5.1.1.1) are conserved bacterial enzymes that belong to the Fold Type III of pyridoxal phosphate (PLP)-dependent enzymes. Crystallographic studies of Alr's from different bacterial species revealed a shared, conserved fold consisting of an eight-stranded α/β barrel at the N-terminal domain and a second, C-terminal domain mainly consisting of β -sheets. The PLP cofactor is bound to a very conserved lysine residue at the N-terminal side of the last helix of the barrel. In all studies, Alr's crystals consist of homo-dimers, with residues from both monomers participating in the formation of the active site. Nevertheless, in-solution studies indicated an equilibrium between monomeric and homo-dimeric states in solution, with the homo-dimer being the catalytically active form (Ju *et al.*, 2011, Strych *et al.*, 2007).

Streptomyces coelicolor is the most widely studied member of the Streptomycetes, which are Gram-positive bacteria with a multicellular mycelial life style that reproduce via sporulation (Claessen *et al.*, 2014). They are of great importance for medicine and biotechnology, accounting for over half of all antibiotics, as well as for many anticancer agents and immunosuppressants available on the market (Hopwood, 2007, Barka *et al.*, 2016). Here we describe the heterologous expression, purification and crystal structure of *S. coelicolor* Alr, encoded by *alr* (SCO4745). An *alr* null mutant of *S. coelicolor* depends on exogenous D-Ala for growth. The purified enzyme catalyzed the racemization of L-Ala to D-Ala *in vitro* and was shown to be a dimer from gel filtration, both in the absence and presence of L-Ala or the inhibitor D-cycloserine (DCS). Furthermore, the crystal structure of the enzyme has been solved both in the absence and in the presence of the inhibitors DCS and propionate. The comparison of the Alr enzymes from *S. coelicolor* and its close relative the DCS-resistant *Streptomyces lavendulae* (Noda *et al.*, 2004b) questions the structural role of Alr in DCS resistance.

MATERIALS AND METHODS

***Streptomyces coelicolor* knock-out mutant and genetic complementation-** *Streptomyces coelicolor* (A3(2) M145 was obtained from the John Innes Centre strain collection and cultured as described (Kieser *et al.*, 2000). *S. coelicolor* *alr* deletion mutants were constructed according to a previously described method (Swiatek *et al.*, 2012). The -1238/-3 and +1167/+2378 regions relative to the start of *alr* were amplified by PCR using primer *alr*_LF and *alr*_LR, and *alr*_RF and *alr*_RR (Table S2) as described (Colson *et al.*, 2007). The left and right flanks were cloned into the unstable, multi-copy vector pWHM3 (Table S1) (Vara *et al.*, 1989), to allow for efficient gene disruption (van Wezel *et al.*, 2005). The apramycin resistance cassette *aac(3)IV* flanked by *loxP* sites was cloned into the engineered XbaI site to create knock-out construct pGWS1151. Media were supplemented with 1 mM D-Ala to allow growth of *alr* mutants. The correct recombination event in the mutant was confirmed by PCR. For genetic complementation, the -575/+1197 region (numbering relative to the *alr* translational start codon) encompassing the promoter and coding region of SCO4745 was amplified from the *S. coelicolor* M145 chromosome using primer 4745FW-575 and 4745RV+1197 (Table S2) and cloned into pHJL401 (van Wezel *et al.*, 2000a). pHJL401 is a low-copy number shuttle vector that is very well suited for genetic complementation experiments (van Wezel *et al.*, 2000b).

Cloning, protein expression and purification

The *alr* gene (SCO4745) was PCR-amplified from genomic DNA of *Streptomyces coelicolor* using primers *alr*-FW and *alr*-RV (Table S2), and cloned into pET-15b with a *N*-terminal His₆ tag. The construct was transformed into *E. coli* BL21 Star (DE3)pLysS electrocompetent cells (Novagen). *E. coli* cultures were incubated in LB medium at 37°C until an OD₆₀₀ of 0.6 and gene expression induced by adding 0.5 mM isopropyl β-D-1-thiogalactopyranoside (IPTG) followed by overnight incubation at 16°C. His₆-tagged Alr was purified using a pre-packed HisTrap FF column (GE Healthcare) as described (Mahr *et al.*, 2000). Briefly, after binding of the protein, the column was washed with ten column volumes of 20 mM sodium phosphate buffer, pH 7.0, 500 mM NaCl and 50 mM imidazole and *N*-terminally His₆-tagged Alr eluted with the same buffer but containing 250 mM imidazole. Fractions containing the Alr were desalted using a PD-10 column (GE Healthcare) to remove the imidazole and Alr purified further by gel-filtration using a Superose-12 column (GE Healthcare). The collected fractions were analyzed by SDS-PAGE and those containing pure Alr were pooled, concentrated using a Centrprep centrifugal filter unit (10 kDa cut-off, Millipore), and flash-frozen in liquid nitrogen.

Crystallization conditions and data collection

Purified Alr was concentrated to 20 mg mL⁻¹ and crystallization conditions were screened by sitting-drop vapor-diffusion using the JCSG+ and PACT *premier* (Molecular Dimensions) screens at 20°C with 500-nL drops. The reservoir (75 μL) was pipetted by a Genesis RS200 robot (Tecan). Drops were made by an Oryx6 robot (Douglas Instruments). After 1 day, crystals grew in condition number 2-38 of PACT *premier*, which consisted of 0.1 M BIS-TRIS propane, pH 8.5, 0.2 M NaBr, 20% (w/v) PEG3350. Bigger crystals were grown in 1-μL drops. Prior to flash-cooling in liquid nitrogen, crystals were soaked in a cryosolution consisting of mother liquor, 10% glycerol and 10, 5, or 1 mM inhibitor to obtain the DCS- and propionate-bound

structures.

X-ray data collection was performed at the ESRF (Grenoble, France) on beamline ID23-1 (Kabsch, 2010) using a PIXEL, Pilatus_6M_F X-ray detector. A total of 1127 frames were collected for the native Alr, with an oscillation of 0.15° , an exposure time of 0.378 s, total 426.006 s. The data set was processed by XDS (Kabsch, 2010) and scaled by AIMLESS (Evans & Murshudov, 2013) to a resolution of 2.8 Å. For the DCS-bound Alr 960 frames were collected, with an oscillation range of 0.15° , an exposure time of 0.071 s per image and a total time of 68.16 s. For the propionate-bound structure, 1240 images were collected, with an oscillation degree of 0.1° , an exposure time per image of 0.037 s, and a total time of 45.88 s. Both inhibitor-bound data sets were auto-processed by the EDNA Autoprocessing package in the mxCuBE (Gabadinho *et al.*, 2010) to a resolution of 1.64 Å and 1.51 Å for the DCS-bound and propionate-bound Alr, respectively. The structures were solved by molecular replacement with *MOLREP* (Vagin & Teplyakov, 1997) using 1VFH as a search model from the *CCP4* suite (Winn *et al.*, 2011) and iteratively refined with *REFMAC* (Murshudov *et al.*, 2011). Manual model building was done using *Coot* (Emsley & Cowtan, 2004).

Enzyme kinetics

The racemization activity of Alr was determined by quantifying the derivatization product of L- and D-Ala by HPLC, as previously described (Hashimoto *et al.*, 1992, Ju *et al.*, 2005). The derivatization reagent consisted of a methanol solution of 10 mg mL⁻¹ *o*-phthalaldehyde (OPA, Sigma-Aldrich) and 10 mg mL⁻¹ Boc-L-Cys (Sigma-Aldrich). A 0.4 M boric acid solution was adjusted to pH 9.0 with sodium hydroxide. The reaction mixture consisted of 20 μL of 20 mM sodium phosphate buffer, pH 7.0 containing varying amounts of L- or D-Ala from 281 μM to 20 mM. The reaction was started by adding 100 nM of enzyme and stopped after 10 min at 25°C by adding 20 μL of 2 N HCl. The reaction mixture was neutralized by NaOH. After adding 350 μL of boric acid buffer and 100 μL of derivatization reagent, derivatization was conducted for 5 min at 25°C. The fluorescent products were separated on a Kinetex EVO C18 column (Phenomenex) by a gradient from 24% to 46.75% of acetonitrile in water in 30 min and detected by a Shimadzu RF-10AXL fluorescence detector.

RESULTS AND DISCUSSION

Creation of an *alr* null mutant of *S. coelicolor*

To study the role of *alr* in amino acid metabolism and in morphogenesis of *S. coelicolor*, a deletion mutant was created by removal of the entire coding region (see Materials & Methods). In line with its expected role in biosynthesis of the essential D-amino acid D-Ala, *alr* null mutants depended on exogenously added D-Ala (50 μ M) for growth (Fig 1a). Re-introducing a copy of the *alr* gene via plasmid pGWS1151 complemented the mutant phenotype, allowing growth in the absence of added D-Ala (Fig 1a).

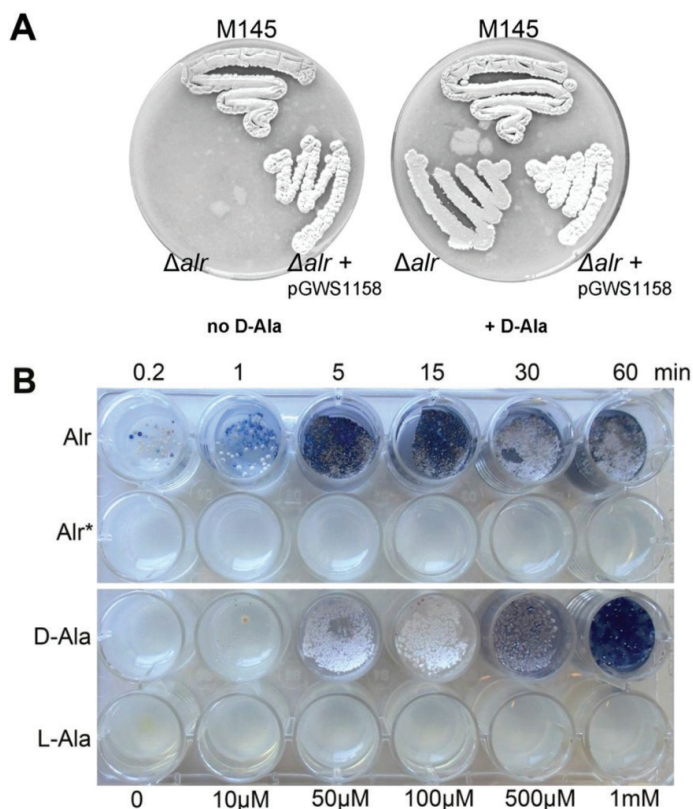


Figure 1. SCO4547 encodes alanine racemase Alr. (A) A *S. coelicolor* *alr* null mutant fails to grow in the absence of added D-Ala. This phenotype is rescued by the introduction of plasmid pGWS1151 which expresses Alr. Strains were grown for 5 days on SFm agar plates. (B) Rescue of an *S. coelicolor* *alr* null mutant with D-Ala produced *in vitro* by Alr. Alr (0.2 nM) was incubated with 10 mM L-Ala for 0, 1, 5, 15, 30 or 60 min, followed by heat inactivation. The reaction mixture was then added to MM agar in 24 well plates and growth of the *alr* null mutant assessed. As a control, the same experiment was done with heat inactivated Alr (Alr*). Note the restoration of growth to the *alr* mutant after addition of the reaction mixture with active Alr, but not with heat-shocked Alr. The bottom rows show control experiments with added D-Ala or L-Ala (ranging from 0-1 mM).

Alr is the only alanine racemase in *S. coelicolor*

The Alr from *S. coelicolor* (Alr_{Sco}) shares 74.9% aa sequence identity with the Alr from the DCS-producing *Streptomyces lavendulae* (Alr_{Sla}) (Noda *et al.*, 2004b) and 37.9% with the well-studied Alr from *Geobacillus stearothermophilus* (Alr_{Gst}) (Shaw *et al.*, 1997) (Fig. 2). To analyze the activity and kinetics of the enzyme, recombinant His₆-tagged Alr was expressed in *E. coli* BL21 Star cells and purified to homogeneity (Materials and Methods). Around 45 mg of pure Alr was obtained from 1 L of bacterial culture and Alr was identified using mass spectrometry (Table S4).

To establish if Alr_{Sco} converts L-Ala into D-Ala, we designed a combined *in vitro* and *in vivo* assay, whereby 10 mM L-Ala was incubated with 0.2 nM purified Alr-His₆ for 10 sec to 60 min, after which the enzyme was heat-inactivated and the mixture was added to minimal media (MM) agar plates, followed by plating of 10⁶ spores of the *alr* null mutant and incubation of 5 days at 30°C (Fig. 1b). If Alr converts L-Ala into D-Ala, the reaction should generate sufficient D-Ala to allow restoration of growth to *alr* null mutants. Indeed, sufficient D-Ala was produced to allow growth of the *alr* null mutant, whereby biomass accumulation was proportional to the incubation time, while a control experiment with extracts from heat-inactivated Alr did not give any growth (Fig. 1b). Addition of D-Ala also restored growth of *alr* mutants, while no growth was seen for cultures grown in the presence of added L-Ala. Taken together, this shows that no Alr activity is present in *S. coelicolor alr* mutants, and that Alr actively converts L-Ala into D-Ala *in vitro*.

The kinetic parameters of recombinant Alr_{Sco} were determined using both L- and D-Ala as substrates. The enzyme shows a K_m of 6.3 mM and 8.9 mM towards L- and D-Ala, respectively (Table S5). For comparison, kinetic parameters of Alr_{Sla} (Noda *et al.*, 2004b) and Alr_{Gst} are also shown in Table S5. To analyze possible multimerization of Alr_{Sco}, analytical gel filtration was used, which established an apparent molecular weight for the protein of 83 kDa in solution both in the absence and in the presence of L-Ala and DCS (Figure S1); this corresponds roughly to two Alr proteins (43.4 kDa per subunit). These data suggest that Alr_{Sco} forms a dimer in solution, both in the presence and in the absence of ligands.

Structural and Functional Characterization of the Alanine Racemase from *Streptomyces coelicolor* A3(2)

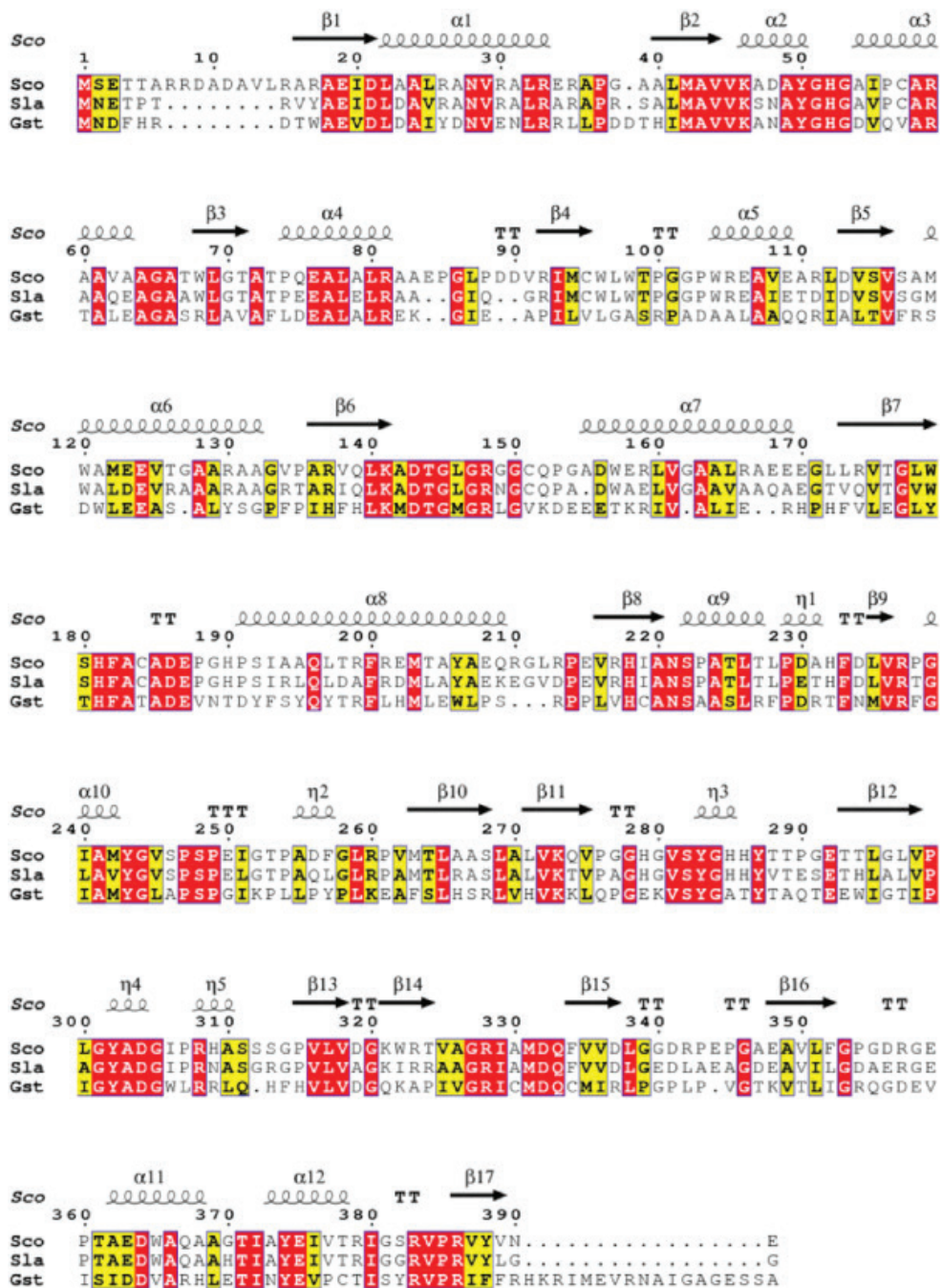


Figure 2. Multiple amino acid sequence alignment of the Alr's from *S. coelicolor* (Sco), *S. lavendulae* (Sla; PDB 1VFT) and *G. stearothermophilus* (Gst; PDB 1XQK). The sequence alignment showing structural elements of Alr_{Sco} was generated with ESPript3.0. α -helices are shown as large coils labeled α , 3_{10} -helices are shown as small coils labeled η , β -strands are shown as arrows labeled β and β -turns are labeled TT. Identical residues are shown on a red background, conserved residues are shown in red and conserved regions are shown in boxes.

Overall structure of Alr from *Streptomyces coelicolor*

The crystal structure of ligand-free Alr_{Sc_o} was determined to a resolution of 2.8 Å (Table S6). The overall structure is similar to that of other prokaryotic Alr proteins (Noda *et al.*, 2004b, Shaw *et al.*, 1997). The asymmetric unit contains four protein molecules (A-D), which interact in a head-to-tail manner to form two dimers (dimer A-B and C-D, Fig. 3a). Each monomer has two structurally distinct domains. The N-terminal domain, comprising residues 1-259, has an eight-stranded α/β -barrel fold, typical of phosphate-binding proteins. The C-terminal domain, residues 260-391, contains mostly β -strands (Fig. 3b). 96% of the amino acids are in the preferred regions of the Ramachandran plot, 4% are in the allowed regions and no residues are in the unfavored areas. After refinement, the r.m.s. deviation between Ca's of the two interacting molecules A and B is 0.0794 Å, and between C and D is 0.1431 Å.

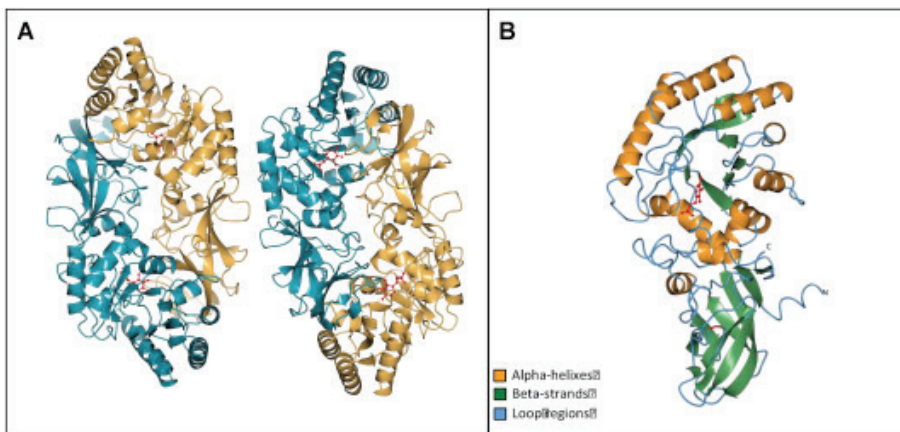


Figure 3. Ribbon representation of the Alr from *S. coelicolor*. (a) The asymmetric unit contains two homo-dimers. The two chains within one dimer are colored in gold and dark cyan. (b) The N-terminal domain (1-259) is a α/β -barrel. The C-terminal domain (260-391) mostly comprises β -strands. The catalytic Tyr283 is highlighted in red.

There are two active sites per dimer, which are located at the interface between each α/β -barrel of one subunit and the C-terminal domain of the other. The catalytic core (Fig. 4a) consists of the PLP cofactor, a Lys, and a Tyr, which is contributed by the other subunit. The PLP is bound through an internal aldimine bond to the amino group of Lys46, located at the C-terminal side of the first β -strand of the α/β -barrel. The side chain of the catalytic Lys46 points out of the α/β -barrel, towards the C-terminal domain of the interacting subunit, and in particular, towards Tyr283'. The phosphate group of the PLP is stabilized by hydrogen bonds with the side chains of Tyr50, Ser222 and Tyr374, and with the backbone of Gly239, Ser222 and Ile240. The pyridine ring of the PLP is stabilized by a hydrogen bond between the N-1 of the cofactor and N ϵ of Arg237. The C2A of the PLP also interacts with oxygen Q1 of the carboxylated Lys141. All residues stabilizing the PLP cofactor (Tyr50, Ser222, Gly239, Ile240, Arg237, Tyr374) are conserved among Alr's (Shaw *et al.*, 1997). However, the Alr_{Sc_o} lacks one important hydrogen bond between Arg148 and the phenolic oxygen of the PLP molecule, as already observed for the Alr_{S_{la}} (Noda *et*

al., 2004a) (Noda *et al.*, 2004b). Among the residues involved in PLP-stabilization, Tyr374, which corresponds to Tyr354 in the well-studied Alr_{Gst}¹, is particularly interesting. In fact, while always regarded as a PLP-stabilizer, Tyr354 was shown to be actually anchored by the hydrogen bond with the PLP so to ensure substrate specificity of the Alr (Patrick *et al.*, 2002).

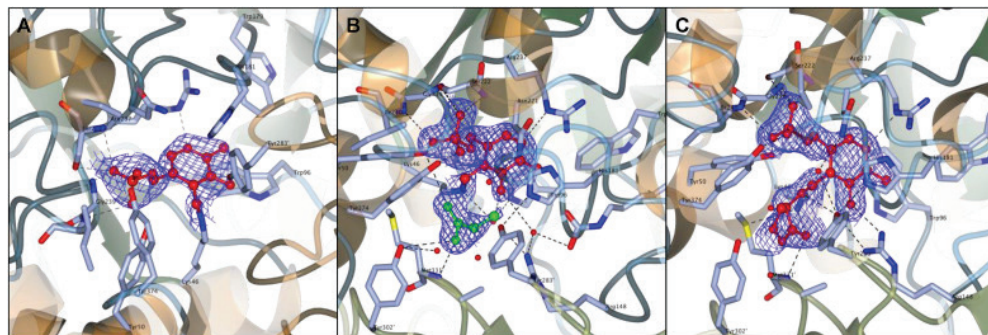


Figure 4. Active site of the Alr without ligands (a) and in complex with propionate (b) and D-cycloserine (c). The electron density $2F_o - F_c$ map is shown for the PLP and the two inhibitors. The residues in the active site which are contributed from the monomer not bound to the PLP are indicated as primed numbers. Dotted lines indicate interatomic distances shorter than 3 Å.

Alr crystal structures bound to propionate and DCS

The structure of Alr_{Sco} was solved in the presence of the two inhibitors propionate (Morollo *et al.*, 1999) and DCS (Noda *et al.*, 2004b) to a resolution of 1.51 Å and 1.64 Å, respectively. In Alr_{Sco}, the carboxylic group of propionate binds in the same orientation in all four active sites present in the crystal unit. One of the carboxylic oxygens of propionate forms hydrogen bonds with the amino group of Met331', the phenolic oxygen and CE2 of Tyr283' and a water molecule, which bridges the substrate to several other water molecules in the active site. The second carboxylic oxygen of propionate interacts with Nz of Lys46, C4A of PLP, the phenolic oxygen of Tyr283' and a water molecule. The electron density around C3 of propionate shows that this atom can have several orientations in the active site. In fact, it can either interact with O4 of the phosphate of PLP, the phenolic oxygen of Tyr283' and a water molecule, or with the phenolic oxygen of Tyr50, the CE of Met331', Nz of Lys46 and C4A of PLP (Fig. 4b). Both in Alr_{Sco} and Alr_{Gst} the hydrogen-bonding network stabilizing the propionate is very conserved. As argued by (Morollo *et al.*, 1999), the propionate-bound form of the Alr can be considered a mimic of the Michaelis complex formed between the enzyme and its natural substrate L-Ala.

DCS is an antibiotic produced by *S. lavendulae* and *Streptomyces garyphalus*, which covalently inhibits Alr (Noda *et al.*, 2004b, Fenn *et al.*, 2003, Asojo *et al.*, 2014, Priyadarshi *et al.*, 2009, Wu *et al.*, 2008, Lambert & Neuhaus, 1972). The structure of the Alr_{Sco} in complex with DCS shows that the amino group of the inhibitor replaces the Lys46 in forming a covalent bond with the PLP C4 (Fig. 4c). The nitrogen and oxygen atoms in the isoxazole ring form hydrogen bonds with Tyr302', Met331' and a water molecule. The hydroxyl group of the DCS ring also interacts with Met331' and Arg148 (Fig. 4c). The catalytic Tyr283' is at hydrogen-bond distance from the amino group of DCS. DCS molecules superpose well in three of the active sites of the crys-

tal (A, B and C). However, the DCS-PMP adduct in the fourth site showed a shift of the DCS compared to the other sites, while PLP still superposed well. Comparison of the hydrogen bonds in the proximity of the active site in the free and in the DCS-bound form of Alr, revealed a role for Arg148 in substrate stabilization. In fact, while the side chain of Arg148 is hydrogen-bonded to Gln333 in free Alr, it shifted towards the hydroxyl moiety of the DCS upon binding of the inhibitor. Gln333 was stabilized by interaction with carboxylated Lys141. The rearrangement of the hydrogen bonds involving Arg148, Gln333 and Lys141 does not occur in the propionate-bound structure, suggesting that Arg148 is involved in stabilization of the carboxylic group of the substrate.

Alr and DCS resistance

Alr_{SCO} shows high sequence and structural similarity to Alr_{Sla}. Based on crystallographic studies, Alr_{Sla} was proposed as one determinant of DCS resistance in the producer strain (Noda *et al.*, 2004b). However, detailed structural comparison of different Alr proteins based on interatomic distances between active site residues, dimerization areas and hinge angles (SI), failed to establish a clear correlation between structural features and DCS resistance. It therefore remains unclear what the role of Alr is in DCS resistance in the producer strain.

In conclusion, we showed that SCO4745 encodes the only Alr in *S. coelicolor* A3(2) and that it is essential for growth. Our structural studies on Alr_{SCO} and comparison to Alr_{Sla} suggest that Alr is not the only factor that contributes to DCS resistance, and further investigation is required, in line with recent studies on DCS-producing Streptomyces (Matsuo *et al.*, 2003) and DCS-resistant strains of *M. tuberculosis* (Desjardins *et al.*, 2016, Hong *et al.*, 2014, Feng & Barletta, 2003, Chen *et al.*, 2012).

CHAPTER 7

General Discussion

The bacterial cell wall is an extremely dynamic macromolecule subject to constant construction and deconstruction depending on the requirements that are imposed by cell growth. New cell wall material is incorporated in a manner which still supports cell structure and survives the turgor pressure – there is no room for weak spots. Correct regulation of cell wall synthesis is essential for several processes in *Streptomyces*. After dormancy, spores need to germinate in a favorable environment, a process tightly regulated by the cAMP receptor protein CRP and Resuscitation Promoting Factors (RPFs) (Piette *et al.*, 2005, Sexton *et al.*, 2015). After germination, DivIVA driven apical growth drives the formation of a large vegetative mycelial structure (Flårdh *et al.*, 2012). During vegetative growth, cross-membranes and vegetative septa are formed to compartmentalize the vegetative mycelium, an SsgB-independent but FtsZ-dependent process (Celler *et al.*, 2016, Yague *et al.*, 2016). Later, spores are formed by a process where SsgB recruits FtsZ, resulting in Z-rings that are spaced by approximately 1 μM , followed by septation and eventually spores (Willemse *et al.*, 2011). After spore dispersal, the life cycle starts anew. This complexity and the necessity for regulation is expressed in the 7-11 SsgA-like proteins in streptomycetes that serve to control processes relating to cell wall remodeling, including germination, branching and sporulation (Traag & van Wezel, 2008), in the nine penicillin binding proteins (PBPs) and seven putative L,D-transpeptidases (LDTs) which together serve to cross-link the peptidoglycan, and in the 50-60 genes predicted to be involved in peptidoglycan hydrolysis (Haiser *et al.*, 2009). This regulation and modification is visible in the diverse mucopeptide pattern, which shows more than 60 separate mucopeptides, as shown in this thesis. As one of the most well-conserved cellular entities, the bacterial cell wall is a major target for antibiotics, and many of these are produced by actinobacteria (Barka *et al.*, 2016). To protect themselves against their own antibiotics, *Streptomyces* carry antibiotic resistance mechanisms that vary from modifying the function of a single protein, like D-cycloserine resistance, to a complete cluster of genes that modifies a part of the cell wall, as seen in vancomycin resistance (Schaberle *et al.*, 2011). Not surprisingly, there are many aspects of *Streptomyces* biology that have not been resolved. In this thesis, I investigated how the actinobacterial cell wall contributes to species differentiation, cell growth and antibiotic resistance.

Cell wall research in actinobacteria finds its origins in the taxonomic separation of different species. Beginning with the pioneering work by Lechevalier and Lechevalier, the composition of the cell wall has served as a useful tool for actinomycete classification (Lechevalier *et al.*, 1971, Cummins, 1962). They showed that all actinomycete cell walls contain *N*-acetyl-glucosamine, *N*-acetyl-muramic acid, alanine and glutamic acid. Diagnostic differences between different actinomycetes species can be found in the presence of glycine, lysine and either LL- or LD(*meso*)-diaminopimelic acid, together with a set of diagnostic sugars: arabinose, galactose, xylose and madurose. In their analysis, the authors also detected the sugars arabinose and galactose, which form the arabinogalactan layer of *Mycobacterium* and *Nocardia* species.

Chapter 2 shows a polyphasic taxonomic approach to the characterization of *Streptomyces roseifaciens*, a novel species of *Streptomyces* originally isolated from the QinLing mountains in China (Zhu *et al.*, 2014a, Zhu *et al.*, 2014b). This *Streptomyces* species is a morphological outlier of the *Streptomyces*, as this does not

make long spore chains, but verticillate spores which branch out of the side of aerial hyphae (Hatano *et al.*, 2003). On analyzing the distribution of the SsgA-like proteins (SALPS), it became apparent that verticillate *Streptomyces* typically lack SsgE. In *Streptomyces coelicolor*, *ssgE* deletion mutants predominately produce single spores, rather than spore chains, suggesting a role in spore chain morphology. This correlates well with the fact that verticillate streptomycetes have an entirely different way of producing spore chains, namely many short chains at the lateral side of the aerial hyphae instead of conversion of the aerial hyphae in a single long spore chain.

Whereas cell wall research has started as a taxonomic indicator, current cell wall research is performed to generate insight in bacterial cell growth and development. In Chapter 3 the cell wall composition of *S. coelicolor* was analyzed in growing vegetative hyphae and of spores to look for trends and changes in peptidoglycan composition, and more importantly, to get a hint on the mechanisms of tip growth. Therefore, the muropeptide profile was analyzed by LC-MS, which allows direct detection of the masses associated with different muropeptides, even with overlapping retention times. This study identified over 60 different muropeptides over the course of growth and development. Especially interesting was the high amount of 3-3 cross-links, produced by L, D-transpeptidases (LDTs). LDTs are recognized as transpeptidases that function similarly to Penicillin Binding Proteins (PBPs), although cross-linking at a different point. Importantly, PBPs require the presence of pentapeptides to form a 3-4 cross-link, whereas LDTs require tetrapeptides to form a 3-3 cross-link. The abundance of 3-3 cross-links is especially high in actinobacteria (which grow at the tip) and LDTs are suggested to remodel the cell wall in the post-tip area (Baranowski *et al.*, 2018). The work described in Chapter 3 also revealed that the amount of 3-3 cross-links increases as vegetative mycelium ages, and hyphae grow longer. Cell wall hydrolysis was clearly visible in our data, especially vegetative mycelium showed a high amount of dimers lacking a set of glycans, indicating constant cell wall hydrolysis. In addition, we show that a single muropeptide increases in abundance over the course of development, namely a MurN-tri peptide, which lacks GlcNAc and carries a de-acetylated MurNAc. Possibly, this muropeptide has no function itself but is the result of hydrolysis or spore separation.

The muropeptide profile of *S. coelicolor* showed that the most apparent difference between the cell wall composition of vegetative mycelium and spores relates to the abundance of certain muropeptides, while no muropeptides were uniquely associated with either vegetative mycelium or spores. To investigate this further, we looked back at the taxonomy of streptomycetes. The presence of either LL-DAP, *meso*-DAP or both is indicative of the genus. This proves invaluable to distinguish *Streptomyces* from *Kitasatosporae*, which are very similar in respect to morphology and 16S rRNA and resulted in the inclusion of *Kitasatospora* within the genus *Streptomyces* (Kim *et al.*, 2004). However, *Kitasatosporae* have different SsgA-like proteins, and lack orthologues of *mbI*, *bldB* and *whiJ*, suggesting that development is regulated in a different manner (Girard *et al.*, 2014). The main diagnostic difference between the cell walls of the two genera within the *Streptomycetaceae* is that *Streptomyces* cell walls contain LL-DAP, whereas *Kitasatospora* cell walls carry *meso*-DAP in the vegetative mycelium and LL-DAP in the spores (Takahashi, 2017, Girard *et al.*, 2014). DAP is a key component of the peptidoglycan, as this amino acid is at the connecting part of cross-links between peptide chains, either a 3-3 or a 3-4 cross-link. We sus-

pected that the difference in stereochemistry could be related to a difference in the peptidoglycan household. Indeed, the work in Chapter 4 shows that two species of *Kitasatospora*, *K. setae* and *K. viridifaciens*, heavily remodel the peptidoglycan between vegetative growth and reproductive growth. It is almost as if the mucopeptide profiles from vegetative mycelium and spores had been obtained from different organisms. This shows that not only the DAP isometry is different between two stages of development, but the entire PG architecture changes radically. The regulation of incorporation of either *meso*- or LL-DAP is unclear, as is the function of this chemical difference between vegetative mycelium and spores.

As mentioned above, the bacterial cell wall is a very important target for antimicrobial compounds. Vancomycin is a glycopeptide antibiotic, mostly used as a last-resort compound, when infections of Gram-positive bacteria are unresponsive to other antibiotics. Chapter 5 discusses the vancomycin resistance cluster of *S. coelicolor*, which largely resembles resistance clusters as found in vancomycin resistant *Enterococci* (Hong et al., 2004). Vancomycin targets the D-Ala-D-Ala terminus of Lipid II, before this is incorporated into the mature peptidoglycan. Resistance against vancomycin is gained by replacing the D-Ala-D-Ala terminus by D-Ala-D-Lac, performed by a combination of seven genes. A two-component regulatory system, VanR and VanS recognize vancomycin in the environment, VanH produces D-Lactic acid, VanA ligates D-Alanine and D-Lactic acid and VanX is a dipeptidase that cleaves D-Ala-D-Ala. We show that the addition of D-Alanine increases the sensitivity of bacteria to vancomycin due to the bifunctional activity of the D-Alanine-D-Lactate ligase VanA. VanA is in essence a modified version of the D-Alanine-D-Alanine ligase Ddl and VanA is able to ligate D-Ala and D-Ala when this is available in the environment. This effect becomes especially clear in a knock-out mutant of *vanX* with the addition of exogenous D-Ala. When the amount of D-Ala in the environment is high, VanA produces D-Ala-D-Ala and when this is not broken down by VanX, the strain regains sensitivity to vancomycin. This emphasizes that antibiotic resistance mechanisms do not function perfectly, but serve to function good enough as to secure survival. A small molecule screen should facilitate the discovery of drugs that target VanX. If such a drug is found, it may be an efficient enhancer of the bioactivity of vancomycin.

The pentapeptide chain in the peptidoglycan consists of interchanging L- and D-amino acids, of the MurNAc-bound D-Lac, L-Ala, D-Glu, LL-DAP and D-Ala-D-Ala (Vollmer *et al.*, 2008a). This interchange serves to deter unspecific peptidases as regular peptidases only target L-amino acids, and a relatively simple mirror image of a peptidase could target a chain of D-amino acids (Radkov & Moe, 2014). A chain of interchanging L- and D- amino acids requires highly specific endopeptidases, such a phenomenon is also found in lantibiotics (Knerr & van der Donk, 2013). In Chapter 6 we have explored the role of the alanine racemase Alr, which is essential for growth, and mutants can only be produced in the presence of D-Ala. This feature was used to show the *in vitro* bioactivity of the enzyme; *alr* null mutants cannot grow when media are supplemented with L-Ala, but if the amino acid is preincubated with Alr enzyme, the mixtures contained sufficient D-Ala to support growth. This clearly showed the *in vitro* racemase bioactivity of the enzyme, and this enzyme prep was subsequently used to determine its crystal structure. The Alr protein is pyridoxal phosphate-dependent and forms a heterodimer. The crystal structure of the protein is solved both with and without its inhibitor D-cycloserine (DCS), a D-Ala analogue that acts as a sui-

cide substrate for Alr. We expected that the DCS producer *Streptomyces lavendulae* might have significant changes in its Alr homologue, but comparison of the crystal structures of the Alr orthologues of *S. coelicolor* and *S. lavendulae* did not reveal any changes that could directly be related to obvious differences in substrate specificity. We therefore suspect that the D-alanine-D-alanine ligase (Ddl) plays an additional role in DCS resistance, and this idea needs to be worked out further.

OUTLOOK

The work presented in this thesis features different approaches to characterize actinomycetes and their cell wall, from the small scale of protein isolation and characterization, peptidoglycan architecture analysis, to taxonomy and antibiotic resistance mechanisms. Each of the research directions in this thesis leaves questions unanswered. In the case of the verticillate *Streptomyces*, we have identified a different set of SALPS from *Streptomyces* with canonical spores, but we do not know how sporulation along the lateral wall is regulated. If this is resolved, it will deliver important cues as to how sporulation-specific cell division is controlled in time and space. The cell wall analysis of *Streptomyces* showed which mucopeptides are available in a complete culture at different moments in time, but a mucopeptide analysis requires an entire culture so we do not yet have spatial knowledge of different PG modifications. Analysis of *Kitasatospora* PG showed that vegetative PG had *meso*-DAP and spore PG LL-DAP. We can only wonder whether the difference in stereochemistry acts as a signal, or whether the stereochemistry is functional at all. The work on vancomycin resistance showed how a deletion of *vanX* increased sensitivity in Vancomycin-resistant strains by a thousand fold, showing major potential for a solution to the high amount of vancomycin resistant infections. Here, the missing component is a chemical inhibitor of the VanX protein. This thesis describes a working fluorescence-based assay to screen for VanX-inhibitors, perhaps this can inspire future scientists to continue the research.

We are currently at a time where genome sequencing becomes commonplace, among others due to ever-decreasing cost, and chemical toolboxes are expanding with new high-throughput methods for cell wall analysis. Imaging is becoming more informative and broadly applicable with fluorescent dyes such as the fluorescent D-amino acid HADA, that binds to PG at the position of D-Ala and allows scientists to localize sites of cell wall remodeling (Kuru *et al.*, 2015). This combination of genomics, biochemical tools and biological insights provides scientists with the perfect opportunity to work with understudied organisms and to investigate how the different modes of growth are executed and controlled. Future work might show why *Kitasatospora* have different stereoisomers of DAP at different developmental stages, how sporulation is regulated in verticillate *Streptomyces*, or how *Streptomyces* know where septal sites in aerial mycelia need to be in order to produce a long chain of equal sized spores. Exiting times are ahead!

Nederlandse samenvatting

De bacteriële celwand is een dynamisch molecuul dat constant wordt afgebroken en wederopgebouwd om celgroei en celdeling te faciliteren. Nieuw celwandmateriaal wordt ingebouwd terwijl de cel onder constante turgordruk staat; er is geen ruimte voor zwakke plekken. De juiste organisatie van celwandsynthese is essentieel voor meerdere processen in het leven van Streptomycten. Als *Streptomyces* sporen een gunstige omgeving hebben gevonden zullen ze ontkiemen, een proces dat strak gereguleerd wordt door het cAMP receptor eiwit CRP en Resuscitation Promoting Factors (RPFs) (Piette *et al.*, 2005, Sexton *et al.*, 2015). Na ontkieming groeien vegetatieve hyfen verder vanuit de top, ondersteund door eiwit DivIVA, waarna de hyfen uitgroeien tot een meercellig mycelium (Flårdh *et al.*, 2012). Tijdens de vegetatieve groei van deze lange hyfen ontstaan er compartimenten binnen de hyfen zelf door cross-membranen en vegetatieve septa, een proces waarvoor het eiwit FtsZ essentieel is, maar wat onafhankelijk is van SsgB (Celler *et al.*, 2016, Yague *et al.*, 2016). Sporen worden later gevormd door de lange luchthyfen in kleine compartimenten te delen, waarvoor SsgB het celdelingseiwit FtsZ rekruteert. FtsZ vormt later FtsZ-ringen op precies 1 μM afstand van elkaar. Hierop vernauwen de ringen om een septum te vormen, en uiteindelijk de sporen zelf (Willemse *et al.*, 2011). Na het verspreiden van sporen begint deze levenscyclus weer van begin af aan. De complexiteit en de noodzaak voor de regulatie van de groei wordt uitgedrukt in de 7-11 SsgA-like proteïnes (SALPS) in Streptomycten. Deze eiwitten reguleren processen gerelateerd aan de celwand, waaronder de ontkieming, vertakking en sporenvorming (Traag & van Wezel, 2008). Behalve de celwand regulatie via SALPS, codeert het DNA van Streptomyces ook voor negen penicillin binding proteïnes (PBPs), en zeven L,D-transpeptidases (LDTs), die samen het peptidoglycaan cross-linken. De noodzaak voor regulatie zien we terug in de 50-60 genen waarvan verondersteld wordt dat zij verantwoordelijk zijn voor het afbreken van het peptidoglycaan (Haiser *et al.*, 2009). Als een van de best geconserveerde onderdelen van de cel is de bacteriële celwand ook een geliefd doelwit voor antibiotica, waarvan er veel geproduceerd worden door actinobacteriën zelf (Barka *et al.*, 2016). Om zichzelf te beschermen tegen hun eigen geproduceerde antibiotica dragen *Streptomyces* antibiotica-resistentie mechanismen. Deze mechanismen variëren: van het modificeren van de functie van een enkel gen, zoals we zien in D-cycloserine resistentie, tot een compleet cluster van genen dat een onderdeel van de celwand verandert, zoals we zien in vancomycine resistentie (Schaberle *et al.*, 2011). Het komt niet als een verrassing dat er veel aspecten zijn van de *Streptomyces* biologie nog onbekend zijn. In dit proefschrift heb ik onderzocht hoe de actinobacteriële celwand bijdraagt aan soortvorming, celgroei en antibiotica resistentie.

Celwandonderzoek in actinobacteriën vindt zijn origine in de taxonomische scheiding van verschillende nauw verwante bacteriële soorten. Het pionierende werk van Lechevalier en Lechevalier heeft als eerst de precieze samenstelling van de celwand bepaald van alle destijds bekende actinomycten, om zo een basis te leggen voor de chemische classificatie van deze soorten (Lechevalier *et al.*, 1971, Cummins, 1962). Zij hebben aangetoond dat de celwanden van alle actinomycten N-acetyl-glucosamine, N-acetyl

muraminezuur, alanine en glutaminezuur bevatten. De verschillen tussen de verschillende soorten actinomyceten zit in de aanwezigheid van glycine, lysine en ofwel de celwand LL- of LD (*meso*)-diaminopimelic acid, evenals de aanwezigheid van een set diagnostische suikers: arabinose, galactose, xylose en madurose. In dit onderzoek werden de suikers arabinose en galactose, de onderdelen van de arabinogalactanlaag van Mycobacterien en Nocardia, al aangetoond.

Hoofdstuk 2 bevat een taxonomische benadering tot de karakterisatie van *Streptomyces roseifaciens*, een nieuwe soort binnen de streptomyceten die origineel geïsoleerd is in de QinLing bergen in China (Zhu *et al.*, 2014a, Zhu *et al.*, 2014b). Deze soort is een morfologische vreemde eend binnen de *Streptomyces*: *S. roseifaciens* maakt geen lange sporenketen, maar maakt sporen in een krans rond luchthyfen (Hatano *et al.*, 2003). Wanneer we naar de SsgA-like proteïns (SALPS) keken bleek dat streptomyceten met kransvormige sporenketens typisch SsgE missen. In *Streptomyces coelicolor* heeft een *ssgE*-gedeelteerde mutant voornamelijk enkele sporen in plaats van lange sporenketens, wat een rol in sporenketenuiterlijk suggereert. Dit past in de lijn dat kranssporulerende streptomyceten een andere sporenketenmorfologie hebben, namelijk met korte sporenketens aan de zijkant van luchthyfen in plaats van een lange luchthyfe dat wordt opgedeeld in kleine compartimenten om sporen te maken.

Waar celwandonderzoek begonnen is als taxonomisch hulpmiddel, wordt de celwand tegenwoordig voornamelijk onderzocht om inzicht te krijgen in de groei en ontwikkeling van bacteriën. In hoofdstuk 3 is de celwandsamenstelling van *Streptomyces coelicolor* geanalyseerd in groeiende vegetatieve mycelia en in sporen om zo te zoeken naar trends en veranderingen in peptidoglycaancompositie. Het doel hiervan is om inzicht te verkrijgen in de mechanismen achter topgroei. Het muropeptide profiel was geanalyseerd met behulp van LC-MS, deze techniek staat toe dat de massa's direct gemeten wordt na de chromatografie, ook als de retentietijden overlappen. Deze studie identificeerde meer dan 60 verschillende muropeptiden gedurende de groei en ontwikkeling. Vooral interessant was de hoge hoeveelheid 3-3 cross-links, geproduceerd door L, D-transpeptidases (LDTs). LDTs zijn transpeptidases die een werking hebben lijkend op die van penicilline bindende eiwitten (PBPs), maar een link vormen op een andere positie. Essentieel is dat PBPs pentapeptiden als substraat nodig hebben om 3-4 cross-links te kunnen vormen, terwijl LDTs tetrapeptiden nodig hebben om 3-3 cross-links te kunnen vormen. De hoeveelheid van 3-3 cross-links is bijzonder hoog in actinobacteriën, die allemaal van de top groeien en het is gesuggereerd dat LDTs de celwand veranderen in het gebied na de groeiende top (Baranowski *et al.*, 2018). Het werk beschreven in hoofdstuk 3 toont dat de hoeveelheid 3-3 cross-links toeneemt terwijl het mycelium groeit en ouder wordt. Celwand afbraak was duidelijk zichtbaar in onze data, wat laat zien dat er constante peptidoglycaanhydrolyse plaats vindt. Hierbij tonen we aan dat er een enkele muropeptide in hoeveelheid toeneemt bij sporenvorming. Deze MurN-tripeptide mist GlcNAc en heeft een gede-acetylerde MurNAc. Mogelijkerwijs heeft dit peptide geen eigen functie maar is het een gevolg van hydrolyse of

sporenvorming.

Het muropeptideprofiel van *S. coelicolor* laat zien dat het grootste verschil in celwandprofiel tussen vegetatief mycelium en sporen in de relatieve hoeveelheid van de muropeptiden zit, niet zozeer in de aan- of afwezigheid. Verder onderzoek naar de celwand begon door opnieuw te kijken naar de taxonomische achtergrond van de familie streptomyceten. De aanwezigheid van ofwel LL-DAP of meso-DAP is een indicatie van het genus; op deze wijze kunnen *Streptomyces* en *Kitasatospora* van elkaar worden onderscheiden, ondanks dat deze twee soorten wat betreft morfologie en 16S rRNA enorm veel op elkaar lijken. (Kim et al., 2004). Een ander verschil in *Kitasatosporae* is de huishouding in SALPs en het ontbreken van orthologen van de genen *mbl*, *bldB* en *whiH*. Dit suggereert dat de ontwikkeling anders gereguleerd wordt in *Kitasatospora* dan in *Streptomyces* (Girard et al., 2014). Het verschil tussen deze twee genera is dat de *Streptomyces* celwand LL-DAP bevat, terwijl de *Kitasatospora* celwand meso-DAP in het vegetatieve mycelium heeft en LL-DAP in de celwand van de sporen (Takahashi, 2017, Girard et al., 2014). DAP is een sleutelcomponent van het peptidoglycaan: dit aminozuur vormt het verbindende gedeelte van een cross-link tussen peptide ketens, als ofwel een 4-3 dan wel een 3-3 cross-link. We verwachten dat het verschil in stereochemie gerelateerd kan zijn aan de peptidoglycaanhuishouding. Het werk in hoofdstuk 4 betreft twee soorten *Kitasatosporae*, *K. setae* en *K. viridifaciens*. Deze twee soorten herstructureren het peptidoglycaan tussen vegetatieve groei en het vormen van sporen, waardoor er bij de analyse van deze twee groeistadia de indruk wordt gewekt dat het peptidoglycaanprofiel van andere organismen afkomstig zijn. Dit toont aan dat niet alleen de DAP isometrie anders is tussen deze twee stadia, maar de hele peptidoglycaan architectuur verandert. De genetische regulatie van het aanmaken van meso- of LL-DAP is onduidelijk, net als de functie achter dit verschil tussen vegetatief mycelium en sporen.

Zoals eerder genoemd is de bacteriële celwand een geliefd aanhechtingpunt voor antimicrobiële compounds. Vancomycine is een glycopeptide antibioticum dat wordt gebruikt bij het behandelen van complexe infecties met Gram positieve bacteriën die niet meer op andere antibiotica reageren. Hoofdstuk 5 betreft het vancomycine resistentie cluster van *S. coelicolor*, die grotendeels overeenkomt met resistentie clusters van infectieuze stammen zoals de vancomycine-resistente Enterokok(Hong et al., 2004). Vancomycine werkt op het 'D-Ala-D-Ala' uiteinde van Lipid II, voordat deze wordt ingebouwd in het peptidoglycaan. Resistentie tegen vancomycine wordt verkregen door de 'D-Ala-D-Ala' terminus te vervangen door een 'D-Ala-D-Lac' uiteinde, een proces dat wordt uitgevoerd door een set van 7 genen in *S. coelicolor*. Dit proces start met een twee-component regulatie systeem, VanR en VanS, die de aanwezigheid van vancomycine in de omgeving kan herkennen. VanH produceert D-lactaat, waarop VanA dit koppelt aan D-alanine om 'D-Ala-D-Lac' te vormen. VanX is een dipeptidase die de overige 'D-Ala-D-Ala' afbreekt. Wij laten zien dat de toevoeging van D-Alanine de stam gevoeliger maakt voor vancomycine dankzij de tweeledigeactiviteit van de 'D-Alanine-D-Lactaat' ligase VanA. VanA is in essentie een gemod-

ificeerde versie van de 'D-Alanine-D-Alanine' ligase Ddl en VanA is in staat deze zelfde functie te vervullen als D-Alanine in overvloed aanwezig is in de omgeving. Dit effect is overduidelijk als zowel het gen *vanX* is uitgeschakeld en er extra D-Alanine wordt toegevoegd aan het groeimedium. Wanneer de hoeveelheid D-alanine in het medium hoog is, dan produceert VanA een D-Ala-D-Ala verbinding die niet wordt afgebroken door VanX, waardoor de stam gevoelig wordt voor vancomycine. Dit effect benadrukt dat antibioti-carestenties niet perfect zijn maar in essentie goed genoeg om de stam te helpen overleven. Een small-molecule screening zou het ontdekken van VanX-bindende moleculen kunnen faciliteren; een dergelijk molecuul zou de bioactiviteit van vancomycine verder kunnen versterken.

De pentapeptideketen in het peptidoglycaan bestaat uit een afwisseling van L- en D-aminozuren, beginnend bij de MurNAC-gebonden D-Lac, L-Ala, D-Glu, LL-DAP en 'D-Ala-D-Ala' (Vollmer *et al.*, 2008). Deze afwisseling zorgt voor een minder efficiënte binding van specifieke peptidasen, gezien reguliere peptidasen alleen ketens van L-aminozuren of simpele spiegelbeeldisomerie ketens van D-aminozuren kunnen afbreken (Radkov & Moe, 2014). Om een keten van afwisselend L- en D-aminozuren af te breken heb je hoog specifieke endopeptidasen nodig; antibiotica maken gebruik van dit fenomeen om de stabiliteit te verhogen (Knerr & van der Donk, 2013). In hoofdstuk 6 hebben we de rol van de alanine racemase Alr onderzocht, een eiwit essentieel voor groei van *S. coelicolor* en waarvan mutanten alleen kunnen worden gemaakt in aanwezigheid van D-Alanine. Deze eigenschap kan gebruikt worden om de in vitro bioactiviteit van het eiwit aan te tonen. Bij mutanten met een *alr* deletie is er geen sprake van groei wanneer L-alanine toegevoegd is aan het medium. Indien L-Ala eerst samen met Alr geïncubeerd is heeft het reagens wel genoeg D-Ala, waardoor de cultuur toch kan groeien. Dit toont duidelijk aan dat Alr in vitro actief is. Dit preparaat is gebruikt om de kristalstructuur te bepalen. Het Alr eiwit is pyridoxal phosphate afhankelijk en vormt een heterodimeer. De kristalstructuur van het eiwit is bepaald met en zonder de inhibitor D-cycloserine (DCS), een D-alanine analoog die aan Alr hecht en vervolgens niet loslaat. We hadden verwacht dat de producent van DCS, *Streptomyces lavendulae*, wellicht veranderingen had in zijn Alr homoloog, maar een vergelijking van de kristalstructuren van de Alr orthologen van *S. coelicolor* en *S. lavendulae* toonde geen veranderingen die gekoppeld zijn aan de duidelijke verschillen in substraat specificiteit. Hierom denken we dat de D-alanine-D-Alanine ligase (Ddl) een belangrijke rol speelt in DCS resistentie, wat verder uitgewerkt zou kunnen worden.

Vooruitblik:

Het werk in dit proefschrift toont verschillende benaderingen om de celwand van actinomyceten te karakteriseren en analyseren: van eiwit isolatie, peptidoglycaan architectuuranalyses, tot taxonomie en antibiotica resistentiemechanismen. Ieder van deze onderzoeksrichtingen heeft vragen beantwoord, maar ook een aantal nieuwe vragen opgebracht. In het geval van de kranssporulerende *Streptomyces* hebben we een andere set SALPS geïdentificeerd dan we vinden bij *Streptomyces* met normale sporenketens,

echterweten we nog niet hoe sporulatie langs de wand gereguleerd is. Verder onderzoek zou ons kunnen vertellen hoe sporulatie langs de laterale wand georganiseerd is over ruimte en tijd. De celwandanalyse van *Streptomyces coelicolor* toonde welke muropeptiden aanwezig waren in een volledige cultuur op verschillende momenten over tijd, echter weten we nog niet welke muropeptiden aanwezig zijn op specifieke plekken in de celwand. Een analyse van *Kitasatospora* peptidoglycaan toonde dat vegetatief peptidoglycaan meso-DAP en sporen peptidoglycaan LL-DAP bevat. De functie van dit verschil in stereo isomerie is nog onduidelijk. Het werk aan vancomycine resistentie toonde aan dat een deletie van *vanX* de gevoeligheid voor vancomycine in duizendvoud verhoogt in vancomycine-resistente stammen. Dit toont veelpotentie als oplossing voor het groeiende probleem van vancomycine resistente infecties. Voor deze oplossing moet nog een chemische inhibitor van het VanX eiwit worden gevonden. Dit proefschrift beschrijft een assay waarmee de functie van VanX gevolgd kan worden met een fluorescent signaal, wat in de toekomst zou kunnen helpen om een inhibitor te vinden.

Wij bevinden ons in een tijd waar genomesequenties algemeen worden, waarbij scheikundige hulpmiddelen steeds uitgebreider worden en we meer methoden ontwikkelen om snelle celwandanalyses te doen. Microscopie ook wordt steeds informatiever en breder toepasbaar. Een voorbeeld hiervan is het gebruik van fluorescente kleurstoffen zoals het fluorescente D-amino zuur HADA, die aan het peptidoglycaan bindt op de positie van D-Ala, waarmee onderzoekers kunnen zien waar nieuw celwandmateriaal wordt ingebouwd (Kuru *et al.*, 2015). Deze combinatie van genetica, biochemie en biologisch inzicht geeft wetenschappers de perfecte gelegenheid om met onderbestudeerde organismen te werken en om te onderzoeken hoe verschillende manieren van groei worden uitgevoerd en gecontroleerd. Toekomstig werk zou kunnen laten zien waarom *Kitasatosporae* verschillende stereoisomeren van DAP hebben, hoe sporulatie gereguleerd is in kranssporulerende *Streptomyces* of hoe *Streptomyces* weten waar de tussenschotten tussen honderden sporen horen te komen in lange hyphen. Spannende tijden komen ons tegemoet!

References

- Ahmed, L., Jensen, P.R., Freel, K.C., Brown, R., Jones, A.L., Kim, B.Y., and Goodfellow, M. (2013) *Salinispora pacifica* sp. nov., an actinomycete from marine sediments. *Antonie Van Leeuwenhoek* **103**: 1069-1078.
- Ainsa, J.A., Bird, N., Ryding, N.J., Findlay, K.C., and Chater, K.F. (2010) The complex *whiJ* locus mediates environmentally sensitive repression of development of *Streptomyces coelicolor* A3(2). *Antonie Van Leeuwenhoek* **98**: 225-236.
- Ainsa, J.A., Parry, H.D., and Chater, K.F. (1999) A response regulator-like protein that functions at an intermediate stage of sporulation in *Streptomyces coelicolor* A3(2). *Mol Microbiol* **34**: 607-619.
- Ainsa, J.A., Ryding, N.J., Hartley, N., Findlay, K.C., Bruton, C.J., and Chater, K.F. (2000) WhiA, a protein of unknown function conserved among gram-positive bacteria, is essential for sporulation in *Streptomyces coelicolor* A3(2). *J Bacteriol* **182**: 5470-5478.
- Allen, H.K., Donato, J., Wang, H.H., Cloud-Hansen, K.A., Davies, J., and Handelsman, J. (2010) Call of the wild: antibiotic resistance genes in natural environments. *Nat Rev Microbiol* **8**: 251-259.
- Aráoz, R., Anhalt, E., René, L., Badet-Denisot, M.-A., Courvalin, P., and Badet, B. (2000) Mechanism-based inactivation of VanX, a D-alanyl-D-alanine dipeptidase necessary for vancomycin resistance. *Biochemistry* **39**: 15971-15979.
- Arbeloa, A., Hugonnet, J.E., Sentilhes, A.C., Josseaume, N., Dubost, L., Monsempes, C., Blanot, D., Brouard, J.P., and Arthur, M. (2004) Synthesis of mosaic peptidoglycan cross-bridges by hybrid peptidoglycan assembly pathways in Gram-positive bacteria. *J Biol Chem* **279**: 41546-41556.
- Arias, C.A., and Murray, B.E. (2009) Antibiotic-resistant bugs in the 21st century--a clinical super-challenge. *N Engl J Med* **360**: 439-443.
- Arthur, M., Depardieu, F., Cabanie, L., Reynolds, P., and Courvalin, P. (1998) Requirement of the VanY and VanX D,D-peptidases for glycopeptide resistance in Enterococci. *Mol Microbiol* **30**: 819-830.
- Arthur, M., Depardieu, F., Gerbaud, G., Galimand, M., Leclercq, R., and Courvalin, P. (1997) The VanS sensor negatively controls VanR-mediated transcriptional activation of glycopeptide resistance genes of Tn1546 and related elements in the absence of induction. *J Bacteriol* **179**: 97-106.
- Arthur, M., Depardieu, F., Snaith, H.A., Reynolds, P.E., and Courvalin, P. (1994) Contribution of VanY D,D-carboxypeptidase to glycopeptide resistance in *Enterococcus faecalis* by hydrolysis of peptidoglycan precursors. *Antimicrob Agents Chemother* **38**: 1899-1903.
- Aslangul, E., Baptista, M., Fantin, B., Depardieu, F., Arthur, M., Courvalin, P., and Carbon, C. (1997) Selection of glycopeptide-resistant mutants of VanB-type *Enterococcus faecalis* BM4281 in vitro and in experimental endocarditis. *J Infect Dis* **175**: 598-605.
- Asojo, O.A., Nelson, S.K., Mootien, S., Lee, Y., Rezende, W.C., Hyman, D.A., Matsumoto, M.M., Reiling, S., Kelleher, A., Ledizet, M., Koski, R.A., and Anthony, K.G. (2014) Structural and biochemical analyses of alanine racemase from the multidrug-resistant *Clostridium difficile* strain 630. *Acta Crystallographica Section D: Biological Crystallography* **70**: 1922-1933.
- Aziz, R.K., Bartels, D., Best, A.A., DeJongh, M., Disz, T., Edwards, R.A., Formsma, K., Gerdes, S., Glass, E.M., Kubal, M., Meyer, F., Olsen, G.J., Olson, R., Osterman, A.L., Overbeek, R.A., McNeil, L.K., Paarmann, D., Paczian, T., Parrello, B., Pusch, G.D., Reich, C., Stevens, R., Vassieva, O., Vonstein, V., Wilke, A., and Zagnitko, O. (2008) The RAST Server: rapid annotations using subsystems technology. *BMC genomics* **9**: 75.

- Baldacci, E., Farina, G., and Locci, R. (1966) Emendation of Genus *Streptovorticillium* Baldacci (1958) and Revision of Some Species. *Giorn Microbiol* **14**: 153.
- Baldacci, E., and Locci, R., (1974) Genus II. *Streptovorticillium* Baldacci 1958, 15, emed. mur. char. Baldacci, Farina and Locci 1966, 168. In: *Bergey's Manual of Determinative Bacteriology*. 8th Ed. R.E. Buchanan & N.E. Gibbons (eds). Baltimore: Williams & Wilkins, pp. 829-842.
- Baranowski, C., Sham, L.-T., Eskandarian, H.A., Welsh, M.A., Lim, H.C., Kieser, K.J., Wagner, J.C., Walker, S., McKinney, J.D., Fantner, G.E., Joerger, T.R., Bernhardt, T.G., Rubin, E.J., and Rego, E.H. (2018) Maturing Mycobacterial Peptidoglycan Requires Non-canonical Crosslinks to Maintain Shape. *bioRxiv*.
- Barka, E.A., Vatsa, P., Sanchez, L., Gaveau-Vaillant, N., Jacquard, C., Klenk, H.-P., Clément, C., Ouhdouch, Y., and van Wezel, G.P. (2016) Taxonomy, Physiology, and Natural Products of Actinobacteria. *Microbiology and Molecular Biology Reviews* **80**: 1-43.
- Bell, J.M., Paton, J.C., and Turnidge, J. (1998) Emergence of vancomycin-resistant Enterococci in Australia: phenotypic and genotypic characteristics of isolates. *J Clin Microbiol* **36**: 2187-2190.
- Benedict, R.G., Dvonch, W., Shotwell, O.L., Pridham, T.G., and Lindenfelser, L.A. (1952) Cinnamycin, an antibiotic from *Streptomyces cinnamoneus* nov. sp. *Antibiot Chemother (Northfield)* **2**: 591-594.
- Bentley, S.D., Chater, K.F., Cerdeno-Tarraga, A.M., Challis, G.L., Thomson, N.R., James, K.D., Harris, D.E., Quail, M.A., Kieser, H., Harper, D., Bateman, A., Brown, S., Chandra, G., Chen, C.W., Collins, M., Cronin, A., Fraser, A., Goble, A., Hidalgo, J., Hornsby, T., Howarth, S., Huang, C.H., Kieser, T., Larke, L., Murphy, L., Oliver, K., O'Neil, S., Rabinowitsch, E., Rajandream, M.A., Rutherford, K., Rutter, S., Seeger, K., Saunders, D., Sharp, S., Squares, R., Squares, S., Taylor, K., Warren, T., Wietzorrek, A., Woodward, J., Barrell, B.G., Parkhill, J., and Hopwood, D.A. (2002) Complete genome sequence of the model actinomycete *Streptomyces coelicolor* A3(2). *Nature* **417**: 141-147.
- Berdy, J. (2012) Thoughts and facts about antibiotics: where we are now and where we are heading. *J Antibiot (Tokyo)* **65**: 385-395.
- Bérdy, J. (2005) Bioactive microbial metabolites. *J Antibiot (Tokyo)* **58**: 1-26.
- Bhullar, K., Waglechner, N., Pawlowski, A., Koteva, K., Banks, E.D., Johnston, M.D., Barton, H.A., and Wright, G.D. (2012) Antibiotic resistance is prevalent in an isolated cave microbiome. *PLoS One* **7**: e34953.
- Bisson-Filho, A.W., Hsu, Y.P., Squyres, G.R., Kuru, E., Wu, F., Jukes, C., Sun, Y., Dekker, C., Holden, S., VanNieuwenhze, M.S., Brun, Y.V., and Garner, E.C. (2017) Treadmilling by FtsZ filaments drives peptidoglycan synthesis and bacterial cell division. *Science* **355**: 739-743.
- Blin, K., Wolf, T., Chevrette, M.G., Lu, X., Schwalen, C.J., Kautsar, S.A., Suarez Duran, H.G., de Los Santos, E.L.C., Kim, H.U., Nave, M., Dickschat, J.S., Mitchell, D.A., Shelest, E., Breitling, R., Takano, E., Lee, S.Y., Weber, T., and Medema, M.H. (2017) antiSMASH 4.0-improvements in chemistry prediction and gene cluster boundary identification. *Nucleic Acids Res*.
- Bornikoel, J., Carrion, A., Fan, Q., Flores, E., Forchhammer, K., Mariscal, V., Mullineaux, C.W., Perez, R., Silber, N., Wolk, C.P., and Maldener, I. (2017) Role of Two Cell Wall Amidases in Septal Junction and Nanopore Formation in the Multicellular *Cyanobacterium Anabaena* sp. PCC 7120. *Front Cell Infect Microbiol* **7**: 386.
- Boucher, H.W., Talbot, G.H., Bradley, J.S., Edwards, J.E., Gilbert, D., Rice, L.B., Scheld, M., Spellberg, B., and Bartlett, J. (2009) Bad bugs, no drugs: no ESCAPE! An update from the Infectious Diseases Society of America. *Clin Infect Dis* **48**: 1-12.
- Braun, V., Gotz, F., Schultz, J.E., and Wohlleben, W. (2015) The bacterial cell envelope: struc-

- ture, function, and infection interface. *Int J Med Microbiol* **305**: 175-177.
- Breukink, E., and de Kruijff, B. (2006) Lipid II as a target for antibiotics. *Nat Rev Drug Disc* **5**: 321-323.
- Bugg, T.D., Braddick, D., Dowson, C.G., and Roper, D.I. (2011) Bacterial cell wall assembly: still an attractive antibacterial target. *Trends Biotechnol* **29**: 167-173.
- Bugg, T.D., Dutka-Malen, S., Arthur, M., Courvalin, P., and Walsh, C.T. (1991a) Identification of vancomycin resistance protein VanA as a D-alanine:D-alanine ligase of altered substrate specificity. *Biochemistry* **30**: 2017-2021.
- Bugg, T.D., Wright, G.D., Dutka-Malen, S., Arthur, M., Courvalin, P., and Walsh, C.T. (1991b) Molecular basis for vancomycin resistance in *Enterococcus faecium* BM4147: biosynthesis of a depsipeptide peptidoglycan precursor by vancomycin resistance proteins VanH and VanA. *Biochemistry* **30**: 10408-10415.
- Bui, N.K., Eberhardt, A., Vollmer, D., Kern, T., Bougault, C., Tomasz, A., Simorre, J.P., and Vollmer, W. (2012) Isolation and analysis of cell wall components from *Streptococcus pneumoniae*. *Anal Biochem* **421**: 657-666.
- Bui, N.K., Gray, J., Schwarz, H., Schumann, P., Blanot, D., and Vollmer, W. (2009) The peptidoglycan sacculus of *Myxococcus xanthus* has unusual structural features and is degraded during glycerol-induced myxospore development. *J Bacteriol* **191**: 494-505.
- Bull, A.T., Asenjo, J.A., Goodfellow, M., and Gomez-Silva, B. (2016) The Atacama Desert: Technical Resources and the Growing Importance of Novel Microbial Diversity. *Annu Rev Microbiol* **70**: 215-234.
- Caceres, N.E., Harris, N.B., Wellehan, J.F., Feng, Z., Kapur, V., and Barletta, R.G. (1997) Overexpression of the D-alanine racemase gene confers resistance to D-cycloserine in *Mycobacterium smegmatis*. *J Bacteriol* **179**: 5046-5055.
- Cameron, T.A., Anderson-Furgeson, J., Zupan, J.R., Zik, J.J., and Zambryski, P.C. (2014) Peptidoglycan synthesis machinery in *Agrobacterium tumefaciens* during unipolar growth and cell division. *MBio* **5**: e01219-01214.
- Cava, F., Lam, H., de Pedro, M.A., and Waldor, M.K. (2011) Emerging knowledge of regulatory roles of D-amino acids in bacteria. *Cell Mol Life Sci* **68**: 817-831.
- Celler, K., Koning, R.I., Koster, A.J., and van Wezel, G.P. (2013) Multidimensional view of the bacterial cytoskeleton. *J Bacteriol* **195**: 1627-1636.
- Celler, K., Koning, R.I., Willemsse, J., Koster, A.J., and van Wezel, G.P. (2016) Cross-membranes orchestrate compartmentalization and morphogenesis in *Streptomyces*. *Nat Commun* **7**: ncomms11836.
- Chang, Y.-P., Tseng, M.-J., and Chu, Y.-H. (2006) Using surface plasmon resonance to directly measure slow binding of low-molecular mass inhibitors to a VanX chip. *Anal Biochem* **359**: 63-71.
- Chater, K.F. (1972) A morphological and genetic mapping study of white colony mutants of *Streptomyces coelicolor*. *J Gen Microbiol* **72**: 9-28.
- Chater, K.F., Bruton, C.J., Plaskitt, K.A., Buttner, M.J., Mendez, C., and Helmann, J.D. (1989) The developmental fate of *S. coelicolor* hyphae depends upon a gene product homologous with the motility sigma factor of *B. subtilis*. *Cell* **59**: 133-143.
- Chen, J.M., Uplekar, S., Gordon, S.V., and Cole, S.T. (2012) A point mutation in *cycA* partially contributes to the D-cycloserine resistance trait of *Mycobacterium bovis* BCG vaccine strains. *PLoS One* **7**: e43467.
- Chun, J., and Rainey, F.A. (2014) Integrating genomics into the taxonomy and systematics of the Bacteria and Archaea. *Int J System Evol Microbiol* **64**: 316-324.
- Claessen, D., Rozen, D.E., Kuipers, O.P., Sogaard-Andersen, L., and van Wezel, G.P. (2014) Bacterial solutions to multicellularity: a tale of biofilms, filaments and fruiting bodies.

- Nat Rev Microbiol* **12**: 115-124.
- Collins, M.D., Goodfellow, M., Minnikin, D.E., and Alderson, G. (1985) Menaquinone Composition of Mycolic Acid-Containing Actinomycetes and Some Sporoactinomycetes. *J Appl Bacteriol* **58**: 77-86.
- Colson, S., Stephan, J., Hertrich, T., Saito, A., van Wezel, G.P., Titgemeyer, F., and Rigali, S. (2007) Conserved cis-acting elements upstream of genes composing the chitinolytic system of streptomycetes are DasR-responsive elements. *J Mol Microbiol Biotechnol* **12**: 60-66.
- Courvalin, P. (2006) Vancomycin resistance in Gram-positive cocci. *Clin Infect Dis* **42 Suppl 1**: S25-34.
- Cummins, C.S. (1962) Chemical composition and antigenic structure of cell walls of *Corynebacterium*, *Mycobacterium*, *Nocardia*, *Actinomyces* and *Arthrobacter*. *J Gen Microbiol* **28**: 35-50.
- Daniel, R.A., and Errington, J. (2003) Control of cell morphogenesis in bacteria: two distinct ways to make a rod-shaped cell. *Cell* **113**: 767-776.
- Daniel, R.A., Harry, E.J., and Errington, J. (2000) Role of penicillin-binding protein PBP 2B in assembly and functioning of the division machinery of *Bacillus subtilis*. *Mol Microbiol* **35**: 299-311.
- Decousser, J.W., Pina, P., Picot, F., Delalande, C., Pangon, B., Courvalin, P., Allouch, P., and Col, B.V.H.S.G. (2003) Frequency of isolation and antimicrobial susceptibility of bacterial pathogens isolated from patients with bloodstream infections: a French prospective national survey. *J Antimicrob Chemother* **51**: 1213-1222.
- den Hengst, C.D., Tran, N.T., Bibb, M.J., Chandra, G., Leskiw, B.K., and Buttner, M.J. (2010) Genes essential for morphological development and antibiotic production in *Streptomyces coelicolor* are targets of BldD during vegetative growth. *Mol Microbiol* **78**: 361-379.
- Desjardins, C.A., Cohen, K.A., Munsamy, V., Abeel, T., Maharaj, K., Walker, B.J., Shea, T.P., Almeida, D.V., Manson, A.L., Salazar, A., Padayatchi, N., O'Donnell, M.R., Mlisana, K.P., Wortman, J., Birren, B.W., Grosset, J., Earl, A.M., and Pym, A.S. (2016) Genomic and functional analyses of *Mycobacterium tuberculosis* strains implicate ald in D-cycloserine resistance. *Nat Genet* **48**: 544-551.
- Edgar, R.C. (2004) MUSCLE: multiple sequence alignment with high accuracy and high throughput. *Nucleic Acids Res* **32**: 1792-1797.
- Egan, A.J., Biboy, J., van't Veer, I., Breukink, E., and Vollmer, W. (2015) Activities and regulation of peptidoglycan synthases. *Philos Trans R Soc Lond B Biol Sci* **370**.
- Egan, A.J., Cleverley, R.M., Peters, K., Lewis, R.J., and Vollmer, W. (2017) Regulation of bacterial cell wall growth. *FEBS J* **284**: 851-867.
- Elliot, M.A., Bibb, M.J., Buttner, M.J., and Leskiw, B.K. (2001) BldD is a direct regulator of key developmental genes in *Streptomyces coelicolor* A3(2). *Mol Microbiol* **40**: 257-269.
- Emami, K., Guyet, A., Kawai, Y., Devi, J., Wu, L.J., Allenby, N., Daniel, R.A., and Errington, J. (2017) RodA as the missing glycosyltransferase in *Bacillus subtilis* and antibiotic discovery for the peptidoglycan polymerase pathway. *Nat Microbiol* **2**: 16253.
- Emsley, P., and Cowtan, K. (2004) Coot: model-building tools for molecular graphics. *Acta Crystallographica Section D* **60**: 2126-2132.
- Engelberg-Kulka, H., Amitai, S., Kolodkin-Gal, I., and Hazan, R. (2006) Bacterial programmed cell death and multicellular behavior in bacteria. *PLoS Genet* **2**: e135.
- Errington, J., Daniel, R.A., and Scheffers, D.J. (2003) Cytokinesis in bacteria. *Microbiol Mol Biol Rev* **67**: 52-65.
- Evans, P.R., and Murshudov, G.N. (2013) How good are my data and what is the resolution?

- Fedorushyn, M., Welle, E., Bechthold, A., and Luzhetskyy, A. (2008) Functional expression of the Cre recombinase in actinomycetes. *Appl Microbiol Biotechnol* **78**: 1065-1070.
- Felsenstein, J. (1981) Evolutionary trees from DNA sequences: a maximum likelihood approach. *J Mol Evol* **17**: 368-376.
- Felsenstein, J. (1985) Confidence Limits on Phylogenies: An Approach Using the Bootstrap. *Evolution* **39**: 783-791.
- Feng, Z., and Barletta, R.G. (2003) Roles of *Mycobacterium smegmatis* D-alanine:D-alanine ligase and D-alanine racemase in the mechanisms of action of and resistance to the peptidoglycan inhibitor D-cycloserine. *Antimicrob Agents Chemother* **47**: 283-291.
- Fenn, T.D., Stamper, G.F., Morollo, A.A., and Ringe, D. (2003) A Side Reaction of Alanine Racemase: Transamination of Cycloserine. *Biochemistry* **42**: 5775-5783.
- Figueiredo, T.A., Sobral, R.G., Ludovice, A.M., Almeida, J.M., Bui, N.K., Vollmer, W., de Lencastre, H., and Tomasz, A. (2012) Identification of genetic determinants and enzymes involved with the amidation of glutamic acid residues in the peptidoglycan of *Staphylococcus aureus*. *PLoS Pathog* **8**: e1002508.
- Fischer, M., Falke, D., and Sawers, R.G. (2013) A respiratory nitrate reductase active exclusively in resting spores of the obligate aerobe *Streptomyces coelicolor* A3(2). *Mol Microbiol* **89**: 1259-1273.
- Fitch, W.M. (1971) Toward Defining Course of Evolution - Minimum Change for a Specific Tree Topology. *Syst Zool* **20**: 406-&.
- Flårdh, K. (2010) Cell polarity and the control of apical growth in *Streptomyces*. *Curr Opin Microbiol* **13**: 758-765.
- Flårdh, K., and Buttner, M.J. (2009) *Streptomyces* morphogenetics: dissecting differentiation in a filamentous bacterium. *Nat Rev Microbiol* **7**: 36-49.
- Flårdh, K., Findlay, K.C., and Chater, K.F. (1999) Association of early sporulation genes with suggested developmental decision points in *Streptomyces coelicolor* A3(2). *Microbiology* **145**: 2229-2243.
- Flårdh, K., Richards, D.M., Hempel, A.M., Howard, M., and Buttner, M.J. (2012) Regulation of apical growth and hyphal branching in *Streptomyces*. *Curr Opin Microbiol*.
- Frieden, T.R., Sterling, T., Pablos-Mendez, A., Kilburn, J.O., Cauthen, G.M., and Dooley, S.W. (1993) The emergence of drug-resistant tuberculosis in New York City. *N Engl J Med* **328**: 521-526.
- Gabardinho, J., Beteva, A., Guijarro, M., Rey-Bakaikoa, V., Spruce, D., Bowler, M.W., Brockhauser, S., Flot, D., Gordon, E.J., Hall, D.R., Lavault, B., McCarthy, A.A., McCarthy, J., Mitchell, E., Monaco, S., Mueller-Dieckmann, C., Nurizzo, D., Ravelli, R.B., Thibault, X., Walsh, M.A., Leonard, G.A., and McSweeney, S.M. (2010) MxCuBE: a synchrotron beamline control environment customized for macromolecular crystallography experiments. *J Synchrotron Radiat* **17**: 700-707.
- Gao, C., Hindra, Mulder, D., Yin, C., and Elliot, M.A. (2012) Crp is a global regulator of antibiotic production in *Streptomyces*. *MBio* **3**: 00407-00412.
- Girard, G., Traag, B.A., Sangal, V., Mascini, N., Hoskisson, P.A., Goodfellow, M., and van Wezel, G.P. (2013) A novel taxonomic marker that discriminates between morphologically complex actinomycetes. *Open Biol* **3**: 130073.
- Girard, G., Willemsse, J., Zhu, H., Claessen, D., Bukarasam, K., Goodfellow, M., and van Wezel, G.P. (2014) Analysis of novel kitasatosporae reveals significant evolutionary changes in conserved developmental genes between *Kitasatospora* and *Streptomyces*. *Antonie Van Leeuwenhoek* **106**: 365-380.
- Glauner, B. (1988) Separation and quantification of mucopeptides with high-performance liq

- uid chromatography. *Anal Biochem* **172**: 451-464.
- Gomez Casanova, N., Siller Ruiz, M., and Munoz Bellido, J.L. (2017) Mechanisms of resistance to daptomycin in *Staphylococcus aureus*. *Rev Esp Quimioter* **30**: 391-396.
- Goodfellow, M., (2012) Phylum XXVI. Actinobacteria phyl. nov. In: Bergey's Manual of Systematic Bacteriology. M. Goodfellow, P. Kämpfer, H.-J. Busse, M.E. Trujillo, K.-I. Suzuki, W. Ludwig & W.B. Whitman (eds). New York: Springer, pp. 1-2083.
- Goodfellow, M., Busarakam, K., Idris, H., Labeda, D.P., Nouioui, I., Brown, R., Kim, B.Y., Del Carmen Montero-Calasanz, M., Andrews, B.A., and Bull, A.T. (2017) *Streptomyces asenjonii* sp. nov., isolated from hyper-arid Atacama Desert soils and emended description of *Streptomyces viridosporus* Pridham et al. 1958. *Antonie Van Leeuwenhoek* **110**: 1133-1148.
- Gray, D.I., Gooday, G.W., and Prosser, J.I. (1990) Apical hyphal extension in *Streptomyces coelicolor* A3(2). *J Gen Microbiol* **136**: 1077-1084.
- Griffith, R.S. (1981) Introduction to vancomycin. *Rev Infect Dis* **3 suppl**: S200-204.
- Gubbens, J., Wu, C., Zhu, H., Filippov, D.V., Florea, B.I., Rigali, S., Overkleef, H.S., and van Wezel, G.P. (2017) Intertwined Precursor Supply during Biosynthesis of the Catecholate-Hydroxamate Siderophores Qinichelins in *Streptomyces* sp. MBT76. *ACS Chem Biol* **12**: 2756-2766.
- Guindon, S., and Gascuel, O. (2003) A simple, fast, and accurate algorithm to estimate large phylogenies by maximum likelihood. *System Biol* **52**: 696-704.
- Guiral, S., Mitchell, T.J., Martin, B., and Claverys, J.P. (2005) Competence-programmed predation of noncompetent cells in the human pathogen *Streptococcus pneumoniae*: genetic requirements. *Proc Natl Acad Sci U S A* **102**: 8710-8715.
- Haiser, H.J., Yousef, M.R., and Elliot, M.A. (2009) Cell wall hydrolases affect germination, vegetative growth, and sporulation in *Streptomyces coelicolor*. *J Bacteriol* **191**: 6501-6512.
- Hammes, W., Schleifer, K.H., and Kandler, O. (1973) Mode of action of glycine on the biosynthesis of peptidoglycan. *J Bacteriol* **116**: 1029-1053.
- Hamoen, L.W., and Errington, J. (2003) Polar targeting of DivIVA in *Bacillus subtilis* is not directly dependent on FtsZ or PBP 2B. *J Bacteriol* **185**: 693-697.
- Hasegawa, T., Takizawa, M., and Tanida, S. (1983) A Rapid Analysis for Chemical Grouping of Aerobic Actinomycetes. *J Gen Appl Microbiol* **29**: 319-322.
- Hashimoto, A., Nishikawa, T., Oka, T., Takahashi, K., and Hayashi, T. (1992) Determination of free amino acid enantiomers in rat brain and serum by high-performance liquid chromatography after derivatization with N-tert.-butyloxycarbonyl-L-cysteine and o-phthalaldehyde. *Journal of Chromatography B: Biomedical Sciences and Applications* **582**: 41-48.
- Hatano, K., Nishii, T., and Kasai, H. (2003) Taxonomic re-evaluation of whorl-forming *Streptomyces* (formerly *Streptoverticillium*) species by using phenotypes, DNA-DNA hybridization and sequences of *gyrB*, and proposal of *Streptomyces luteireticuli* (ex Katoh and Arai 1957) corrig., sp. nov., nom. rev. *Int J Syst Evol Microbiol* **53**: 1519-1529.
- Hayakawa, M., and Nomomura, H. (1989) A new method for the intensive isolation of actinomycetes from soil. *Actinomycetologica* **3**: 95-104.
- Healy, V.L., Mullins, L.S., Li, X., Hall, S.E., Raushel, F.M., and Walsh, C.T. (2000) D-Ala-D-X ligases: evaluation of D-alanyl phosphate intermediate by MIX, PIX and rapid quench studies. *Chem Biol* **7**: 505-514.
- Heidrich, C., Templin, M.F., Ursinus, A., Merdanovic, M., Berger, J., Schwarz, H., de Pedro, M.A., and Holtje, J.V. (2001) Involvement of N-acetylmuramyl-L-alanine amidases in cell separation and antibiotic-induced autolysis of *Escherichia coli*. *Mol Microbiol* **41**: 167-178.

- Heidrich, C., Ursinus, A., Berger, J., Schwarz, H., and Holtje, J.V. (2002) Effects of multiple deletions of murein hydrolases on viability, septum cleavage, and sensitivity to large toxic molecules in *Escherichia coli*. *J Bacteriol* **184**: 6093-6099.
- Hochman, A. (1997) Programmed cell death in prokaryotes. *Crit Rev Microbiol* **23**: 207-214.
- Holmes, N.A., Walshaw, J., Leggett, R.M., Thibessard, A., Dalton, K.A., Gillespie, M.D., Hemmings, A.M., Gust, B., and Kelemen, G.H. (2013) Coiled-coil protein Scy is a key component of a multiprotein assembly controlling polarized growth in *Streptomyces*. *Proc Natl Acad Sci U S A* **110**: E397-406.
- Höltje, J.-V., (1993) "Three for one" — a Simple Growth Mechanism that Guarantees a Precise Copy of the Thin, Rod-Shaped Murein Sacculus of *Escherichia coli*. In: Bacterial Growth and Lysis: Metabolism and Structure of the Bacterial Sacculus. M.A. de Pedro, J.V. Höltje & W. Löffelhardt (eds). Boston, MA: Springer US, pp. 419-426.
- Homma, T., Nuxoll, A., Gandt, A.B., Ebner, P., Engels, I., Schneider, T., Gotz, F., Lewis, K., and Conlon, B.P. (2016) Dual Targeting of Cell Wall Precursors by Teixobactin Leads to Cell Lysis. *Antimicrob Agents Chemother* **60**: 6510-6517.
- Hong, H.J., Hutchings, M.I., and Buttner, M.J. (2008) Vancomycin resistance VanS/VanR two-component systems. *Adv Exp Med Biol* **631**: 200-213.
- Hong, H.J., Hutchings, M.I., Hill, L.M., and Buttner, M.J. (2005) The role of the novel Fem protein VanK in vancomycin resistance in *Streptomyces coelicolor*. *J Biol Chem* **280**: 13055-13061.
- Hong, H.J., Hutchings, M.I., Neu, J.M., Wright, G.D., Paget, M.S., and Buttner, M.J. (2004) Characterization of an inducible vancomycin resistance system in *Streptomyces coelicolor* reveals a novel gene (vanK) required for drug resistance. *Mol Microbiol* **52**: 1107-1121.
- Hong, W., Chen, L., and Xie, J. (2014) Molecular basis underlying *Mycobacterium tuberculosis* D-cycloserine resistance. Is there a role for ubiquinone and menaquinone metabolic pathways? *Expert Opin Ther Targets* **18**: 691-701.
- Hopwood, D.A., (2007) *Streptomyces in nature and medicine: the antibiotic makers*. Oxford University Press, New York.
- Hopwood, D.A., Wright, H.M., Bibb, M.J., and Cohen, S.N. (1977) Genetic recombination through protoplast fusion in *Streptomyces*. *Nature* **268**: 171-174.
- Howden, B.P., Davies, J.K., Johnson, P.D., Stinear, T.P., and Grayson, M.L. (2010) Reduced vancomycin susceptibility in *Staphylococcus aureus*, including vancomycin-intermediate and heterogeneous vancomycin-intermediate strains: resistance mechanisms, laboratory detection, and clinical implications. *Clin Microbiol Rev* **23**: 99-139.
- Hugonnet, J.E., Haddache, N., Veckerle, C., Dubost, L., Marie, A., Shikura, N., Mainardi, J.L., Rice, L.B., and Arthur, M. (2014) Peptidoglycan cross-linking in glycopeptide-resistant *Actinomycetales*. *Antimicrob Agents Chemother* **58**: 1749-1756.
- Hussain, S., Wivagg, C.N., Szwedziak, P., Wong, F., Schaefer, K., Izore, T., Renner, L.D., Holmes, M.J., Sun, Y., Bisson-Filho, A.W., Walker, S., Amir, A., Lowe, J., and Garner, E.C. (2018) MreB filaments align along greatest principal membrane curvature to orient cell wall synthesis. *Elife* **7**.
- Hutchings, M.I., Hong, H.J., and Buttner, M.J. (2006) The vancomycin resistance VanRS two-component signal transduction system of *Streptomyces coelicolor*. *Mol Microbiol* **59**: 923-935.
- Hwang, J.Y., Kim, S.H., Oh, H.R., Kwon, E., and Nam, D.H. (2015) Analysis of a draft genome sequence of *Kitasatospora cheerisanensis* KCTC 2395 producing bafilomycin antibiotics. *J Microbiol* **53**: 84-89.
- Iannazzo, L., Soroka, D., Triboulet, S., Fonvielle, M., Compain, F., Dubée, V., Mainardi, J.L., Hugonnet, J.E., Braud, E., Arthur, M., and Etheve-Quellejeu, M. (2016) Routes of

- Synthesis of Carbapenems for Optimizing Both the Inactivation of L,D-Transpeptidase LdtMt1 of *Mycobacterium tuberculosis* and the Stability toward Hydrolysis by β -Lactamase BlaC. *J Med Chem* **59**: 3427-3438.
- Ikeda, H., Ishikawa, J., Hanamoto, A., Shinose, M., Kikuchi, H., Shiba, T., Sakaki, Y., Hattori, M., and Omura, S. (2003) Complete genome sequence and comparative analysis of the industrial microorganism *Streptomyces avermitilis*. *Nat Biotechnol* **21**: 526-531.
- Inagaki, K., Tanizawa, K., Badet, B., Walsh, C., Tanaka, H., and Soda, K. (1986) Thermostable alanine racemase from *Bacillus stearothermophilus*: molecular cloning of the gene, enzyme purification, and characterization. *Biochemistry* **25**: 3268 - 3274.
- Jakimowicz, D., and van Wezel, G.P. (2012) Cell division and DNA segregation in *Streptomyces*: how to build a septum in the middle of nowhere? *Mol Microbiol* **85**: 393-404.
- Ju, J., Xu, S., Furukawa, Y., Zhang, Y., Misono, H., Minamino, T., Namba, K., Zhao, B., and Ohnishi, K. (2011) Correlation between catalytic activity and monomer-dimer equilibrium of bacterial alanine racemases. *J Biochem* **149**: 83 - 89.
- Ju, J., Yokoigawa, K., Misono, H., and Ohnishi, K. (2005) Cloning of alanine racemase genes from *Pseudomonas fluorescens* strains and oligomerization states of gene products expressed in *Escherichia coli*. *Journal of Bioscience and Bioengineering* **100**: 409-417.
- Jukes, T.H., and Cantor, C.R. (1969) Evolution of protein molecules. *Academic Press, London* **3**: 21-132.
- Kabsch, W. (2010) Integration, scaling, space-group assignment and post-refinement. *Acta Crystallogr D Biol Crystallogr* **66**: 125-132.
- Kämpfer, P., (2012) Family 1. *Streptomycetaceae* Waksman and Henrici 1943, 339AL emend. Rainey, Ward-Rainey and Stackebrandt, 1997, 486 emend. Kim, Lonsdale, Seong and Goodfellow 2003b, 113 emend. Zhi, Li and Stackebrandt 2009, 600. In: Bergey's Manual of Systematic Bacteriology. M. Goodfellow, P. Kämpfer, H.-J. Busse, M.E. Trujillo, K.-I. Suzuki, W. Ludwig & W.B. Whitman (eds). New York: Springer, pp.
- Karoui, M.E., and Errington, J. (2001) Isolation and characterization of topological specificity mutants of *minD* in *Bacillus subtilis*. *Mol Microbiol* **42**: 1211-1221.
- Kato, S., Hemmi, H., and Yoshimura, T. (2012) Lysine racemase from a lactic acid bacterium, *Oenococcus oeni*: structural basis of substrate specificity. *J Biochem* **152**: 505-508.
- Keep, N.H., Ward, J.M., Cohen-Gonsaud, M., and Henderson, B. (2006) Wake up! Peptidoglycan lysis and bacterial non-growth states. *Trends Microbiol* **14**: 271-276.
- Keijser, B.J., Noens, E.E., Kraal, B., Koerten, H.K., and van Wezel, G.P. (2003) The *Streptomyces coelicolor* *ssgB* gene is required for early stages of sporulation. *FEMS Microbiol Lett* **225**: 59-67.
- Kelley, L.A., Mezulis, S., Yates, C.M., Wass, M.N., and Sternberg, M.J. (2015) The Phyre2 web portal for protein modeling, prediction and analysis. *Nat Protoc* **10**: 845-858.
- Kelly, K. (1964) Centroid notations for revised ISCC-NBS colour name blocks *J Res Nat Bur Stand USA*: 472.
- Kieser, T., Bibb, M.J., Buttner, M.J., Chater, K.F., and Hopwood, D.A., (2000) *Practical Streptomyces genetics*. John Innes Foundation, Norwich, U.K.
- Kim, B.J., Kim, C.J., Chun, J., Koh, Y.H., Lee, S.H., Hyun, J.W., Cha, C.Y., and Kook, Y.H. (2004) Phylogenetic analysis of the genera *Streptomyces* and *Kitasatospora* based on partial RNA polymerase beta-subunit gene (*rpoB*) sequences. *Int J Syst Evol Microbiol* **54**: 593-598.
- Kimura, M. (1980) A simple method for estimating evolutionary rates of base substitutions through comparative studies of nucleotide sequences. *J Mol Evol* **16**: 111-120.
- Knerr, P.J., and van der Donk, W.A. (2013) Chemical Synthesis of the lantibiotic lacticin 481

- reveals the importance of lanthionine stereochemistry. *J Am Chem Soc* **135**: 7094-7097.
- Koch, A.L. (1990) Additional Arguments for the Key Role of Smart Autolysins in the Enlargement of the Wall of Gram-Negative Bacteria. *Res Microbiol* **141**: 529-541.
- Kolter, R., and van Wezel, G.P. (2016) Goodbye to brute force in antibiotic discovery? *Nat Microbiol* **1**: 15020.
- Kühner, D., Stahl, M., Demircioglu, D.D., and Bertsche, U. (2014) From cells to muropeptide structures in 24 h: peptidoglycan mapping by UPLC-MS. *Sci Rep* **4**: 7494.
- Kumar, S., Stecher, G., and Tamura, K. (2016) MEGA7: Molecular Evolutionary Genetics Analysis Version 7.0 for Bigger Datasets. *Mol Biol Evol* **33**: 1870-1874.
- Kumar, Y., and Goodfellow, M. (2010) Reclassification of *Streptomyces hygrosopicus* strains as *Streptomyces aldersoniae* sp. nov., *Streptomyces angustmyceticus* sp. nov., comb. nov., *Streptomyces ascomycinicus* sp. nov., *Streptomyces decoyicus* sp. nov., comb. nov., *Streptomyces milbemycinicus* sp. nov. and *Streptomyces wellingtoniae* sp. nov. *Int J System Evol Microbiol* **60**: 769-775.
- Kuru, E., Tekkam, S., Hall, E., Brun, Y.V., and Van Nieuwenhze, M.S. (2015) Synthesis of fluorescent D-amino acids and their use for probing peptidoglycan synthesis and bacterial growth in situ. *Nat Protoc* **10**: 33-52.
- Kwun, M.J., Novotna, G., Hesketh, A.R., Hill, L., and Hong, H.J. (2013) *In vivo* studies suggest that induction of VanS-dependent vancomycin resistance requires binding of the drug to D-Ala-D-Ala termini in the peptidoglycan cell wall. *Antimicrob Agents Chemother* **57**: 4470-4480.
- Kysela, D.T., Randich, A.M., Caccamo, P.D., and Brun, Y.V. (2016) Diversity Takes Shape: Understanding the Mechanistic and Adaptive Basis of Bacterial Morphology. *PLoS Biol* **14**: e1002565.
- Labeda, D.P. (2011) Multilocus sequence analysis of phytopathogenic species of the genus *Streptomyces*. *Int J System Evol Microbiol* **61**: 2525-2531.
- Labeda, D.P., Dunlap, C.A., Rong, X., Huang, Y., Doroghazi, J.R., Ju, K.S., and Metcalf, W.W. (2017) Phylogenetic relationships in the family *Streptomycetaceae* using multi-locus sequence analysis. *Antonie Van Leeuwenhoek* **110**: 563-583.
- Labeda, D.P., Goodfellow, M., Brown, R., Ward, A.C., Lanoot, B., Vanncanneyt, M., Swings, J., Kim, S.B., Liu, Z., Chun, J., Tamura, T., Oguchi, A., Kikuchi, T., Kikuchi, H., Nishii, T., Tsuji, K., Yamaguchi, Y., Tase, A., Takahashi, M., Sakane, T., Suzuki, K.I., and Hatano, K. (2012) Phylogenetic study of the species within the family *Streptomycetaceae*. *Antonie Van Leeuwenhoek* **101**: 73-104.
- Lam, H., Oh, D.C., Cava, F., Takacs, C.N., Clardy, J., de Pedro, M.A., and Waldor, M.K. (2009) D-amino acids govern stationary phase cell wall remodeling in bacteria. *Science* **325**: 1552-1555.
- Lambert, M.P., and Neuhaus, F.C. (1972) Mechanism of D-cycloserine Action: Alanine Race-mase from *Escherichia coli* W. *J Bacteriol* **110**: 978-987.
- Larson, J.L., and Hershberger, C.L. (1986) The minimal replicon of a streptomycete plasmid produces an ultrahigh level of plasmid DNA. *Plasmid* **15**: 199-209.
- Lavollay, M., Arthur, M., Fourgeaud, M., Dubost, L., Marie, A., Riegel, P., Gutmann, L., and Mainardi, J.L. (2009) The beta-lactam-sensitive D,D-carboxypeptidase activity of Pbp4 controls the L,D and D,D transpeptidation pathways in *Corynebacterium jeikeium*. *Mol Microbiol* **74**: 650-661.
- Lavollay, M., Arthur, M., Fourgeaud, M., Dubost, L., Marie, A., Veziris, N., Blanot, D., Gutmann, L., and Mainardi, J.L. (2008) The peptidoglycan of stationary-phase *Mycobacterium tuberculosis* predominantly contains cross-links generated by L,D-transpeptidation. *J Bacteriol* **190**: 4360-4366.

- Lavollay, M., Fourgeaud, M., Herrmann, J.L., Dubost, L., Marie, A., Gutmann, L., Arthur, M., and Mainardi, J.L. (2011) The peptidoglycan of *Mycobacterium abscessus* is predominantly cross-linked by L,D-transpeptidases. *J Bacteriol* **193**: 778-782.
- Lawlor, E.J., Baylis, H.A., and Chater, K.F. (1987) Pleiotropic morphological and antibiotic deficiencies result from mutations in a gene encoding a tRNA-like product in *Streptomyces coelicolor* A3(2). *Genes Dev* **1**: 1305-1310.
- Laxminarayan, R., Duse, A., Wattal, C., Zaidi, A.K., Wertheim, H.F., Sumpradit, N., Vlieghe, E., Hara, G.L., Gould, I.M., Goossens, H., Greko, C., So, A.D., Bigdeli, M., Tomson, G., Woodhouse, W., Ombaka, E., Peralta, A.Q., Qamar, F.N., Mir, F., Kariuki, S., Bhutta, Z.A., Coates, A., Bergstrom, R., Wright, G.D., Brown, E.D., and Cars, O. (2013) Antibiotic resistance-the need for global solutions. *Lancet Infect Dis* **13**: 1057-1098.
- Lechevalier, H., and Lechevalier, M.P. (1965) Classification of aerobic actinomycetes based on their morphology and their chemical composition. *Ann Inst Pasteur (Paris)* **108**: 662-673.
- Lechevalier, H.A., Lechevalier, M.P., and Gerber, N.N. (1971) Chemical composition as a criterion in the classification of actinomycetes. *Adv Appl Microbiol* **14**: 47-72.
- Leclercq, R., Derlot, E., Duval, J., and Courvalin, P. (1988) Plasmid-mediated resistance to vancomycin and teicoplanin in *Enterococcus faecium*. *N Engl J Med* **319**: 157-161.
- Leclercq, S., Derouaux, A., Olatunji, S., Fraipont, C., Egan, A.J., Vollmer, W., Breukink, E., and Terrak, M. (2017) Interplay between Penicillin-binding proteins and SEDS proteins promotes bacterial cell wall synthesis. *Sci Rep* **7**: 43306.
- Leskiw, B.K., Bibb, M.J., and Chater, K.F. (1991) The use of a rare codon specifically during development? *Mol Microbiol* **5**: 2861-2867.
- Lessard, I.A., Healy, V.L., Park, I.S., and Walsh, C.T. (1999) Determinants for differential effects on D-Ala-D-lactate vs D-Ala-D-Ala formation by the VanA ligase from vancomycin-resistant Enterococci. *Biochemistry* **38**: 14006-14022.
- Lessard, I.A., and Walsh, C.T. (1999) VanX, a bacterial D-alanyl-D-alanine dipeptidase: resistance, immunity, or survival function? *Proc Natl Acad Sci U S A* **96**: 11028-11032.
- Levefaudes, M., Patin, D., de Sousa-d'Auria, C., Chami, M., Blanot, D., Hervé, M., Arthur, M., Houssin, C., and Mengin-Lecreulx, D. (2015) Diaminopimelic Acid Amidation in *Corynebacteriales*: New insights into the role of LtsA in peptidoglycan modification. *J Biol Chem* **290**: 13079-13094.
- Ling, L.L., Schneider, T., Peoples, A.J., Spoering, A.L., Engels, I., Conlon, B.P., Mueller, A., Schaberle, T.F., Hughes, D.E., Epstein, S., Jones, M., Lazarides, L., Steadman, V.A., Cohen, D.R., Felix, C.R., Fetterman, K.A., Millett, W.P., Nitti, A.G., Zullo, A.M., Chen, C., and Lewis, K. (2015) A new antibiotic kills pathogens without detectable resistance. *Nature* **517**: 455-459.
- Lutkenhaus, J. (2007) Assembly dynamics of the bacterial MinCDE system and spatial regulation of the Z ring. *Annu Rev Biochem* **76**: 539-562.
- Lyons, N.A., and Kolter, R. (2015) On the evolution of bacterial multicellularity. *Curr Opin Microbiol* **24**: 21-28.
- MacNeil, D.J., Gewain, K.M., Ruby, C.L., Dezeny, G., Gibbons, P.H., and MacNeil, T. (1992) Analysis of *Streptomyces avermitilis* genes required for avermectin biosynthesis utilizing a novel integration vector. *Gene* **111**: 61-68.
- Mahr, K., van Wezel, G.P., Svensson, C., Krengel, U., Bibb, M.J., and Titgemeyer, F. (2000) Glucose kinase of *Streptomyces coelicolor* A3(2): large-scale purification and biochemical analysis. *Antonie Van Leeuwenhoek* **78**: 253-261.
- Mainardi, J.L., Fourgeaud, M., Hugonnet, J.E., Dubost, L., Brouard, J.P., Ouazzani, J., Rice, L.B., Gutmann, L., and Arthur, M. (2005) A novel peptidoglycan cross-linking enzyme for a beta-lactam-resistant transpeptidation pathway. *J Biol Chem* **280**: 38146-38152.

- Mainardi, J.L., Morel, V., Fourgeaud, M., Cremniter, J., Blanot, D., Legrand, R., Frehel, C., Arthur, M., Van Heijenoort, J., and Gutmann, L. (2002) Balance between two transpeptidation mechanisms determines the expression of beta-lactam resistance in *Enterococcus faecium*. *J Biol Chem* **277**: 35801-35807.
- Mainardi, J.L., Villet, R., Bugg, T.D., Mayer, C., and Arthur, M. (2008) Evolution of peptidoglycan biosynthesis under the selective pressure of antibiotics in Gram-positive bacteria. *FEMS Microbiol Rev* **32**: 386-408.
- Maldonado, L.A., Fenical, W., Jensen, P.R., Kauffman, C.A., Mincer, T.J., Ward, A.C., Bull, A.T., and Goodfellow, M. (2005) *Salinispora arenicola* gen. nov., sp. nov. and *Salinispora tropica* sp. nov., obligate marine actinomycetes belonging to the family *Micromonosporaceae*. *Int J Syst Evol Microbiol* **55**: 1759-1766.
- Manteca, A., Alvarez, R., Salazar, N., Yague, P., and Sanchez, J. (2008) Mycelium differentiation and antibiotic production in submerged cultures of *Streptomyces coelicolor*. *Appl Environ Microbiol* **74**: 3877-3886.
- Manteca, A., Fernandez, M., and Sanchez, J. (2005) Mycelium development in *Streptomyces antibioticus* ATCC11891 occurs in an orderly pattern which determines multiphase growth curves. *BMC Microbiol* **5**: 51.
- Manteca, A., Mader, U., Connolly, B.A., and Sanchez, J. (2006) A proteomic analysis of *Streptomyces coelicolor* programmed cell death. *Proteomics* **6**: 6008-6022.
- Margolin, W. (2005) FtsZ and the division of prokaryotic cells and organelles. *Nat Rev Mol Cell Biol* **6**: 862-871.
- Marshall, C.G., Broadhead, G., Leskiw, B.K., and Wright, G.D. (1997) D-Ala-D-Ala ligases from glycopeptide antibiotic-producing organisms are highly homologous to the enterococcal vancomycin-resistance ligases VanA and VanB. *Proc Natl Acad Sci U S A* **94**: 6480-6483.
- Marshall, C.G., Lessard, I.A., Park, I., and Wright, G.D. (1998) Glycopeptide antibiotic resistance genes in glycopeptide-producing organisms. *Antimicrob Agents Chemother* **42**: 2215-2220.
- Matsuo, H., Kumagai, T., Mori, K., and Sugiyama, M. (2003) Molecular cloning of a D-cycloserine resistance gene from D-cycloserine-producing *Streptomyces garyphalus*. *J Antibiot (Tokyo)* **56**: 762-767.
- Mazza, P., Noens, E.E., Schirner, K., Grantcharova, N., Mommaas, A.M., Koerten, H.K., Muth, G., Flardh, K., van Wezel, G.P., and Wohlleben, W. (2006) MreB of *Streptomyces coelicolor* is not essential for vegetative growth but is required for the integrity of aerial hyphae and spores. *Mol Microbiol* **60**: 838-852.
- McCormick, J.R. (2009) Cell division is dispensable but not irrelevant in *Streptomyces*. *Curr Opin Microbiol* **12**: 689-698.
- McCormick, J.R., Su, E.P., Driks, A., and Losick, R. (1994) Growth and viability of *Streptomyces coelicolor* mutant for the cell division gene *ftsZ*. *Mol Microbiol* **14**: 243-254.
- McHenney, M.A., Hosted, T.J., Dehoff, B.S., Rosteck, P.R., Jr., and Baltz, R.H. (1998) Molecular cloning and physical mapping of the daptomycin gene cluster from *Streptomyces roseosporus*. *J Bacteriol* **180**: 143-151.
- Meeske, A.J., Riley, E.P., Robins, W.P., Uehara, T., Mekalanos, J.J., Kahne, D., Walker, S., Kruse, A.C., Bernhardt, T.G., and Rudner, D.Z. (2016) SEDS proteins are a widespread family of bacterial cell wall polymerases. *Nature* **537**: 634-638.
- Meeske, A.J., Sham, L.T., Kimsey, H., Koo, B.M., Gross, C.A., Bernhardt, T.G., and Rudner, D.Z. (2015) MurJ and a novel lipid II flippase are required for cell wall biogenesis in *Bacillus subtilis*. *Proc Natl Acad Sci U S A* **112**: 6437-6442.
- Meier-Kolthoff, J.P., Auch, A.F., Klenk, H.P., and Göker, M. (2013) Genome sequence-based species delimitation with confidence intervals and improved distance functions. *BMC*

- Bioinformatics* **14**: 60.
- Merrick, M.J. (1976) A morphological and genetic mapping study of bald colony mutants of *Streptomyces coelicolor*. *J Gen Microbiol* **96**: 299-315.
- Meyrand, M., Boughammoura, A., Courtin, P., Mezange, C., Guillot, A., and Chapot-Chartier, M.P. (2007) Peptidoglycan N-acetylglucosamine deacetylation decreases autolysis in *Lactococcus lactis*. *Microbiology* **153**: 3275-3285.
- Migueluez, E.M., Hardisson, C., and Manzanal, M.B. (1999) Hyphal death during colony development in *Streptomyces antibioticus*: morphological evidence for the existence of a process of cell deletion in a multicellular prokaryote. *J Cell Biol* **145**: 515-525.
- Migueluez, E.M., Hardisson, C., and Manzanal, M.B. (2000) Streptomycetes: a new model to study cell death. *Int Microbiol* **3**: 153-158.
- Mohammadi, T., Sijbrandi, R., Lutters, M., Verheul, J., Martin, N.I., den Blaauwen, T., de Kruijff, B., and Breukink, E. (2014) Specificity of the transport of lipid II by FtsW in *Escherichia coli*. *J Biol Chem* **289**: 14707-14718.
- Mohammadi, T., van Dam, V., Sijbrandi, R., Vernet, T., Zapun, A., Bouhss, A., Diepeveen-de Bruin, M., Nguyen-Disteche, M., de Kruijff, B., and Breukink, E. (2011) Identification of FtsW as a transporter of lipid-linked cell wall precursors across the membrane. *Embo J* **30**: 1425-1432.
- Molle, V., Palframan, W.J., Findlay, K.C., and Buttner, M.J. (2000) WhiD and WhiB, homologous proteins required for different stages of sporulation in *Streptomyces coelicolor* A3(2). *J Bacteriol* **182**: 1286-1295.
- Morales Angeles, D., Liu, Y., Hartman, A.M., Borisova, M., de Sousa Borges, A., de Kok, N., Beilharz, K., Veening, J.W., Mayer, C., Hirsch, A.K., and Scheffers, D.J. (2017) Pentapeptide-rich peptidoglycan at the *Bacillus subtilis* cell-division site. *Mol Microbiol* **104**: 319-333.
- Morollo, A., Petsko, G., and Ringe, D. (1999) Structure of a Michaelis complex analogue: propionate binds in the substrate carboxylate site of alanine racemase. *Biochemistry* **38**: 3293 - 3301.
- Mukamolova, G.V., Murzin, A.G., Salina, E.G., Demina, G.R., Kell, D.B., Kaprelyants, A.S., and Young, M. (2006) Muralytic activity of *Micrococcus luteus* Rpf and its relationship to physiological activity in promoting bacterial growth and resuscitation. *Mol Microbiol* **59**: 84-98.
- Mukamolova, G.V., Turapov, O.A., Kazarian, K., Telkov, M., Kaprelyants, A.S., Kell, D.B., and Young, M. (2002) The rpf gene of *Micrococcus luteus* encodes an essential secreted growth factor. *Mol Microbiol* **46**: 611-621.
- Murray, B.E. (2000) Vancomycin-resistant enterococcal infections. *N Engl J Med* **342**: 710-721.
- Murray, P., Barron, E., Phaller, M., Ternover, J., and Yolken, R. (1999) Manual of Clinical Microbiology. *Mycopathologia* **146**: 107-108.
- Murshudov, G.N., Skubak, P., Lebedev, A.A., Pannu, N.S., Steiner, R.A., Nicholls, R.A., Winn, M.D., Long, F., and Vagin, A.A. (2011) REFMAC5 for the refinement of macromolecular crystal structures. *Acta Crystallogr D Biol Crystallogr* **67**: 355-367.
- Muthyala, R., Rastogi, N., Shin, W.S., Peterson, M.L., and Sham, Y.Y. (2014) Cell permeable VanX inhibitors as vancomycin re-sensitizing agents. *Bioorg Med Chem Lett* **24**: 2535-2538.
- Nagatsu, J., and Suzuki, S. (1963) Studies on an Antitumor Antibiotic, Cervicarcin. Iii. Taxonomic Studies on the Cervicarcin-Producing Organism, *Streptomyces Ogaensis* Nov. Sp. *J Antibiot (Tokyo)* **16**: 203-206.
- Nei, M., and Kumar, S. (2000) Molecular evolution and phylogenetics. *Oxford University Press, New York*.

- Nikitushkin, V.D., Demina, G.R., Shleeva, M.O., and Kaprelyants, A.S. (2013) Peptidoglycan fragments stimulate resuscitation of “non-culturable” Mycobacteria. *Antonie Van Leeuwenhoek* **103**: 37-46.
- Ning, S.B., Guo, H.L., Wang, L., and Song, Y.C. (2002) Salt stress induces programmed cell death in prokaryotic organism *Anabaena*. *J Appl Microbiol* **93**: 15-28.
- Noda, M., Kawahara, Y., Ichikawa, A., Matoba, Y., Matsuo, H., Lee, D.G., Kumagai, T., and Sugiyama, M. (2004a) Self-protection mechanism in D-cycloserine-producing *Streptomyces lavendulae*. Gene cloning, characterization, and kinetics of its alanine racemase and D-alanyl-D-alanine ligase, which are target enzymes of D-cycloserine. *J Biol Chem* **279**: 46143-46152.
- Noda, M., Matoba, Y., Kumagai, T., and Sugiyama, M. (2004b) Structural evidence that alanine racemase from a D-cycloserine-producing microorganism exhibits resistance to its own product. *J Biol Chem* **279**: 46153-46161.
- Noda, M., Matoba, Y., Kumagai, T., and Sugiyama, M. (2005) A novel assay method for an amino acid racemase reaction based on circular dichroism. *Biochem J* **389**: 491 - 496.
- Noens, E.E., (2007) Control of sporulation-specific cell division in *Streptomyces coelicolor*. In: PhD Thesis. Leiden: Leiden University, pp.
- Noens, E.E., Mersinias, V., Traag, B.A., Smith, C.P., Koerten, H.K., and van Wezel, G.P. (2005) SsgA-like proteins determine the fate of peptidoglycan during sporulation of *Streptomyces coelicolor*. *Mol Microbiol* **58**: 929-944.
- Noens, E.E., Mersinias, V., Willemse, J., Traag, B.A., Laing, E., Chater, K.F., Smith, C.P., Koerten, H.K., and van Wezel, G.P. (2007) Loss of the controlled localization of growth stage-specific cell-wall synthesis pleiotropically affects developmental gene expression in an *ssgA* mutant of *Streptomyces coelicolor*. *Mol Microbiol* **64**: 1244-1259.
- Nothhaft, H., Rigali, S., Boomsma, B., Swiatek, M., McDowall, K.J., van Wezel, G.P., and Titgemeyer, F. (2010) The permease gene *nagE2* is the key to N-acetylglucosamine sensing and utilization in *Streptomyces coelicolor* and is subject to multi-level control. *Mol Microbiol* **75**: 1133-1144.
- Novotna, G., Hill, C., Vincent, K., Liu, C., and Hong, H.J. (2012) A novel membrane protein, VanJ, conferring resistance to teicoplanin. *Antimicrob Agents Chemother* **56**: 1784-1796.
- Ogawara, H., Kawamura, N., Kudo, T., Suzuki, K.I., and Nakase, T. (1999) Distribution of beta-lactamases in actinomycetes. *Antimicrob Agents Chemother* **43**: 3014-3017.
- Okanishi, M., Suzuki, K., and Umezawa, H. (1974) Formation and reversion of *Streptomyces* protoplasts: cultural condition and morphological study. *J Gen Microbiol* **80**: 389-400.
- Okoro, C.K., Brown, R., Jones, A.L., Andrews, B.A., Asenjo, J.A., Goodfellow, M., and Bull, A.T. (2009) Diversity of culturable actinomycetes in hyper-arid soils of the Atacama Desert, Chile. *Antonie Van Leeuwenhoek* **95**: 121-133.
- Park, J.T., and Strominger, J.L. (1957) Mode of action of penicillin. *Science* **125**: 99-101.
- Parker, C.T., Tindall, B.J., and Garrity, G.M. (2015) International Code of Nomenclature of Prokaryotes. *Int J System Evol Microbiol*: 10.1099/ijsem.1090.000778.
- Patrick, W., Weisner, J., and Blackburn, J. (2002) Site-directed mutagenesis of Tyr354 in *Geobacillus stearothermophilus* alanine racemase identifies a role in controlling substrate specificity and a possible role in the evolution of antibiotic resistance. *Chem-biochem* **3**: 789 - 792.
- Perry, J.A., and Wright, G.D. (2013) The antibiotic resistance “mobilome”: searching for the link between environment and clinic. *Front Microbiol* **4**: 138.
- Peters, K., Kannan, S., Rao, V.A., Biboy, J., Vollmer, D., Erickson, S.W., Lewis, R.J., Young, K.D., and Vollmer, W. (2016) The Redundancy of Peptidoglycan Carboxypeptidases

- Ensures Robust Cell Shape Maintenance in *Escherichia coli*. *MBio* **7**.
- Piette, A., Derouaux, A., Gerken, P., Noens, E.E., Mazzucchelli, G., Vion, S., Koerten, H.K., Titgemeyer, F., De Pauw, E., Leprince, P., van Wezel, G.P., Galleni, M., and Rigali, S. (2005) From dormant to germinating spores of *Streptomyces coelicolor* A3(2): new perspectives from the crp null mutant. *J Proteome Res* **4**: 1699-1708.
- Pisabarro, A.G., de Pedro, M.A., and Vazquez, D. (1985) Structural modifications in the peptidoglycan of *Escherichia coli* associated with changes in the state of growth of the culture. *J Bacteriol* **161**: 238-242.
- Pluskal, T., Castillo, S., Villar-Briones, A., and Oresic, M. (2010) MZmine 2: modular framework for processing, visualizing, and analyzing mass spectrometry-based molecular profile data. *BMC Bioinformatics* **11**: 395.
- Pope, M.K., Green, B., and Westpheling, J. (1998) The *bldB* gene encodes a small protein required for morphogenesis, antibiotic production, and catabolite control in *Streptomyces coelicolor*. *J Bacteriol* **180**: 1556-1562.
- Pope, M.K., Green, B.D., and Westpheling, J. (1996) The *bld* mutants of *Streptomyces coelicolor* are defective in the regulation of carbon utilization, morphogenesis and cell-cell signalling. *Mol Microbiol* **19**: 747-756.
- Popham, D.L. (2002) Specialized peptidoglycan of the bacterial endospore: the inner wall of the lockbox. *Cell Mol Life Sci* **59**: 426-433.
- Popham, D.L., Helin, J., Costello, C.E., and Setlow, P. (1996) Analysis of the peptidoglycan structure of *Bacillus subtilis* endospores. *J Bacteriol* **178**: 6451-6458.
- Priyadarshi, A., Lee, E., Sung, M., Nam, K., Lee, W., Kim, E., and Hwang, K. (2009) Structural insights into the alanine racemase from *Enterococcus faecalis*. *Biochim Biophys Acta* **1794**: 1030 - 1040.
- Radkov, A.D., and Moe, L.A. (2014) Bacterial synthesis of D-amino acids. *Appl Microbiol Biotechnol* **98**: 5363-5374.
- Ramijan, K., Ultee, E., Willemse, J., Wondergem, J., Heinrich, D., Briegel, A., van Wezel, G., and Claessen, D. (2018) Stress-induced formation of cell wall-deficient cells in filamentous actinomycetes. *bioRxiv*.
- Ramijan, K., van Wezel, G.P., and Claessen, D. (2017) Genome Sequence of the Filamentous Actinomycete *Kitasatospora viridifaciens*. *Genome Announc* **5**.
- Reading, C., and Cole, M. (1977) Clavulanic acid: a beta-lactamase-inhibiting beta-lactam from *Streptomyces clavuligerus*. *Antimicrob Agents Chemother* **11**: 852-857.
- Reynolds, P.E. (1989) Structure, biochemistry and mechanism of action of glycopeptide antibiotics. *European journal of clinical microbiology & infectious diseases : official publication of the European Society of Clinical Microbiology* **8**: 943-950.
- Reynolds, P.E., Depardieu, F., Dutka-Malen, S., Arthur, M., and Courvalin, P. (1994) Glycopeptide resistance mediated by enterococcal transposon Tn1546 requires production of VanX for hydrolysis of D-alanyl-D-alanine. *Mol Microbiol* **13**: 1065-1070.
- Rice, K.C., and Bayles, K.W. (2003) Death's toolbox: examining the molecular components of bacterial programmed cell death. *Mol Microbiol* **50**: 729-738.
- Rice, L.B. (2001) Emergence of vancomycin-resistant Enterococci. *Emerg Infect Dis* **7**: 183.
- Richter, M., and Rossello-Mora, R. (2009) Shifting the genomic gold standard for the prokaryotic species definition. *Proc Natl Acad Sci U S A* **106**: 19126-19131.
- Rigali, S., Titgemeyer, F., Barends, S., Mulder, S., Thomae, A.W., Hopwood, D.A., and van Wezel, G.P. (2008) Feast or famine: the global regulator DasR links nutrient stress to antibiotic production by *Streptomyces*. *EMBO Rep* **9**: 670-675.
- Rioseras, B., Yague, P., Lopez-Garcia, M.T., Gonzalez-Quinonez, N., Binda, E., Marinelli, F., and Manteca, A. (2016) Characterization of SCO4439, a D-alanyl-D-alanine car-

- boxypeptidase involved in spore cell wall maturation, resistance, and germination in *Streptomyces coelicolor*. *Sci Rep* **6**: 21659.
- Rocaboy, M., Herman, R., Sauvage, E., Remaut, H., Moonens, K., Terrak, M., Charlier, P., and Kerff, F. (2013) The crystal structure of the cell division amidase AmiC reveals the fold of the AMIN domain, a new peptidoglycan binding domain. *Mol Microbiol* **90**: 267-277.
- Rong, X., and Huang, Y. (2012) Taxonomic evaluation of the *Streptomyces hygroscopicus* clade using multilocus sequence analysis and DNA-DNA hybridization, validating the MLSA scheme for systematics of the whole genus. *Systematic and applied microbiology* **35**: 7-18.
- Rong, X., and Huang, Y. (2014) Multi-locus sequence analysis: taking prokaryotic systematics to the next level. *Methods Microbiol* **41**: 221–251.
- Roper, D.I., Huyton, T., Vagin, A., and Dodson, G. (2000) The molecular basis of vancomycin resistance in clinically relevant Enterococci: crystal structure of D-alanyl-D-lactate ligase (VanA). *Proc Natl Acad Sci U S A* **97**: 8921-8925.
- Rutledge, P.J., and Challis, G.L. (2015) Discovery of microbial natural products by activation of silent biosynthetic gene clusters. *Nat Rev Microbiol* **13**: 509-523.
- Sacco, E., Hugonnet, J.E., Josseaume, N., Cremniter, J., Dubost, L., Marie, A., Patin, D., Blannot, D., Rice, L.B., Mainardi, J.L., and Arthur, M. (2010) Activation of the L,D-transpeptidation peptidoglycan cross-linking pathway by a metallo-D,D-carboxypeptidase in *Enterococcus faecium*. *Mol Microbiol* **75**: 874-885.
- Saitou, N., and Nei, M. (1987) The neighbor-joining method: a new method for reconstructing phylogenetic trees. *Mol Biol Evol* **4**: 406-425.
- Sambrook, J., Fritsch, E.F., and Maniatis, T., (1989) *Molecular cloning: a laboratory manual*. Cold Spring Harbor laboratory press, Cold Spring harbor, N.Y.
- Sanders, A.N., Wright, L.F., and Pavelka, M.S., Jr. (2014) Genetic characterization of mycobacterial L,D-transpeptidases. *Microbiology* **160**: 1795-1806.
- Sasser, M. (1990) Identification of bacteria by gas chromatography of cellular fatty acids *MIDI Inc. Technical Notes* **101**: 1.
- Schaberle, T.F., Vollmer, W., Frasch, H.J., Huttel, S., Kulik, A., Rottgen, M., von Thaler, A.K., Wohlleben, W., and Stegmann, E. (2011) Self-resistance and cell wall composition in the glycopeptide producer *Amycolatopsis balhimycina*. *Antimicrobial agents and chemotherapy* **55**: 4283-4289.
- Scheffers, D.J., and Tol, M.B. (2015) LipidIII: Just Another Brick in the Wall? *PLoS Pathog* **11**: e1005213.
- Schleifer, K.H., and Kandler, O. (1972) Peptidoglycan types of bacterial cell walls and their taxonomic implications. *Bacteriol Rev* **36**: 407-477.
- Schneider, T., and Sahl, H.G. (2010) An oldie but a goodie - cell wall biosynthesis as antibiotic target pathway. *Int J Med Microbiol* **300**: 161-169.
- Sexton, D.L., St-Onge, R.J., Haiser, H.J., Yousef, M.R., Brady, L., Gao, C., Leonard, J., and Elliot, M.A. (2015) Resuscitation-promoting factors are cell wall-lytic enzymes with important roles in the germination and growth of *Streptomyces coelicolor*. *J Bacteriol* **197**: 848-860.
- Sham, L.T., Butler, E.K., Lebar, M.D., Kahne, D., Bernhardt, T.G., and Ruiz, N. (2014) MurJ is the flippase of lipid-linked precursors for peptidoglycan biogenesis. *Science* **345**: 220-222.
- Shapiro, J.A. (1988) Bacteria as multicellular organisms. *Sci Am* **256**: 82-89.
- Shaw, J.P., Petsko, G.A., and Ringe, D. (1997) Determination of the Structure of Alanine Racemase from *Bacillus stearothermophilus* at 1.9-Å Resolution. *Biochemistry* **36**:

- 1329-1342.
- Shinobu, R. (1955) On *Streptomyces hirosimensis* nov. sp. *Seibutsugakkaishi* **6**: 43-46.
- Shirling, E., and Gottlieb, D. (1966) Methods for characterization of *Streptomyces* species. *Int J Syst Evol Microbiol* **16**:313-340.
- Silver, L.L. (2013) Viable screening targets related to the bacterial cell wall. *Ann N Y Acad Sci* **1277**: 29-53.
- Smith, C.A. (2006) Structure, function and dynamics in the mur family of bacterial cell wall ligases. *J Mol Biol* **362**: 640-655.
- Smith, T.L., Pearson, M.L., Wilcox, K.R., Cruz, C., Lancaster, M.V., Robinson-Dunn, B., Tenover, F.C., Zervos, M.J., Band, J.D., and White, E. (1999) Emergence of vancomycin resistance in *Staphylococcus aureus*. *N Engl J Med* **340**: 493-501.
- Sogaard-Andersen, L., and Yang, Z. (2008) Programmed cell death: role for MazF and MrpC in *Myxococcus* multicellular development. *Curr Biol* **18**: R337-339.
- Steen, A., Palumbo, E., Deghorain, M., Coconcelli, P.S., Delcour, J., Kuipers, O.P., Kok, J., Buist, G., and Hols, P. (2005) Autolysis of *Lactococcus lactis* is increased upon D-alanine depletion of peptidoglycan and lipoteichoic acids. *J Bacteriol* **187**: 114-124.
- Strych, U., Davlieva, M., Longtin, J.P., Murphy, E.L., Im, H., Benedik, M.J., and Krause, K.L. (2007) Purification and preliminary crystallization of alanine racemase from *Streptococcus pneumoniae*. *BMC Microbiol* **7**: 40.
- Susstrunk, U., Pidoux, J., Taubert, S., Ullmann, A., and Thompson, C.J. (1998) Pleiotropic effects of cAMP on germination, antibiotic biosynthesis and morphological development in *Streptomyces coelicolor*. *Mol Microbiol* **30**: 33-46.
- Swiatek, M.A., Tenconi, E., Rigali, S., and van Wezel, G.P. (2012) Functional analysis of the N-acetylglucosamine metabolic genes of *Streptomyces coelicolor* and role in the control of development and antibiotic production. *J Bacteriol* **194**: 1136-1144.
- Sycuro, L.K., Wyckoff, T.J., Biboy, J., Born, P., Pincus, Z., Vollmer, W., and Salama, N.R. (2012) Multiple peptidoglycan modification networks modulate *Helicobacter pylori*'s cell shape, motility, and colonization potential. *PLoS Pathog* **8**: e1002603.
- Takacs, C.N., Hocking, J., Cabeen, M.T., Bui, N.K., Poggio, S., Vollmer, W., and Jacobs-Wagner, C. (2013) Growth medium-dependent glycine incorporation into the peptidoglycan of *Caulobacter crescentus*. *PLoS One* **8**: e57579.
- Takahashi, Y. (2017) Genus *Kitasatospora*, taxonomic features and diversity of secondary metabolites. *J Antibiot (Tokyo)* **70**: 506-513.
- Takahashi, Y., Seino, A., Iwai, Y., and Omura, S. (1999) Taxonomic study and morphological differentiation of an actinomycete genus, *Kitasatospora*. *Zentralbl Bakteriol* **289**: 265-284.
- Tamura, K., Peterson, D., Peterson, N., Stecher, G., Nei, M., and Kumar, S. (2011) MEGA5: molecular evolutionary genetics analysis using maximum likelihood, evolutionary distance, and maximum parsimony methods. *Mol Biol Evol* **28**: 2731-2739.
- Tan, A.L., Loke, P., and Sim, T.S. (2002) Molecular cloning and functional characterisation of VanX, a D-alanyl-D-alanine dipeptidase from *Streptomyces coelicolor* A3(2). *Res Microbiol* **153**: 27-32.
- Tassoni, R., van der Aart, L.T., Ubbink, M., van Wezel, G.P., and Pannu, N.S. (2017) Structural and functional characterization of the alanine racemase from *Streptomyces coelicolor* A3(2). *Biochem Biophys Res Commun* **483**: 122-128.
- Taylor, S.D., and Palmer, M. (2016) The action mechanism of daptomycin. *Bioorg Med Chem* **24**: 6253-6268.
- Tenconi, E., Traxler, M.F., Hoebreck, C., van Wezel, G.P., and Rigali, S. (2018) Production of prodiginines is part of a programmed cell death process in *Streptomyces coelicolor*.

Frontiers Microbiol: in press.

- Thaker, M.N., Kalan, L., Waglechner, N., Eshaghi, A., Patel, S.N., Poutanen, S., Willey, B., Coburn, B., McGeer, A., Low, D.E., and Wright, G.D. (2015) Vancomycin-variable enterococci can give rise to constitutive resistance during antibiotic therapy. *Antimicrob Agents Chemother* **59**: 1405-1410.
- Thompson, J.D., Higgins, D.G., and Gibson, T.J. (1994) CLUSTAL W: improving the sensitivity of progressive multiple sequence alignment through sequence weighting, position-specific gap penalties and weight matrix choice. *Nucleic Acids Res* **22**: 4673-4680.
- Traag, B.A., and van Wezel, G.P. (2008) The SsgA-like proteins in actinomycetes: small proteins up to a big task. *Antonie Van Leeuwenhoek* **94**: 85-97.
- Uehara, T., Parzych, K.R., Dinh, T., and Bernhardt, T.G. (2010) Daughter cell separation is controlled by cytokinetic ring-activated cell wall hydrolysis. *Embo J* **29**: 1412-1422.
- Urem, M., Swiatek-Polatynska, M.A., Rigali, S., and van Wezel, G.P. (2016) Intertwining nutrient-sensory networks and the control of antibiotic production in *Streptomyces*. *Mol Microbiol* **102**: 183-195.
- Vagin, A., and Teplyakov, A. (1997) MOLREP: an Automated Program for Molecular Replacement. *Journal of Applied Crystallography* **30**: 1022-1025.
- van der Aart, L.T., Spijksma, G.K., Harms, A., Vollmer, W., Hankemeier, T., and van Wezel, G.P. (2018) High-resolution analysis of the peptidoglycan composition in *Streptomyces coelicolor*. *J Bacteriol*.
- van der Heul, H.U., Bilyk, B.L., McDowall, K.J., Seipke, R.F., and van Wezel, G.P. (2018) Regulation of antibiotic production in Actinobacteria: new perspectives from the post-genomic era. *Nat Prod Rep* **35**: 575-604.
- van der Meij, A., Worsley, S.F., Hutchings, M.I., and van Wezel, G.P. (2017) Chemical ecology of antibiotic production by actinomycetes. *FEMS Microbiol Rev* **41**: 392-416.
- van Dissel, D., Claessen, D., and Van Wezel, G.P. (2014) Morphogenesis of *Streptomyces* in submerged cultures. *Adv Appl Microbiol* **89**: 1-45.
- van Wageningen, A.M., Kirkpatrick, P.N., Williams, D.H., Harris, B.R., Kershaw, J.K., Lennard, N.J., Jones, M., Jones, S.J., and Solenberg, P.J. (1998) Sequencing and analysis of genes involved in the biosynthesis of a vancomycin group antibiotic. *Chem Biol* **5**: 155-162.
- van Wezel, G.P., Krabben, P., Traag, B.A., Keijser, B.J., Kerste, R., Vijgenboom, E., Heijnen, J.J., and Kraal, B. (2006) Unlocking *Streptomyces* spp. for use as sustainable industrial production platforms by morphological engineering. *Appl Environ Microbiol* **72**: 5283-5288.
- van Wezel, G.P., Mahr, K., Konig, M., Traag, B.A., Pimentel-Schmitt, E.F., Willimek, A., and Titgemeyer, F. (2005) GlcP constitutes the major glucose uptake system of *Streptomyces coelicolor* A3(2). *Mol Microbiol* **55**: 624-636.
- van Wezel, G.P., and McDowall, K.J. (2011) The regulation of the secondary metabolism of *Streptomyces*: new links and experimental advances. *Nat Prod Rep* **28**: 1311-1333.
- van Wezel, G.P., van der Meulen, J., Kawamoto, S., Luiten, R.G., Koerten, H.K., and Kraal, B. (2000a) *ssgA* is essential for sporulation of *Streptomyces coelicolor* A3(2) and affects hyphal development by stimulating septum formation. *J Bacteriol* **182**: 5653-5662.
- van Wezel, G.P., White, J., Hoogvliet, G., and Bibb, M.J. (2000b) Application of *redD*, the transcriptional activator gene of the undecylprodigiosin biosynthetic pathway, as a reporter for transcriptional activity in *Streptomyces coelicolor* A3(2) and *Streptomyces lividans*. *J Mol Microbiol Biotechnol* **2**: 551-556.
- Vara, J., Lewandowska-Skarbek, M., Wang, Y.G., Donadio, S., and Hutchinson, C.R. (1989)

- Cloning of genes governing the deoxysugar portion of the erythromycin biosynthesis pathway in *Saccharopolyspora erythraea* (*Streptomyces erythreus*). *J Bacteriol* **171**: 5872-5881.
- Verkade, P. (2008) Moving EM: the Rapid Transfer System as a new tool for correlative light and electron microscopy and high throughput for high-pressure freezing. *Journal of microscopy* **230**: 317-328.
- Vollmer, W. (2008) Structural variation in the glycan strands of bacterial peptidoglycan. *FEMS Microbiol Rev* **32**: 287-306.
- Vollmer, W., Blanot, D., and de Pedro, M.A. (2008a) Peptidoglycan structure and architecture. *FEMS Microbiol Rev* **32**: 149-167.
- Vollmer, W., Joris, B., Charlier, P., and Foster, S. (2008b) Bacterial peptidoglycan (murein) hydrolases. *FEMS Microbiol Rev* **32**: 259-286.
- Waksman, S.A., and Henrici, A.T. (1943) The Nomenclature and Classification of the Actinomycetes. *J Bacteriol* **46**: 337-341.
- Walsh, C.T. (1989) Enzymes in the D-alanine branch of bacterial cell wall peptidoglycan assembly. *J Biol Chem* **264**: 2393-2396.
- Walsh, C.T., Fisher, S.L., Park, I.S., Prahallad, M., and Wu, Z. (1996) Bacterial resistance to vancomycin: five genes and one missing hydrogen bond tell the story. *Chem Biol* **3**: 21-28.
- Wang, Z.M., Li, X., Cocklin, R.R., Wang, M., Fukase, K., Inamura, S., Kusumoto, S., Gupta, D., and Dziarski, R. (2003) Human peptidoglycan recognition protein-L is an N-acetylmuramoyl-L-alanine amidase. *J Biol Chem* **278**: 49044-49052.
- Wayne, L.G., Brenner, D.J., Colwell, R.R., Grimont, P.A.D., Kandler, O., Krichevsky, M.I., Moore, L.H., Moore, W.E.C., Murray, R.G.E., Stackebrandt, E., Starr, M.P., and Truper, H.G. (1987) Report of the Ad-Hoc-Committee on Reconciliation of Approaches to Bacterial Systematics. *Int J Syst Bacteriol* **37**: 463-464.
- WHO, (2014) *Antimicrobial Resistance: Global Report on Surveillance*. Geneva, Switzerland.
- Wiener, P., Egan, S., and Wellington, E. (1998) Evidence for transfer of antibiotic resistance genes in soil populations of streptomycetes. *Mol Ecol* **7**: 1205-1216.
- Willemse, J., Borst, J.W., de Waal, E., Bisseling, T., and van Wezel, G.P. (2011) Positive control of cell division: FtsZ is recruited by SsgB during sporulation of *Streptomyces*. *Genes Dev* **25**: 89-99.
- Willemse, J., and van Wezel, G.P. (2009) Imaging of *Streptomyces coelicolor* A3(2) with Reduced Autofluorescence Reveals a Novel Stage of FtsZ Localization. *PLoS ONE* **4**: e4242.
- Williams, S.T., Goodfellow, M., Alderson, G., Wellington, E.M., Sneath, P.H., and Sackin, M.J. (1983) Numerical classification of *Streptomyces* and related genera. *J Gen Microbiol* **129**: 1743-1813.
- Winn, M.D., Ballard, C.C., Cowtan, K.D., Dodson, E.J., Emsley, P., Evans, P.R., Keegan, R.M., Krissinel, E.B., Leslie, A.G.W., McCoy, A., McNicholas, S.J., Murshudov, G.N., Pannu, N.S., Potterton, E.A., Powell, H.R., Read, R.J., Vagin, A., and Wilson, K.S. (2011) Overview of the CCP4 suite and current developments. *Acta Crystallographica Section D: Biological Crystallography* **67**: 235-242.
- Witt, D., and Stackebrandt, E. (1990) Unification of the Genera *Streptoverticillum* and *Streptomyces*, and Amendment of *Streptomyces*-Waksman and Henrici-1943, 339a. *Syst Appl Microbiol* **13**: 361-371.
- Wolanski, M., Wali, R., Tilley, E., Jakimowicz, D., Zakrzewska-Czerwinska, J., and Herron, P. (2011) Replisome trafficking in growing vegetative hyphae of *Streptomyces coelicolor* A3(2). *J Bacteriol* **193**: 1273-1275.

- Wright, G.D., and Walsh, C.T. (1992) D-Alanyl-D-Alanine Ligases and the Molecular Mechanism of Vancomycin Resistance. *Accounts Chem Res* **25**: 468-473.
- Wu, C., Du, C., Ichinose, K., Choi, Y.H., and van Wezel, G.P. (2017a) Discovery of C-Glycosylpyranonaphthoquinones in *Streptomyces* sp. MBT76 by a Combined NMR-Based Metabolomics and Bioinformatics Workflow. *J Nat Prod* **80**: 269-277.
- Wu, C., Ichinose, K., Choi, Y.H., and van Wezel, G.P. (2017b) Aromatic polyketide GTRI-02 is a previously unidentified product of the *act* gene cluster in *Streptomyces coelicolor* A3(2). *Chembiochem* **18**: 1428-1434.
- Wu, C., Zacchetti, B., Ram, A.F., van Wezel, G.P., Claessen, D., and Hae Choi, Y. (2015) Expanding the chemical space for natural products by *Aspergillus-Streptomyces* co-cultivation and biotransformation. *Sci Rep* **5**: 10868.
- Wu, C., Zhu, H., van Wezel, G.P., and Choi, Y.H. (2016) Metabolomics-guided analysis of isocoumarin production by *Streptomyces* species MBT76 and biotransformation of flavonoids and phenylpropanoids. *Metabolomics* **12**: 90.
- Wu, D., Hu, T., Zhang, L., Chen, J., Du, J., Ding, J., Jiang, H., and Shen, X. (2008) Residues Asp164 and Glu165 at the substrate entryway function potently in substrate orientation of alanine racemase from *E. coli*: Enzymatic characterization with crystal structure analysis. *Protein Sci* **17**: 1066 - 1076.
- Wu, L.J., and Errington, J. (2011) Nucleoid occlusion and bacterial cell division. *Nat Rev Microbiol* **10**: 8-12.
- Wu, Z., Wright, G.D., and Walsh, C.T. (1995) Overexpression, purification, and characterization of VanX, a D-, D-dipeptidase which is essential for vancomycin resistance in *Enterococcus faecium* BM4147. *Biochemistry* **34**: 2455-2463.
- Xia, J., Sinelnikov, I.V., Han, B., and Wishart, D.S. (2015) MetaboAnalyst 3.0--making metabolomics more meaningful. *Nucleic Acids Res* **43**: W251-257.
- Xie, J., Pierce, J.G., James, R.C., Okano, A., and Boger, D.L. (2011) A redesigned vancomycin engineered for dual D-Ala-D-ala And D-Ala-D-Lac binding exhibits potent antimicrobial activity against vancomycin-resistant bacteria. *J Am Chem Soc* **133**: 13946-13949.
- Yague, P., Lopez-Garcia, M.T., Rioseras, B., Sanchez, J., and Manteca, A. (2013) Pre-sporulation stages of *Streptomyces* differentiation: state-of-the-art and future perspectives. *FEMS Microbiol Lett* **342**: 79-88.
- Yague, P., Manteca, A., Simon, A., Diaz-Garcia, M.E., and Sanchez, J. (2010) New method for monitoring programmed cell death and differentiation in submerged *Streptomyces* cultures. *Appl Environ Microbiol* **76**: 3401-3404.
- Yague, P., Willemse, J., Koning, R.I., Rioseras, B., Lopez-Garcia, M.T., Gonzalez-Quinonez, N., Lopez-Iglesias, C., Shliaha, P.V., Rogowska-Wrzesinska, A., Koster, A.J., Jensen, O.N., van Wezel, G.P., and Manteca, A. (2016) Subcompartmentalization by cross-membranes during early growth of *Streptomyces* hyphae. *Nat Commun* **7**: 12467.
- Yamasaki, M., Miyashita, K., Cullum, J., and Kinashi, H. (2000) A complex insertion sequence cluster at a point of interaction between the linear plasmid SCP1 and the linear chromosome of *Streptomyces coelicolor* A3 (2). *J Bacteriol* **182**: 3104-3110.
- Yang, D.C., Peters, N.T., Parzych, K.R., Uehara, T., Markovski, M., and Bernhardt, T.G. (2011a) An ATP-binding cassette transporter-like complex governs cell-wall hydrolysis at the bacterial cytokinetic ring. *Proc Natl Acad Sci U S A* **108**: E1052-1060.
- Yang, K.-W., Cheng, X., Zhao, C., Liu, C.-C., Jia, C., Feng, L., Xiao, J.-M., Zhou, L.-S., Gao, H.-Z., and Yang, X. (2011b) Synthesis and activity study of phosphoramidate dipeptides as potential inhibitors of VanX. *Bioorg Med Chem Lett* **21**: 7224-7227.
- Yoon, S.H., Ha, S.M., Kwon, S., Lim, J., Kim, Y., Seo, H., and Chun, J. (2017a) Introducing

- EzBioCloud: a taxonomically united database of 16S rRNA gene sequences and whole-genome assemblies. *Int J System Evol Microbiol* **67**: 1613-1617.
- Yoon, S.H., Ha, S.M., Lim, J., Kwon, S., and Chun, J. (2017b) A large-scale evaluation of algorithms to calculate average nucleotide identity. *Antonie Van Leeuwenhoek* **110**: 1281-1286.
- Zarlenga, L.J., Gilmore, M.S., and Sahm, D.F. (1992) Effects of amino acids on expression of enterococcal vancomycin resistance. *Antimicrob Agents Chemother* **36**: 902-905.
- Zhang, L., Willemse, J., Claessen, D., and van Wezel, G.P. (2016a) SepG coordinates sporulation-specific cell division and nucleoid organization in *Streptomyces coelicolor*. *Open Biol* **6**: 150164.
- Zhang, Z., Claessen, D., and Rozen, D.E. (2016b) Understanding Microbial Divisions of Labor. *Front Microbiol* **7**: 2070.
- Zhang, Z., Wang, Y., and Ruan, J. (1997) A proposal to revive the genus *Kitasatospora* (Omu-
ra, Takahashi, Iwai, and Tanaka 1982). *Int J Syst Bacteriol* **47**: 1048-1054.
- Zhu, H., Sandiford, S.K., and van Wezel, G.P. (2014a) Triggers and cues that activate antibiotic production by actinomycetes. *J Ind Microbiol Biotechnol* **41**: 371-386.
- Zhu, H., Swierstra, J., Wu, C., Girard, G., Choi, Y.H., van Wamel, W., Sandiford, S.K., and van Wezel, G.P. (2014b) Eliciting antibiotics active against the ESKAPE pathogens in a collection of actinomycetes isolated from mountain soils. *Microbiology* **160**: 1714-1725.
- Ziemert, N., Lechner, A., Wietz, M., Millan-Aguinaga, N., Chavarria, K.L., and Jensen, P.R. (2014) Diversity and evolution of secondary metabolism in the marine actinomycete genus *Salinispora*. *Proc Natl Acad Sci U S A* **111**: E1130-1139.

Curriculum vitae

Lizah Tanja van der Aart was born on the 7th of August 1991 in Haarlem, the Netherlands. In 2009, she graduated with a Nature and Health profile from the Kennemer Lyceum in Overveen. That same year, she started her Bachelor's programme at the Institute of Biology, Leiden University. She finished her Bachelor's studies in 2012 with a research internship p on the topic of *Streptomyces* L-forms in the group of Dr. Dennis Claessen. Lizah then followed a Masters programme in Molecular Biotechnology and Health at the Leiden University where she did a research project on *Streptomyces* development in the lab of Prof. Gilles van Wezel. In the summer of 2014 she joined a Top Sector competition hosted by the NWO with the team "Pulp Fraction" and worked on the reduction of orange peel waste using Natural Deep Eutectic Solvents (NADES) under the supervision of Prof. Dr. Geert-Jan Witkamp and Dr. Young Choi at the Plant Sciences and Natural Products lab at the Leiden University. She obtained her Master degree, cum laude, in 2014. That same year, Lizah began as a PhD student under the supervision of Prof. Gilles van Wezel and Prof. Thomas Hankemeier; the results of this work are presented in this thesis. During her work as a PhD student, she has spent 3 weeks in Prof. Waldemar Vollmer's lab to learn about peptidoglycan isolation and analysis. She received an EMBO short-term fellowship to spend two months in the Lab of Prof. Michael Goodfellow to perform taxonomy on *Streptomyces roseifaciens*. She participated at several conferences, among which the ISBA17 in Turkey, The Great Wall Symposium 2017 in Portugal, and the GRC Cell Surface Conference at Mount Snow, USA, 2018. After her PhD, she will join the lab of Prof. Jeff Errington at the Centre for Bacterial Cell Biology in Newcastle upon Tyne (United Kingdom).

List of publications:

Lizah T. van der Aart, Imen Nouioui, Alexander Kloosterman, Joost Willemse, Hua Zhu, Michael Goodfellow, Gilles P. van Wezel. (2019) Classification of *Streptomyces roseifaciens* sp. nov. as a novel verticillate strain with high potential for specialized metabolite production. *IJSEM*, Jan 9.

Lizah T. van der Aart, Gerwin K. Spijksma, Amy Harms, Waldemar Vollmer, Thomas Hankemeier, Gilles P. van Wezel. (2018) High-resolution analysis of the peptidoglycan composition in *Streptomyces coelicolor*. *J Bacteriol* 200:e00290-18. (with Cover image)

Raffaella Tassoni, Lizah T. van der Aart, Marcellus Ubbink, Gilles P. van Wezel, Navraj S. Pannu. (2017) Structural and functional characterization of the alanine racemase from *Streptomyces coelicolor* A3(2) *Biochemical and Biophysical Research Communications* Vol. 483, Issue 1, 29 January 2017, Pages 122-128

Lizah T. van der Aart, Nicole Lemmens, Willem J van Wamel, Gilles P. van Wezel. (2016) Substrate inhibition of VanA by D-alanine reduces vancomycin resistance in a VanX-dependent manner. *Antimicrob. Agents Chemother.* vol. 60 no. 8 4930-4939

Patent application:

Lizah T. van der Aart, Nicole Lemmens, Willem J van Wamel, Gilles P. van Wezel. (2016) Composition and method for treating infections caused by vancomycin-resistant infectious agents in a subject. European Patent Application PCT/NL2016/050919

Popular Scientific blog posts (Dutch):

Lizah van der Aart and Anne van der Meij write about microbiology for Wetenschap.nu
<https://wetenschap.nu/auteur/lizah-van-der-aart-en-anne-van-der-meij/>